ISTANBUL TECHNICAL UNIVERSITY ★ GRADUATE SCHOOL OF SCIENCE ENGINEERING AND TECHNOLOGY

FABRICATION AND CHARACTERIZATION OF SUPPORT LAYER FOR THIN FILM NANOCOMPOSITE DESALINATION MEMBRANES

M.Sc. THESIS

Kader ÖZGÜR

Nano Science and Nano Engineering

Nano Science and Nano Engineering Programme

MAY 2016

ISTANBUL TECHNICAL UNIVERSITY ★ GRADUATE SCHOOL OF SCIENCE ENGINEERING AND TECHNOLOGY

FABRICATION AND CHARACTERIZATION OF SUPPORT LAYER FOR THIN FILM NANOCOMPOSITE DESALINATION MEMBRANES

M.Sc. THESIS

Kader ÖZGÜR
513131015

Nano Science and Nano Engineering

Nano Science and Nano Engineering Programme

Thesis Advisor: Prof. Dr. M. Göktuğ AHUNBAY

MAY 2016

İSTANBUL TEKNİK ÜNİVERSİTESİ ★ FEN BİLİMLERİ ENSTİTÜSÜ

İNCE FİLM NANOKOMPOZİT DESALİNASYON MEMBRANLARI İÇİN DESTEK TABAKASI ÜRETİMİ VE KARAKTERİZASYONU

YÜKSEK LİSANS TEZİ

Kader ÖZGÜR
(513131015)

Nano Bilim ve Nano Mühendislik

Nano Bilim ve Nano Mühendislik Programı

Tez Danışmanı: Prof. Dr. M. Göktuğ AHUNBAY

MAYIS 2016

Kader Özgür, a M.Sc. student of ITU Graduate School of Science Engineering and Technology student ID 513131015, successfully defended the thesis entitled "FABRICATION AND CHARACTERIZATION OF SUPPORT LAYER FOR THIN FILM NANOCOMPOSITE DESALINATION MEMBRANES", which she prepared after fulfilling the requirements specified in the associated legislations, before the jury whose signatures are below.

Thesis Advisor :	**Prof. Dr. M. Göktuğ AHUNBAY** İstanbul Technical University	.....
Jury Members :	**Prof. Dr. Birgül TANTEKİN-ERSOLMAZ** İstanbul Technical University	.....
	Prof. Dr. Sacide ALSOY ALTINKAYA İzmir Institute of Technology	.....

Date of Submission : 12 April 2016
Date of Defense : 3 May 2016

To my family and all beloved ones,

FOREWORD

First of all, I would like to express my sincere thanks and gratitude to my research advisor Prof. Dr. Göktuğ AHUNBAY for his time, support, patience, and encouragement during this study.

I would like to express my indebtedness to Prof. Dr. Ş. Birgül TANTEKİN-ERSOLMAZ who is the architecture of this research. She has supported and encouraged me from the beginning of this study and shared her deep knowledge and experience. Without her support and guidance, this thesis would not have been possible. I would not be where I am today with my research.

I would like to acknowledge my mentor and co-worker Dr. Sadiye VELİOĞLU who shared her knowledge and experience generously throughout this study and spent all her efforts for making the best in this research as well.

I would also like to thank to my project partner Res. Asst. Süer KÜRKLÜ with whom we carried out all the experiments and tried to overcome all the problems encountered together. She was always there with her generous help and big smile.

I am especially indebted to Prof. William B. Krantz for his invaluable comments and enlightening discussions.

Special thanks to Ress. Asst. Dr. Çiğdem ORAL who always made suggestions for solving the problems and of course for supplying everything what we need.

Also, I must thank all the MeMaSep Group members, past and present, for their help and companion for this two year-period.

Finally, I would like to thank my father Nurhan ÖZGÜR, my mother Aliye ÖZGÜR, my brother Gürdal ÖZGÜR, and last but not least thank you to Burak BÜYÜKSAKALLI who as always were my most important supporters and moral sources during this research with their endless love and patience. Therefore, this work is dedicated to them for their love and encouragement during the past years.

This study was financially supported by 1001 program of TÜBİTAK under the project number of 114Y165.

April 2016

Kader ÖZGÜR
(Chemist)

TABLE OF CONTENTS

Page

ABBREVIATIONS

PSf **:** Polysulfone
RO : Reverse osmosis
TFC **:** Thin film composite
PA : Polyamide
IP : Interfacial polymerization
CNT : Carbon nanotube
TFN **:** Thin film nanocomposite
SWCNT : Singled-walled carbon nanotube
PVP : Polyvinylpyrrolidone
MPD : m-Phenylenediamine
TMC : Trimesoyl chloride
NMP : 1-Methyl-2-pyrrolidone
IPA : 2-Propanol
MeOH : Methanol
SWRO : Sea Water Reverse Osmosis
MF : Microfiltration
UF : Ultrafiltartion
NF : Nanofiltration
TDS : Total Dissolved Solids
PEG : Poly(ethylene glycol)
PES : Polyethersulfone
TEA : Triethylamine
TEOMA : Triethanolamine
ODA : Octadecylamine
ICIC : 5-isocyanato-isophthaloyl chloride
OD : Outer diameter
FO : Forward Osmosis
PRO : Pressure Retarded Osmosis
EtOH : Ethanol
SDBS : Sodium dodecylbenzenesulfonate
MWCNT : Multi-walled carbon nanotube

LIST OF TABLES

Page

LIST OF FIGURES

Page

FABRICATION AND CHARACTERIZATION OF SUPPORT LAYER FOR THIN FILM NANOCOMPOSITE DESALINATION MEMBRANES

SUMMARY

The production of potable water has become a global concern; for many communities, conventional available water resources are inadequate in supplying the demand due to rapid population growth and industrialization. Desalination of brackish or seawater has become an important source of both drinking water production and irrigation. The leading technology is reverse osmosis (RO) membrane process and is accounted for producing more than half of the world's desalination capacity. Significant development in membrane materials and technologies; in terms of module and process design, feed pre-treatment and energy recovery in the past few decades have greatly improved the cost effectiveness and performance capability of membrane processes and have made the RO technology dominating in the desalination market. Owing to showing inherently high salt rejection and durability with small footprint and ease of the operation, polymeric membranes have governed the RO membrane industry. On the other hand, there are several severe problems need to be eliminated such as comparatively low permeability due to their characteristic hyrophobicities, low boron removal and fouling issues.

In order to resolve aforementioned problems, different approaches were developed. Among them, thin film composite (TFC) membranes have drawn substantial attention since their invention by Cadotte et al. in the 1970s in which a thin selective polyamide (PA) layer is formed on top of a microporous support by in-situ interfacial polymerization (IP) technique and these membranes have high salt rejection values over 99%. Although, commercially available PA-TFC membranes can remove almost all ions in the seawater, their boron removal values are around 95% under normal test conditions. Recently, a new concept of mixed-matrix composite RO membranes was reported by incorporation of nanoparticles such as carbon nanotubes (CNTs) and zeolites into the thin selective PA barrier in the course of IP process. Both experimental and molecular simulation studies have shown that the use of CNTs in PA layer resulted with enhanced water flux and improved salt rejection values compared with conventional counterparts that are mainly because of their preeminent characteristics, and ease of functionalization with various functional groups. This thesis aims to develop a novel fabrication method of thin film nanocomposite (TFN) membrane for RO technology in which single-walled CNTs are embedded in PA selective layer during IP process on top of a microporous polysulfone (PSf) substrate with the purpose of increasing the boron rejection capacity and improving the water flux as well. Experiments were performed at three stages: i) preparation of porous polysulfone (PSf) substrate by phase inversion method and optimization of the process parameters such as addition of pore-former agents, changing the type of non-solvent and modifying the temperature of precipitation medium, ii) the development of TFC membranes on PSf supports

having different pore sizes and optimization of the IP process conditions such as altering the monomer concentrations and reaction time, iii) fabrication of TFN membranes by means of filtration of commercially available –COOH functionalized SWCNTs on PSf support prior to IP process for the semi-alignment of the nanotubes. For the characterization of the resultant membranes field emission scanning electron microscopy (FESEM) and contact angle measurements were employed to investigate both the surface and cross-sectional morphology, and surface hydrophilicity, respectively. Performance evaluations of the fabricated membranes were conducted using a laboratory scale cross-flow membrane test unit.

According to the results, the ideal PSf substrate membrane for the incorporation of SWCNT into PA layer was obtained from the recipe of 15 wt.% PSf with the addition of 10 wt.% pore-forming agent which was polyvinylpyrrolidone (PVP) and precipitated in cold isopropyl alcohol.

On the other hand, regarding to TFC results; SEM micrographs have shown that pore size of the PSf support has great impact on the resultant PA layer. Relatively smaller pores produced thicker PA layer due to the limited diffusion of aqueous m-phenylenediamine (MPD) solution into the small pore channels, whereas larger pores produced thinner PA layer mainly because of ability of MPD solution to penetrate deep into the pore channels and at the same time these big pores act like a MPD reservoir in which subsequent trimesoyl chloride (TMC) introduction will produce PA layer. Other than characteristics of PSf substrate, the PA layer thickness was affected by the interfacial polymerization reaction time in such a way that longer the polymerization time is applied, the thicker the cross-linked PA layer is formed. The 15 s reaction time produced around 100 nm PA layer, while doubling the reaction time from 15 s to 30 s formed approximately 1 μm-thick PA barrier. In addition to these, the effect of MPD concentration was also studied. Increasing the amount of MPD can caused to form thicker layer than its low concentration counterpart produced. All the results were consistent with the literature.

In order to test the fabricated membranes in the testing cell having 140 cm^2 test area, various masking techniques with Al tape and foil were tried and finally the most proper method has been developed. This newly developed technique enables to test the performance of the membranes having smaller areas than the test cell. Technique was tested with a membrane having a known specification. Results showed that the developed method works successfully without any leaking. In this regard, one of the fabricated membranes TFC-5 was tested in order to determine the performance of synthesized membranes so that to reflect a representative result. Salt rejection was calculated by measuring conductivity of the solutions before and after, which were feed and permeate, respectively. The rejection value was calculated as ~85% at 2000 ppm NaCl, which was smaller than the commercial membranes. These results have shown that the fabricated membranes can be improved in terms of fabrication technique to obtain better results. Nevertheless, this study contains noteworthy clues with respect to membrane masking and is still a guidance for the fabrication of substrate membranes for high boron rejection TFN membranes that can be used for desalination applications.

İNCE FİLM NANOKOMPOZİT DESALİNASYON MEMBRANLARI İÇİN DESTEK TABAKASI ÜRETİMİ VE KARAKTERİZASYONU

ÖZET

İçme suyu eldesi ve üretimi dünya çapında bir problem halini almıştır; birçok ülke için, kullanılabilir içme suyu kaynakları hızlı nüfus artışı ve endüstrileşmeden dolayı artan talebi karşılamak konusunda yetersiz kalmaktadır. Acı sudan ya da deniz suyunda içme ve sulama suyu eldesi sınırlı su kaynaklarına çözüm olarak ortaya çıkmaktadır. Günümüzde, ters osmoz (RO) bu alandaki lider teknoloji konumda olup dünya kapasitesinin yarıdan fazlasının üretiminden sorumludur. Membran malzeme ve teknolojisinde, modül ve proses tasarımında, besleme akımının ön temizliğinde ve enerji geri dönüşümünde son yıllarda gerçekleşen önemli gelişmeler; membran performans özelliklerini iyileştirirken aynı zamanda uygun maliyeti sebebiyle de ticari olarak RO teknolojisini desalinasyon pazarının lideri konumuna getirmektedir. Yüksek tuz giderme, dayanıklılık, atıklarının az olması ve operasyonel kolaylıklarından dolayı, polimerik membranlar RO endüstrisinin hakimi konumundadır. Öte yandan, bazı polimerler doğası gereği sahip olduğu hidrofob özelliklerinden dolayı göreceli düşük geçirgenlik göstermeleri, düşük bor giderimleri ve membran kirlenmesi; çözülmesi gereken önemli sorunların başında gelmektedir.

Bahsi geçen problemlerin çözümü için değişik yaklaşımlar geliştirilmiştir. Bunların arasında, Cadotte v.d.'nin, 1970'li yıllarda geliştirdiği; gözenekli destek membranı üzerinde arayüz polimerizasyonu yöntemi ile oluşturulan, seçici ince poliamid (PA) film oluşumunu sağlayan ince film kompozit (TFC) membranların keşfi araştırmacıların ilgisini çeken konuların başında gelmektedir. Bu tür membranlar, %99 üzerinde tuz giderimi sağlarlar. Ticari PA-TFC membranlar, deniz suyundan iyonların neredeyse tamamını giderebildiği halde, bor giderme yüzdeleri normal test koşulları altında %95 dolaylarındadır. Yakın zamanda, RO membranları için, karbon nanotüp (CNT) ve zeolit gibi nano boyuttaki yapıların seçici ince PA film içerisine arayüz polimerizasyonu sırasında yerleştirilmesini sağlayan, yeni karışık matrisli kompozit membran üretimi geliştirilmiştir. Karbon nanotüplerin yapılarından ve çeşitli gruplarla fonksiyonelleştirilebilir olmasından dolayı, seçici PA film içerisinde kullanımı; su geçirgenliğini ve tuz giderimini iyileştirdiğini rapor eden deneysel ve simulasyon çalışmaları mevcuttur.

Tez çalışmasında; yüksek bor ayırma kapasitesine sahip, tek duvarlı karbon nanotüplerin seçici PA film içerisine arayüz polimerizasyonu ile yerleştirildiği, yeni nesil ince film nanokompozit (TFN) desalinasyon membranı üretimi ve karakterizasyonu amaçlanmıştır. Çalışmalar üç (3) ana başlıkta toplanabilir: i) polisülfon (PSf) destek membranının faz ayrımı yolu ile üretimi ve membran üretim koşullarının optimize edilmesi, ii) ince film kompozit membran üretimi ve en uygun arayüz polimerizasyon reaksiyon koşullarının belirlenmesi, iii) ticari olarak –COOH gruplu satın alınan tek duvarlı nanotüplerin PSf destek membranı üzerine filtrasyon

yöntemiyle yarı-hizalanması ve takiben arayüz polimerizasyonunun yapılmasıyla ince film nanokompozit membran üretimi ve karakterizasyonu.

İlk olarak, 70'li yıllardan beri kullanılmakta olan faz ayrımı yöntemiyle PSf destek membranı üretimi ve karakterizasyonu yapılmıştır. Membran malzemesi olarak, literatürde ince film kompozit membran üretiminde en çok tercih edilen polimer olan PSf kulanılmış ve çözücüsü olan 1-metil-2-pyrrolidon (NMP) ile karıştırılarak homojen bir karışım elde edilmiştir. Polimer oranı yine literatürde en çok kullanılan oranlar arasından belirlenmiş ve kütlece %15 olarak sabit tutulmuştur. Düz plaka membran dökümünde, homojen dağılımı sağlanmış polimer çözeltisi cam bir yüzey üzerine dökülmüş; sabit kalınlığa ayarlanmış olan döküm bıçağı ve film döküm makinesini yardımıyla polimer film cam yüzeyinde oluşturulmuştur. Oluşturulan filmler, istenen membran özelliklerine göre, koagülasyon banyosuna daldırılmadan önce çözücünün buharlaşması için belirli bir süre atmosferik koşullarda bekletilmiştir. Ardından, dökülen filmler membran oluşumunun tamamlanması için belirli bir süre koagülasyon banyolarına daldırılmıştır. En uygun çözelti reçetesi ve koşulları bulunana kadar farklı konsantasyonlarda katkı malzemeleri, farklı buharlaşma süreleri ve çeşitli non-solventlerden oluşan, sıcaklığı düşürülmüş koagülasyon banyoları denenmiştir.

Non-solvent olarak hem ucuz hem de pek çok polimeri çözmeme özelliğinden dolayı distile su kullanılmaktadır. Bu çalışmada da öncelikli olarak koagülasyon banyosu olarak distile su kullanılmış; ancak oluşan membranların taramalı elektron mikroskobu (SEM) sonuçlarına bakıldığında istenen gözenekli yapıda olmadığı görülmüştür. Bu sebeple, yapılan literatür taramasında koagülasyon banyosundaki non-solventi değiştirmeden önce, dökülen membranların 24 saat koagülasyon banyosunda ve sonrasında 8 saatlik metanol (MeOH) banyosunda tutulması, membran yüzeyinde gözenek oluşumunu sağladığı görülmüştür. Ancak SEM sonuçlarında yine gözenek oluşumu gözlenmediği için farklı yaklaşımlar denenmiştir. Bu kez, kullanılan non-solventi değiştirerek istenen gözenekli yapı elde edilmeye çalışılmıştır. Literatür araştırmasında: non-solvent, solvent ve polimerin Hansen solubilite parametrelerininin biribirine yakın olması gerektiği belirlenmiş ve buna göre izopropil alkol (IPA) non-solvent olarak seçilmiştir. Yine istenen sonuçların elde edilememesiyle polivinilpirolidon (PVP) katkı malzemesi olarak PSf/NMP membran çözeltisine değişik konsantrasyonlarda (kütlece % 2, 5 ve 10) eklenmiştir. SEM analizlerinde gözenek oluşumu görüldü ancak düzenli bir yapıda olmadığı için; farklı buharlaşma süreleri denenmiş ve koagülasyon banyosu sıcaklığı düşürülmüştür. Yapılan çalışmalar sonucunda: % 5 ve % 10 PVP katkılı, soğuk IPA koagülasyon banyosuna daldırılmış, takibinde 8 saat MeOH'de bekletilmiş PSf membranlarının ortalama 30-40 nm civarında gözeneklere sahip olduğu görülmüştür.

Bir sonraki aşama olarak PSf destek membranı üzerine arayüz polimerizasyonu yöntemi uygulandı. Bu amaçla, literatür taraması sonucu optimum monomer konsantrasyonları belirlendi. Oluşturulan TFC membranlarının yüzey özelliklerini gözlemlemek amacıyla SEM ve yüzey ıslanabilirliğinin bir göstergesi olan hidrofilik veya hidrofobik özelliğinin ölçümü için de damlatma yöntemi kullanılarak temas açışı analizi yapılmıştır.

Distile su ile ıslatılan destek membranı, plastik çerçeve ve cam yüzey arasına sıkıştırıldı ve m-phenylenediamine (MPD)'den oluşan sulu çözelti membran yüzeyine döküldü. Belirli bir süre sonunda MPD çözeltisi döküldü ve çözeltinin fazlası plastik bir rulo yardımıyla membrandan uzaklaştırıldı.Membran tekrar

çerçeve arasına alınıp trimesoly chloride (TMC) çözeltisi döküldü. Belirli bir süre reaksiyonundan sonra etüvde ısıtılarak cross-linking reaksiyonu tamamlanması sağlandı.

Öte yandan, TFC membranında PA film oluşumunu ve kalitesini etkileyen farklı parametrelerin etkileri denendi. Bu çalışmada, oluşan ince PA tabakasının kalınlığını etkileyen etmenler arasından; farklı gözenek boyutuna sahip destek membranının etkisi, arayüz polimerizasyon süresi ve MPD konsantrasyonu etkileri incelenmiştir. Elde edilen SEM görüntülerine göre: yüzey gözenek büyüklüğü yaklaşı olarak 60 nm olan PSf destek membranının üzerinde oluşturulan PA filmin yaklaşık olarak 200 nm kalınlığında olduğu; öte yandan gözenek çapı ~ 300 nm olan destek membranında 100 nm civarında bir ince filmin oluştuğu gözlendi. Küçük gözenek boyutlarında daha kalın PA filmi oluşmasının başlıca nedeni: küçük gözeneklerin sulu MPD çözeltisinin daha derinlere nüfuz etmesini engelleyerek yüzeyde kalmasına yol açarak yüzeyde daha kalın bir PA tabakasının oluşmasına sebep olmaktır. Büyük gözenek boyutlu membranda ise durum tam tersidir; MPD çözeltisi geniş gözeneklerin iç çeperlerine kadar nüfuz ederek orada da cross-linking reaksiyonu oluşmasına olanak sağlar ve böylece yüzeyde oluşan film kalınlığı küçük gözenekli destek membranda oluşturulan PA tabakadan daha ince olur. Bunu yanı sıra, TFC membran yapımında reaksiyon süresinin etkisi de incelendi. Buna göre; 15 sn'lik sürede yaklaşık olarak 300 nm kalınlığında PA tabakası oluştuğu gözlenirken, aynı tabakanın kalınlığı süre 30 sn'ye çıkarıldığı zaman ~ 1 µm civarında olduğu görüldü. Bu büyük farklılığın ana nedeni; reaksiyon süresi arttıkça MPD ve TMC arasındaki çapraz bağlanma ile oluşan PA tabakasının oluşumunun da artmış olmasıdır. Son olarak, MPD konsantrasyonun etkisini ölçmek için değişik konsantrasyonlarda MPD sulu çözeltisi uygulandı. MPD miktarını arttırmakla daha kalın bir PA tabaka elde edildi. En uygun TFC koşullarını belirlemek amacıyla yapılan yukarıdaki çalışmaların sonuçları, literatürdeki verilerle de birebir örtüşmektedir.

TFN membranlarının üretimi için; öncelikli olarak ticari olarak satın alınan –COOH gruplu karbon nanotüpler filtrasyon yöntemi kullanılarak PSf destek membranı üzerine süzülmüştür. Bu esnada pompa yardımıyla vakum uygulanmış ve kesme kuvveti ile karbon nanotüplerin yarı-hizalanması amaçlanmıştır. Oluşturulan, karbon nanotüplü membran üzerine arayüz polimerizasyonu yöntemiyle PA film oluşturuldu.

Sentezlenen membranların performans testleri; hazırlanan model çözeltilerde test edilerek membranların tuz giderme yüzdeleri ve su geçirgenlik değerleri laboratuar ölçekli çapraz akımlı ters osmoz cihazında denenmiştir. Test hücre alanının sentezlenen membranlardan büyük olmasından dolayı farklı özelliklere sahip malzemeler ile maskeleme yöntemi geliştirildi. Geliştirilen maskeleme yöntemi performans değerleri bilinen ticari membran ile test edildi. Bunun için maskeli ve maskesiz performans değerleri kıyaslandı. Yöntemin sızıntı olmadan çalıştığı belirlendikten sonra, geliştirilen membranlardan biri olan TFC-5 denendi. 2000 ppm NaCl çözeltisi ve 18 bar basınçta yapılan test sonuçlarına göre; membran ~ %85 tuz giderimine sahip. Elde edilen sonuç; hem literatürde eksik olan maskeleme yöntemi eksiğini kapatmak, hem de desalinasyon uygulamalarında yüksek bor giderme değerlerine sahip TFN membranlarının üretimde kullanılacak destek tabakası üretimi için bir yol gösterici niteliktedir.

1. INTRODUCTION

Water shortage is a world-wide concern. Despite the fact that the 75% of Earth surface is covered by water, only 0.8% is freshwater since the bulk of 95% is salty water sourced from oceans and inland seas. Non-conventional methods gain importance because conventional methods for water and wastewater treatment need huge footprints on land and for land use they are not so efficient. Two of the key technologies are nanotechnology as we can use it for so many environmental related purposes such as water and wastewater purification, remediation, sensing, pollution prevention etc. and membranes that used for water and wastewater treatment. Therefore, combination of these two technologies complement each other to overcome water scarcity problem by solving challenges linked to the issue. Desalination of seawater and reclaimed wastewater became one of the leading method for obtaining clean water.

The purposes of the study are fabrication of porous polysulfone (PSf) support membrane by phase inversion method and optimization of the parameters; development of TFC membrane synthesized in-situ interfacial polymerization and adjustment of IP conditions; incorporation of CNTs into polyamide layer to form TFN membrane; and finally characterization of to-be-fabricated membranes in terms of morphological and performance evaluations.

2. LITERATURE REVIEW

2.1 Background

Increasing demand of safe drinking and irrigation water inevitably causes the freshwater deficiency, which has been identified as one of the most formidable challenge to be overcome in worldwide in the course of maintaining the population growth with improved living standards. Despite the fact that the 75% of Earth surface is covered by water, only 0.8% is freshwater since the bulk of 95% is salty water sourced from oceans and inland seas [1]. Furthermore, this 0.8% of freshwater is divided as of 70% agricultural, 22% industrial, and 8% domestic use [2]. In that case, the search of alternative water resources has been increased. Desalination of seawater and reclaimed wastewater became one of the leading method for obtaining clean water. One way of commonly used method of producing potable water is thermal distillation, which has been employed on remote islands and on ships since 1930s. However, the massive dependency to fossil fuel make thermal distillation less attractive over the years due to the fact that the rise in fuel price, and thus mainly restricted in the Middle East area in which fossil fuel is still affordable [1].

A major competitor of thermal distillation is reverse osmosis (RO) membrane technology since its invention in the 1960s, and today approximately half of the current worldwide desalination capacity is dominated by RO membranes [3]. On the other hand, current membrane technology is not able to separate some trace elements (such as boron) 100% from the feed water yet. RO membrane technology is not as effective as thermal distillation counterpart in which boron removal is accomplished nearly zero concentration. The main reason of insufficient removal of boron lies behind the fact that existence of uncharged boric acid comprising the large proportion of boron in seawater. These uncharged boric acid molecules can pass through membrane similar to diffusion of water molecules, and consequently causing a decrease in the percentage of boron rejection from seawater [4].

Typically, boron naturally occurs in seawater at an average concentration of approximately 4.6 mg/L, ranging in the interval of 0.52 mg/L in the Baltic Sea to 9.57 mg/L in the Mediterranean Sea [1]. In general, the surface water contains lower boron concentration values than 0.5 mg/L. Although, boron is an essential nutrient for humans, plants, and animals, it might cause adverse effects such as intoxicating the plants and disrupting reproduction of animals when they are exposed to higher concentrations of boron [5]. On the other hand, the toxicity of boron to human is not fully identified, and the majority of the researches has been undertaken from the studies of higher exposure of boron on animals, but more specifically from the agricultural crops studies [1, 4]. In order to draw a general conclusion, humans are supposed to tolerate higher level of boron than many plants, therefore the existing guidelines on boron limitations are mostly based on the tolerance of agricultural crops grown in the region [1]. Regulations for boron in drinking water from several organizations and countries are listed in Table 2.1.

Table 2.1: Regulations for boron in drinking water from several organizations and countries [1].

Organization/country	Boron upper value (mg/L)
WHO	2.4
EU	1.0
Israel	0.3
South Korea	1.0
New Zealand	1.4
Saudi Arabia	1.5
Japan	1.5
Canada	5.0

The strictest regulation is in Israel with the value of 0.3 mg/L since they use drinking water for irrigations of crops for example citrus, which has high boron sensitivity. Over the years, the World Health Organization (WHO) recommended varying values of boron concentration in potable water ranging from 0.3 mg/L to the final value of 2.4 mg/L starting in 1998 to 2011, respectively. The reason of this variation was the inadequacy in current removal technology since the existing methods were not able to separate boron as low as of 0.3 mg/L. On the other hand, lack of boron toxicity data on humans led to increase the upper limit of boron to 2.4 mg/L in the 4th Edition of the WHO guidelines [6].

2.2 Boron Chemistry

In seawater, typically boron exists in form of boric acid ($B(OH)_3$) which behaves as a very weak Lewis acid as stated by the dissociation reaction in equation (2.1):

$$B(OH)_3 + H_2O \Leftrightarrow B(OH)_4^- + H^+ \qquad (2.1)$$

The dissociation constant of boric acid that is the pK_a value is 9.25 [5]. In the aqueous medium, at the pH values lower than 9.25, boric acid is the major component; whereas at higher pH values borate ions ($B(OH)_4^-$) dominate [7]. Therefore, boron removal is intensively pH-dependent process. The dissociation of boric acid as a function of pH is illustrated in Figure 2.1. Boric acid can be poorly hydrated due to having small molecular size with Stokes radius twice as much as water molecule that is approximately 0.155 nm [1].

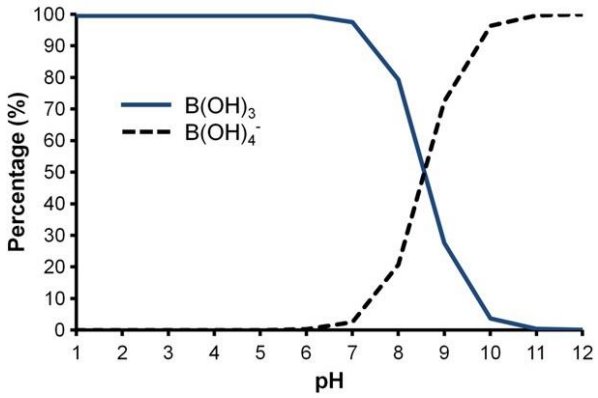

Figure 2.1: The dissociation curve of boric acid in diluted solution (at 25°C, 35,000 ppm salinity, and at 1 atm) [4].

Other than the pH dependency, there are other factors governing the boric acid dissociation and hence the removal efficiency in seawater such as temperature, salinity, and pressure. Studies conducted so far have revealed that at normal pressure range the effect of pressure is trivial while the temperature and salinity increase cause positive impact on the dissociation of boric acid [4, 5].

2.3 Boron Removal Technologies

Due to possessing at least three hydroxyl groups in its structure, boric acid and borate ions can react with multiple hydroxyl compounds called polyols to form complexes. With the aim of that idea, boron specific ion exchange resins were developed early in

the 1970s [4]. The use of boron selective chelating ion exchange resins is in a sense unavoidable for effective separation of boron from water. In fact, removal of boron by ion exchange resins is the most extensively studied technique [7]. The idea behind the principle of boron-selective ion exchange resins is the formation of variety of borate esters as a result of reaction with polyols which are composed of multi hydroxyl groups. The formed esters undergo rapid dissociation releasing protons, as a consequence the complexation increases the acidity of boric acid which is essential for monitoring the reaction [1, 4]. The simplified reaction between a polyol and boric acid is shown in equation (2.2); and schematic illustrations of boric acid and borate complexation with a polyol are represented in Figure 2.2.

$$B(OH)_3 + 3ROH \Leftrightarrow B(OR)_3 + 3H_2O \qquad (2.2)$$

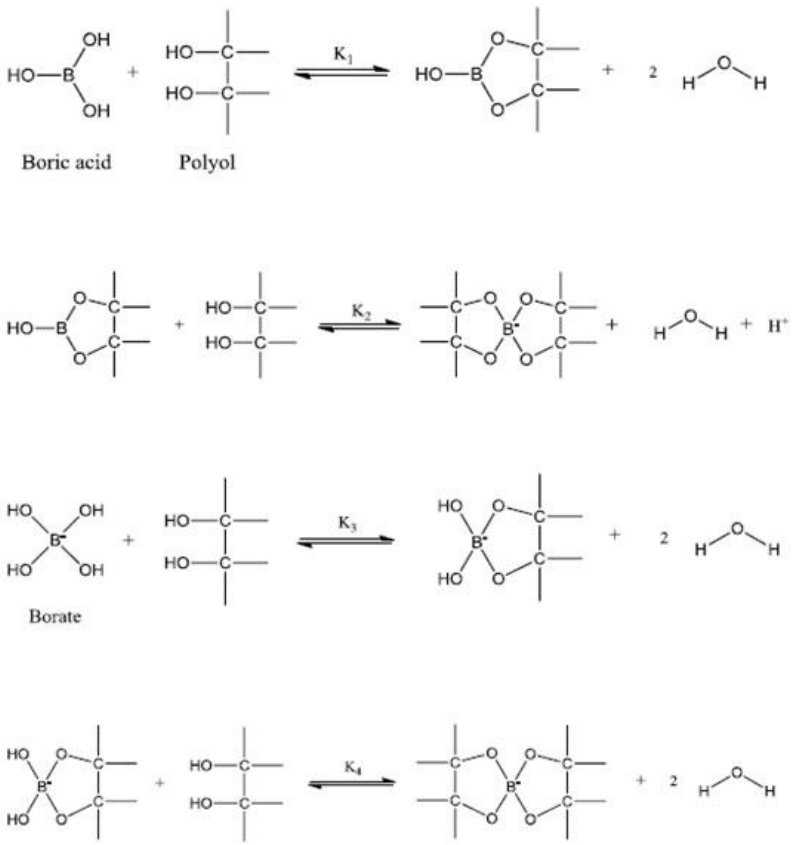

Figure 2.2: Schematic illustrations of boric acid and borate complexation with polyols [1].

There have been extensive research in the field of improving the properties of boron selective resins. On the other hand, there are numerous commercially available resins for boron removal mainly composed of microporous polystyrene matrix, where the

functional group is commonly N-methyl-D-glucamine having tertiary amine end and polyol end [4, 7].

Alternatively, RO process is one of the well-developed technologies for seawater desalination. Operation principal is so simple that facilitating only the water molecule passage, while withholding the dissolved components under applied pressure [7]. The reason for applying an external pressure is to overcome the osmotic pressure on seawater in which the diffusion of the molecules takes place from a concentrated solution to a dilute solution [4]. The foundation of the seawater desalination and water treatment by RO process is based on this phenomenon.

Generally, RO membranes can yield high boron removal but in the form of negatively charged borate ion, $B(OH)_4^-$ which is the dominating component at pH values higher than pK_a. On the other hand, the removal of non-dissociated uncharged boric acid is a big challenge, which is the major constituent at lower pH values. There are varying rejection values reported in the literature depending on the membrane used and operational conditions. For example, boric acid rejection value was reported in the interval of 40-60% at pH ranges from 5.5 to 9.5, whereas under the same conditions borate ion rejection was recorded as more than 95% [4]. In practice, conventional Sea Water Reverse Osmosis (SWRO) membranes can separate boron up to 84.6% under the feed pressure of 55 bar, at 32 g/L of NaCl, and in 8% recovery representing the standard test conditions [8]. In the same study, the pH effect of a commercial membrane was also reported indicating that the boron rejection was recorded as 84% at neutral pH values, while the rejection was increased to 89% when the pH was raised to around 8.2. In another study, two commercially available membranes were compared in terms of their boron rejection performances [9]. From the data obtained, the boron removal was increased from around 90% to 98% when the pH value was raised from 8.2 to 10.5, respectively. The studies reveal that the overall removal of boron is affected by the boric acid/borate ion ratio [4]. Despite the fact that the removal efficiency of boron differs in literature, the general idea is that the use of chemical for adjusting the pH brings additional cost to the overall process. Furthermore, increasing the pH for effective separation causes fouling problems, following the decrease in the water flux are the major obstacles to be overcome. On the other hand, there are studies have been focused on the improvement of the boron removal with compliance of the stringent

conditions as well as for reducing the overall cost of the process by developing several design concepts [4].

Another type of boron removal method is adsorption membrane filtration, which is the combination of the ion exchange process with membrane separation. In this technique, sorption of boron species in water by ion exchangers takes place; subsequent membrane filtration of boron-loaded resins encloses the hybrid process [4]. Although, the studies conducted so far have accomplished high boron removal efficiency, the cost of the process is still high and is a major challenge in front of the hybrid process to overcome.

The outline of the boron removal processes with their advantages and disadvantages is listed in Table 2.2.

Table 2.2: The outline of the boron removal processes with their properties [5].

Technology	Application	Boron level (mg/L)	Properties	
			Advantages	Disadvantages
Ion exchange	Desalination, reclamation, and ultra-pure water	2-500	>99% removal. Selectively remove boron.	Require chemicals for regeneration and disposal of chemical.
Reverse osmosis	Desalination and reclamation	1-35	Good removal at high pH. Flexible to run.	Require high pH for good removal. Risk of short membrane life.
Adsorption	Wastewater	100	Low initial cost and can handle high concentration	Long contact time, unable to procure low level of boron in product water.
Precipitation	Wastewater	5		
Electrodialysis	Pure water	4.5	>99% removal	Need high energy input.
Hybrid membrane	Sea water Reverse Osmosis permeate	5	>99% removal	Require chemicals. Resin abrasion in time.

2.4 Membrane Technology

A membrane is a thin, selective barrier allowing the permeation of certain molecules under the effect of a driving force and eventually rendering the separation of the chemical components from each other. Separation of the different components takes place as a result of selective permeability of one component over others. In general, one might think that a usual filter covers the membrane definition, but it differs in terms of the separation capability from a membrane. A normal filter is usually used for particulate suspensions and can separate the particles larger that 1 to 10 μm [10]. Despite the fact that the development of membrane phenomenon can be initiated in the eighteenth century by Abbé Nolet in 1748, it can be defined as an emerging technology and keep developing in every day. Schematic illustration of a membrane process is shown in Figure 2.3.

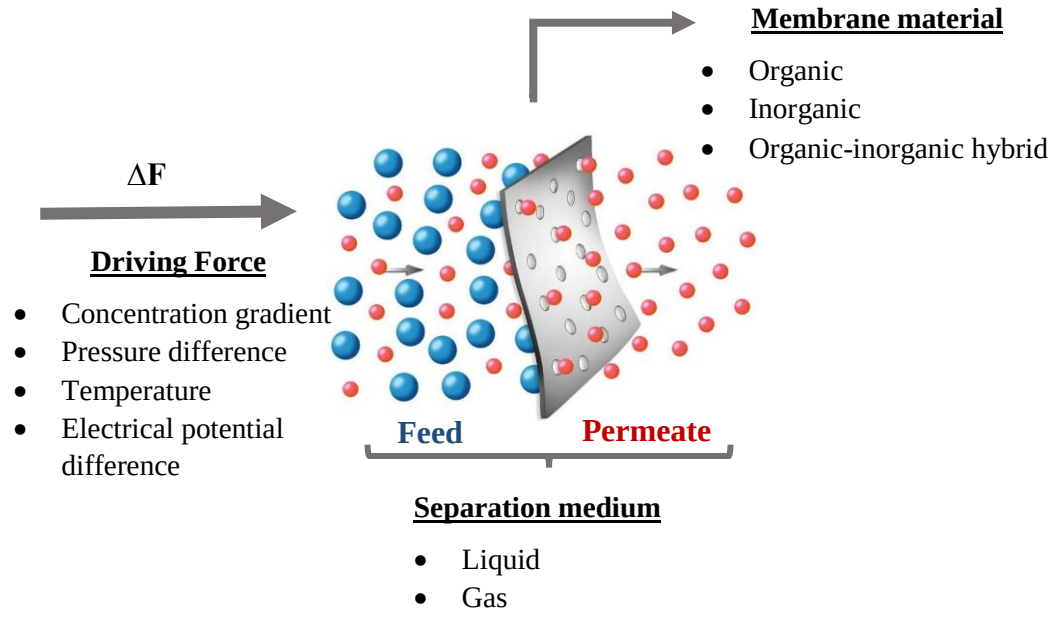

Figure 2.3: Schematic illustration of a membrane process [11].

Driving force can be described as the force or energy creating the movement of the species at the feed side due to the gradient in its chemical potential such as concentration, pressure, temperature, or electrical potential. Even a small difference in one of the above mentioned forces creates a molecular diffusion thus rendering the transportation of the permeants from one side to the other.

Membranes can be divided into two groups in terms of their origin as biological membranes or synthetic membranes. Both types have their own structure and

functionality, hence differ accordingly. Biological membranes are completely dissimilar with synthetic ones, therefore they are beyond the scope of this thesis. On the other hand, synthetic membranes can be sectioned primarily as organic, inorganic and the organic-inorganic hybrid membranes which are subdivided into mixed matrix and metal organic frameworks (MOF). The vast majority of the commercial membranes are composed of organic membranes specifically of polymer-based ones. Polymers having various kinds of combinations with tunable properties have captured a wide application area in industry. Polymeric membranes will be investigated thoroughly in next sections. About inorganic membranes, despite the fact that ceramic, zeolite, and metallic membranes which are the classes of inorganic membranes have gained much attention in recent years due to their better chemical and thermal stability allowing them to be used in aggressive conditions, they still need modifications in some aspects. Ceramic membranes are primarily consisted of metal oxide membranes made from aluminum, titanium or silica oxide and developed for mainly ultrafiltration and microfiltration via sol-gel methods or slip coating- sintering. Particularly, sol-gels techniques can produce membranes with pores between 10 and 100 Å, which is the reason for the extensive research interest for gas separation applications, yet up to now the commercial use is still limited. Zeolite-based membranes have been used for dehydration of alcohols by pervaporation or vapor/vapor permeation. Since the membranes are in tubular form, they exhibit high selectivities and high fluxes with the operation at high temperatures. However, the cost of the membrane module is expensive compared with polymeric counterparts [10]. Metallic membranes can be used mainly in hydrogen- gas mixture separations. The most well-known example is the palladium membrane which can absorb 600 times its volume of hydrogen. Hydrogen permeates several metals including tantalum, niobium, nickel, iron, vanadium, copper, cobalt, and platinum. However, these hydrogen-permeable metal membranes are essentially impermeable to all other gases. Mixed matrix membranes can combine the advantageous aspects of both polymers and inorganics. One example can be to fabricate a membrane that is comprised of the zeolite dispersed in polymer matrix yielding the combination of high selectivity of the zeolite with the low cost and ease of manufacture of the polymer matrix. The key point is the determination of the zeolite loading in the matrix [10].

A more general classification of the synthetic membranes can be built up on the morphological or structural differentiation. The types of membranes are illustrated on Figure 2.4.

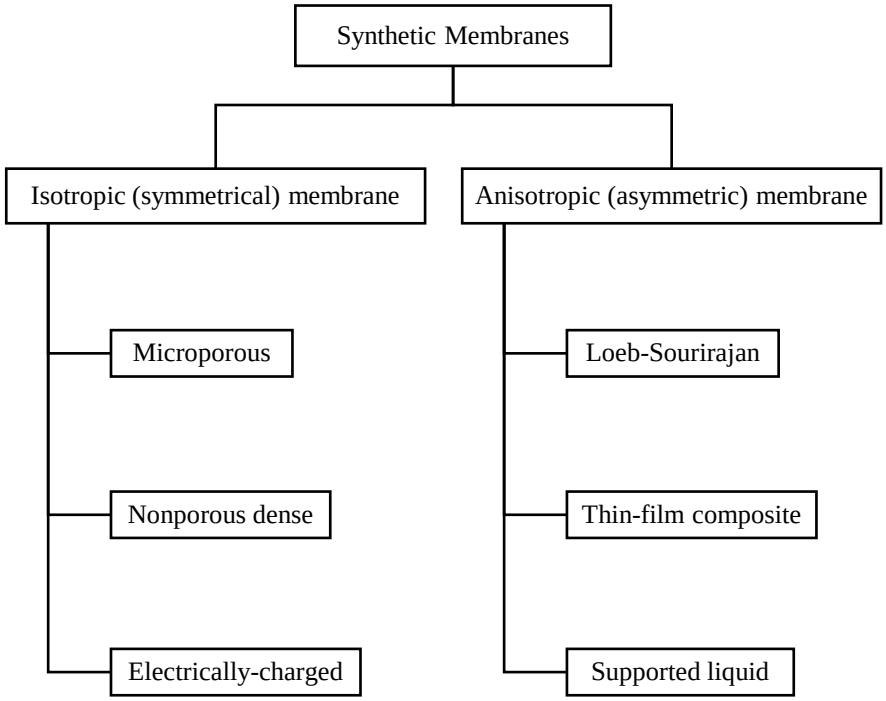

Figure 2.4: General classification of synthetic membranes.

Isotropic membranes have uniform composition and can be formed primarily in two different structures being porous and non-porous or dense. Although electrically charged membranes are categorized as another section of the symmetric membrane area, they can be produced as either a dense or a porous membrane with varying fixed positively or negatively charged ions. They are mostly developed with the purpose of treating the electrolyte solution in electrodialysis. While electrically charged membranes separate via the ion exclusion of the same charge as the fixed ions of the membrane, the separation in porous ones are based on differences in size and shape of the species. Basically, these membranes function according to the molecular size and pore size distribution of the membrane, such as species larger than the largest pores are completely excluded and particles smaller than largest pores can be partially rejected. On the other hand, in dense membranes separation is based on differences in selective adsorption and diffusion of the species in the membrane. Thus, the transportation or permeation of a component is related directly

to relative transport rate of other species within the membrane and requires a driving force of a pressure, concentration, or electrical potential gradient. Since the separation can be achieved by their relative diffusivity or solubility in the membrane material, even particles having similar sizes can be separated effectively. Having non-porous morphology lead these membranes to be used in gas separation, reverse osmosis, and pervaporation applications in which similar size permeants are presented in the same medium and need to be separated. Moreover, these types of membranes are designed as anisotropic structure so that to obtain improved fluxes. Figure 2.5 demonstrates a representation of primary membrane types.

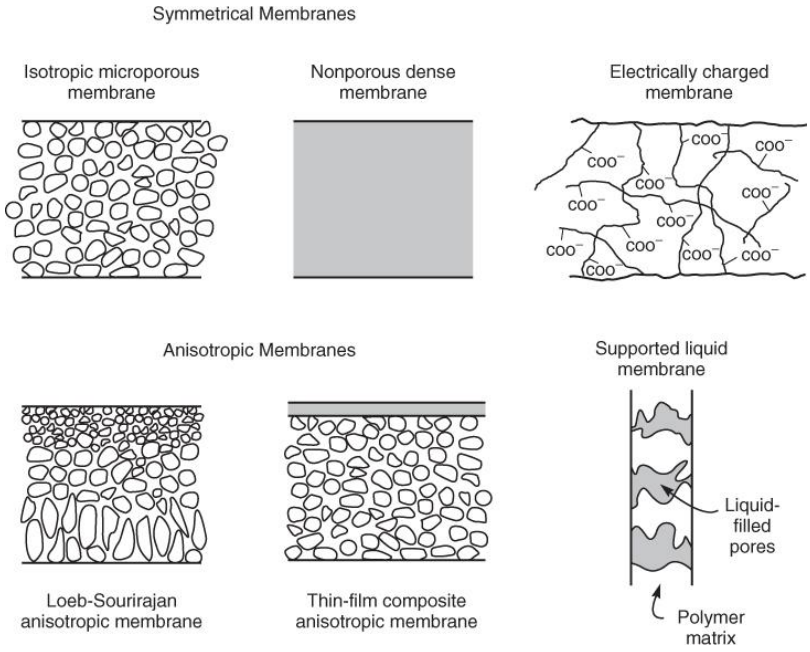

Figure 2.5: The diagram of primary types of membranes [12].

The development of the first anisotropic membrane was introduced by Loeb and Sourirajan in early 1960s [13]. Ultrathin, selective surface film was fabricated on thicker and more permeable microporous support resulting defect-free and high flux membranes. These membranes were the first prototype of reverse osmosis membranes. In the light of these excellent properties, other membrane fabrication techniques have been developed for improved performances. Interfacial polymerization and multilayer composite casting and coating are the methods developed for above-mentioned purposes. Essentially, these techniques direct the scientists to develop the new type of membranes called thin-film composites with skinned asymmetric layer produced with different material than its sublayer [12].

2.5 Membrane Processes

The major developed membrane separation processes are microfiltration (MF), ultrafiltration (UF), nanofiltration (NF), and reverse osmosis (RO). They are all pressure-driven processes that necessitate a pressure difference between feed and permeate side. Basically, MF and UF membranes operate similarly in a way that the separation takes place via molecular sieving. The major difference between them is the ability to exclude the particles that is to say MF membranes filter colloidal particles and bacteria in the interval of 0.1 to 10 μm in diameter while UF ones are utilized to separate dissolved macromolecules from solutions [10]. The pressure must be applied to these membranes are 5-500 kPa and less than 1.0 MPa for MF and UF, respectively. A NF membrane has separation characteristics between UF and RO. Series of studies have been conducted so far for their advantageous properties such as high flux, high retention of multivalent ion salts, and relatively low operation pressure [14]. Reverse osmosis is completely different from other methods in terms of the separation mechanism. The pores are in the range of 3 to 5 Å that only allow water permeation, hence mainly used in desalination applications. Having such small pores requires high pressure gradient from 5 to 10 MPa. Pressure-driven membrane processes and their properties are listed in Table 2.3.

Table 2.3: Pressure-driven membrane processes [15].

Water treatment process	Membrane	Thickness (μm)	Thin Film (μm)	Operating pressure (bar)	Pore size
RO	Asymmetrical	150	1	15-150	3-5 Å
NF	Asymmetrical	150	1	5-35	0.001-0.01 μm
UF	Asymmetrical	150-250	1	1-10	0.001-0.1 μm
MF	Symmetrical, Asymmetrical	10-150	-	< 2	0.1-10 μm

Another type of membrane processes is reverse osmosis, which is used for desalination of water. Operation principal is so simple that these type of membranes allow water permeation while restricting the salt permeation. The word desalination implies that the salt removal process from water to produce fresh water. Fresh water indicates that the salts or total dissolved solids (TDS) are less than 1000mg/L [16].

There are two classes of RO desalination being seawater RO and brackish water RO. These processes differ in terms of foulants, salinity, waste brine disposal options, and plant location [3]. As a result of these differences brackish water RO yields higher water flux but lower salt rejection due to trade-off between permeability and selectivity. In seawater RO membranes, the situation is exact opposite, such that these membranes are designed for maximum salt rejection with a condition to operate at higher pressures to compensate for the elevated osmotic pressure of seawater. There are standard limits on drinking water and these standards can be varied from country to country, for example the World Health Organization recommend a drinking water standard of 1000 mg/L TDS [17]. In addition to this, most desalination facilities are designed to achieve 500 mg/L or less TDS [3]. Seawater contains approximately 3.5 wt % salt, and to obtain a tolerable permeate which is less than 500 ppm salt, a RO membrane must have salt rejection greater than 99%. These levels of rejections can only achieved at high pressures.

The most favored and used material for RO membranes is polymer. Typically, RO membranes are fabricated as dense membranes, hence do not possess distinct pores for water migration from feed side to permeate side. Since the pores are so small that the thermal motion of the polymer chains overlaps with these pore ranges. Due to having dense characteristics and no open pores for pore flow, which is pressure-driven convective flow model, solution-diffusion model explains the transport mechanism taking place in RO membranes. According to this model, the separation achieved in three subsequent steps. First, the water has to be absorbed on the membrane surface at the feed side, then diffusion takes place through the membrane thickness because of concentration gradient, and finally release of the molecule from the permeate side of the membrane by desorption process. Since the focus of this study is to develop a new type of membrane for RO applications, the details on materials and fabrication techniques will be provided in next sections, other membrane applications such as MF, UF, and gas separation areas will be excluded.

2.6 Membrane Materials

Generally, membranes can be made of organic or inorganic materials. Ceramics and metals can be used to fabricate inorganic membranes, while polymers are the sources for organic ones. The main difference between polymeric and inorganic membranes

is the preparation methods. RO membrane technology operates at high pressures to achieve high salt rejection values. Polymers, as membrane materials, are the favored choice for their versatilities, ease of fabrications, and relatively low costs for RO application. Because of these reasons, polymeric membrane materials and fabrication techniques will be discussed in coming sections, inorganic membranes will be left out of this thesis.

Cellulose derivatives membranes were the first example of the high flux RO membranes developed by Loeb and Sourirajan [13]. Recently, these types of membranes have lost their popularities to interfacially produced composite membranes which give higher flux and salt rejection values. Cellulose, being as a natural polymer, is still used in specific membrane applications. Cellulose acetate is the organic esters of the cellulose and the most used type in certain kinds of membranes. The one thing affecting the water and salt permeabilities is the degree of acetylation of the polymer. As an example, cellulose triacetate containing 44.2 wt % acetate, exhibits high water- to-salt ratio representing high selectivity, but due to inevitable trade-off between permeability and selectivity, its water permeability is low. Their enhanced hydrophilic nature makes them an attractive choice for membrane fouling prevention. Moreover, these membranes have resistivity for dissolving because they show high structural uniformity as an addition to their intermolecular hydrogen bonding with hydroxyl groups. On the other hand, they are lack of broad operating temperatures; typically, they operate at 30°C to 40°C. The other disadvantages of these membranes are poor resistivity to chlorine and working at low pH range mostly pH 3 to pH 6. Furthermore, because of having the glass transition temperature at 68.8°C, the application to the higher temperatures and pressures is restricted [18].

Another type of membrane material used in RO process is polyamide membranes. Specifically aromatic membranes were developed to overcome the drawbacks of cellulose acetate membranes. They have better thermal stability and higher pH tolerance, but lower chlorine resistivity compared with cellulose acetate membranes.

In thin film composite membranes, polysulfone (PSf) and polyethersulfone (PES) membranes are mostly used as support membranes providing the porous structure and mechanical stability. They exhibit high rigidity and dimensional stability owing to having diphenylene sulfone repeating units in their aromatic structure. In addition

to these, unlike cellulose acetate membranes they do not suffer from low thermal stability. They can operate fairly high temperatures; for PSf up to 75°C and for PES 125°C, with wider pH operations [18].

2.7 Membrane Fabrication Techniques

In this section, polymeric membrane fabrication techniques for pressure driven processes are described. The choice of proper production method can affect the membrane pore structure, surface properties, and morphology. The most commonly used methods are stretching, track-etching, phase inversion, and interfacial polymerization.

2.7.1 Stretching

Technique was developed in 1970s by a commercial manufacturer and enables to produce porous membranes used in MF and UF applications. In this method, the polymer is heated above its melting point, and then extruded as thin sheet. Finally, the extruded sheet is stretched to obtain porous structure. Pore size between 0.1 μm and 3 μm can be achieved during the mechanical stress. Moreover, it is not necessary to use any kind of solvent, basically it is solvent free. Crystalline polymers such as polyethylene and polypropylene are the most preferred ones, because the crystalline regions give strength and porous structure is formed by amorphous regions [15].

2.7.2 Track-etching

The basis of this method is following: the exposure of the heavy energetic ions from a radiation source causes damages, basically leaves behind a sensitized track on the thin polymer film. Then, the immersion of this nonporous polymeric film in acid or alkaline solution forms the uniform cylindrical pores with pore size 0.02-10 μm. As a result, this fabrication method enables to control the pore size distribution precisely [10, 15].

2.7.3 Phase inversion

This technique also known as the Loeb-Sourirajan technique or polymer precipitation process. Fundamentally, this method involves a one-phase polymer solution precipitation into the two separate phases as solid and liquid states. The solid phase is polymer rich forming the membrane matrix, while liquid phase is polymer poor

creating the membrane pores [10]. There are several ways to achieve phase separation as described below:

a) Water precipitation, the Loeb-Sourirajan process. Immersion into a nonsolvent bath, usually water, allows solvent exchange and results rapid precipitation of polymer from top surface down.
b) Thermally induced phase separation. In this technique, the polymer solution is cast hot. As the cast film cools down, the solvent amount drops to such a point that precipitation is taking place to yield microporous structure.
c) Evaporation induced phase separation. This method is based on evaporation of one of the solvents that was formed a mixture together. Precipitation occurs while solution composition changes.
d) Vapor induced phase separation. The prepared film is subjected to an atmosphere containing high humidity. Concurrent water vapor absorption with the evaporation of one of the more volatile components causes precipitation [10, 15].

Among these methods, water precipitation and thermally induced phase separation are the most favored method for production of polymeric membranes. Specifically, the Loeb-Sourirajan process is commonly used for almost all RO and UF membranes. A skin, dense top layer on porous support can be produced for RO applications, while same general anisotropic nature, this time with finely porous skin layer can be fabricated to be used as a support membrane in UF characteristics for interfacial polymerization membranes.

There are several important aspects of water precipitation method, which are the choice of polymer and casting solution solvent, the precipitation medium, and selection of appropriate casting solution modifiers [10].

In the following sections, the details concerning the effects of varying parameters on UF substrate membrane production will be described; starting with the choice of polymer and solvent, coagulation bath, and following addition of pore former agents. In this technique, every contributor has a significant effect on final structure.

2.7.3.1 Effect of polymer

The polymer that will be used in substrate casting has to be an amorphous, tough, and high-molecular-weight thermoplastic with solubility of water-miscible solvent. The examples are polysulfone, cellulose acetate, polycarbonate, polyethersulfone

(PSf), polyetherimide, aromatic polyamides, and poly(vinylidine fluoride) [10, 19]. Among all the polymers used, polysulfone is the most favored one because of its ease of processing, wide availability, relative stability of thermal, mechanical, chemical, and bacterial attack [20, 21]. However, its hydrophobic nature and solvent resistivity are the main drawbacks [20]. In addition to chemistry of the polymer, the other key parameters is the decision of in what concentration the polymer must be used. Higher concentrations of casting solution can yield lower porosity with reduced pore size. Generally, the concentration range of polymer solution of 12-20 wt.% produces typical UF membranes, while the concentrations above 20 wt% are used for RO membrane fabrications [10, 15].

2.7.3.2 Effect of solvent

Aprotic solvents such as *N*-methyl pyrrolidone, dimethyl formamide, and dimethyl acetamide are the most appropriate solvents in terms of their ability to dissolve a wide variety of polymers. On one hand, when one of these solvents are prepared as a casting solution, after immersion into the non-solvent, typically water, they can quickly precipitate to yield porous and anisotropic membrane [10]. Basically, rapid precipitation gives high porosity. On the other hand, the selected solvent must have good miscibility with the polymer in order to obtain porous membranes, otherwise nonporous membranes are the results of the low miscibility of polymer with the solvent [15].

2.7.3.3 Effect of coagulation solution

The most popular non-solvent used for coagulation solution is water. The water is chosen for practical and economical purposes, but organic non-solvents can be employed as well especially when the casting solution solvent is water-immiscible such as methanol, ethanol, propanol, and acetone. Besides, the mixture of above-mentioned solvents with water is also widely applicable [22]. The mission of the non-solvent is to make the polymer precipitates from the casting solution consequently to cause the membrane formation.

The phase inversion membranes are the results of diffusion processes. In order to understand the entire concept, a ternary phase diagram is employed comprising of the polymer, solvent, and non-solvent. In this phase diagram, while membrane is formed by precipitation mechanism, any compositional change can be tracked through the

paths on the diagram. The casting solution concentration is the starting point, following the path to the final membrane composition as a result of a gradual decrease in the solvent concentration and increase in non-solvent amount in the membrane. Figure 2.6 schematically represents the mass transfer paths when the cast membrane is immersed into the precipitation solution [23].

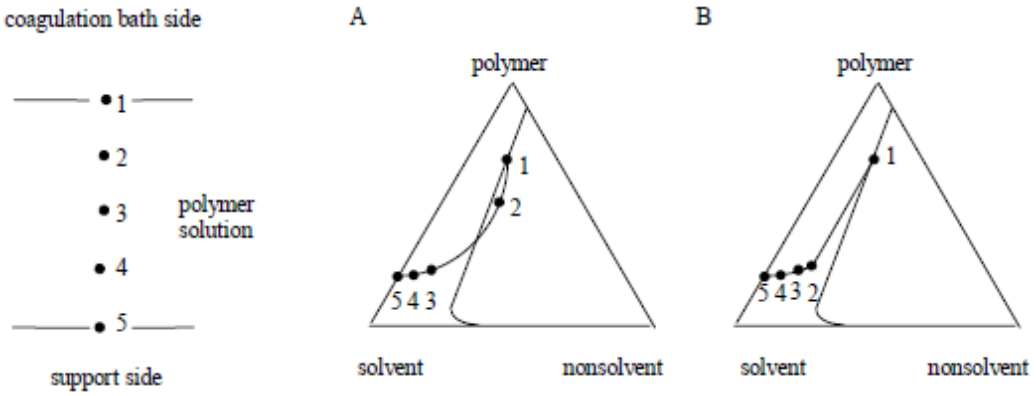

Figure 2.6: Schematic representation of mass transfer paths for A) instantaneous demixing system and B) delayed demixing system [23].

2.7.3.4 Effect of solution modifiers

The one way of modifying the membrane performance, surface, and structure characteristics is to add the solution modifiers to the system. These additives could be introduced by two different ways: the first one is hydrophilic polymers addition to the casting solution and the second one is solvent introduction to the precipitation solution [24]. The latter case produces increased skin layer porosity due to the added solvent can slow down the liquid-liquid demixing process causing to decrease the polymer concentration at the interface [25], while addition of a polymeric modifier decreases the macrovoid formation leading to produce more sponge-like structure with increasing the number pores and the pore interconnectivity [26]. Because of above-mentioned reasons, these modifiers are also identified as pore-former agents. The main requirement in selection of the pore-former is a good solubility in the precipitation medium. Generally, pore-formers can be selected from polyols, polyglycols, alkanols, and cycloketones. Explicitly, the most favored pore formers used with PSf are the high molecular weight polyvinyl pyrrolidone (PVP) and poly(ethylene glycol) (PEG) [22, 27, 28]. The concentration of the pore-formers in the casting solution could be up to 20 wt.%.

There have been numerous systematic studies conducted so far on the effects of PVP and PEG addition and their concentration variation on the membrane morphology and performances. Saljoughi et al. [29] showed that the addition of PVP in the range of 0 to 1.5 wt% leading to improved pure water flux, as the addition of PVP facilitated the macrovoid formation in the membrane sublayer. On the other hand, they also reported that any increase in PVP concentration from 1.5 to 3, 6 and 9 wt.% caused water flux reduction simply because the macrovoid formation had been suppressed gradually. In the other study, Marchese et al. [30] studied on the mechanism of membrane permeability increase with the PVP addition. As a result, they came up with the explanation that when PVP is added to the solution; the presence of macrovoids in the support layer and increased hydrophilicity of the both surfaces on the membrane and inside the pores cause gradual increase in pore density and decrease in the effective thickness of the dense layer. Wang et al. [31] reported that the addition of PVP to the polyethersulfone (PES) membrane yields higher water permeability with lower water contact angles implying that higher hydrophilicity is obtained compared with the pristine PES membrane. Ochoa et al. [32] stated that the PVP-added PES membrane has improved water flux without significant changes in selectivity. In addition to these, there are studies reporting similar results on using PEG as the pore former. Saljoughi et al. [33] proved that the addition of PEG enables the macrovoid formation causing to increase in flux and rejection of human serum albumin.

Other than organic modifiers, numerous inorganics are used as well. Typically, LiCl is employed as the inorganic additive. As general outcomes, LiCl produces open pores, but the concentration has such a significant effect that at higher concentrations the size of the macrovoids are suppressed due to strong interaction of LiCl with the polymer and solvent [34]. In addition to these, inorganic nanoparticles have been also incorporated into the casting solutions for taking advantages of their high strength and modulus in the membranes. Metal/metal oxide nanoparticles are the most used ones such as Ag, TiO_2, and Al_2O_3 [35].

2.7.4 Interfacial polymerization

Interfacial polymerization (IP) is a technique of forming thin and dense separating layer on a porous support membrane with enhanced water fluxes and salt rejections.

It was first developed by Cadotte as thin film composite (TFC) membrane, and today, almost all RO and NF membranes are commercially fabricated by this method [36]. It is a two-step procedure; as the first step a porous support, usually polysulfone UF membrane, is immersed in an aqueous solution of a polyamide. Then, this amine-saturated membrane is soaked into an organic solution containing a reactant such as a diacid chloride in an organic solvent. The reaction of acid chloride and amine at the interface of the support and following heat treatment produce the densely cross-linked and extremely thin membrane layer at the interface of the two solutions. This dense and cross-linked surface is composed of a polyamide (PA) layer, and the thickness is on the order of 0.1 μm or less yielding exceptionally both high permeability and selectivity. This PA layer can be formed via using various monomers; the most common monomers are m-phenylenediamine (MPD), or piperazine as amide source and trimesoyl chloride (TMC) as diacid source [10, 15]. Schematic representation of the reaction between MPD and TMC is shown in Figure 2.7.

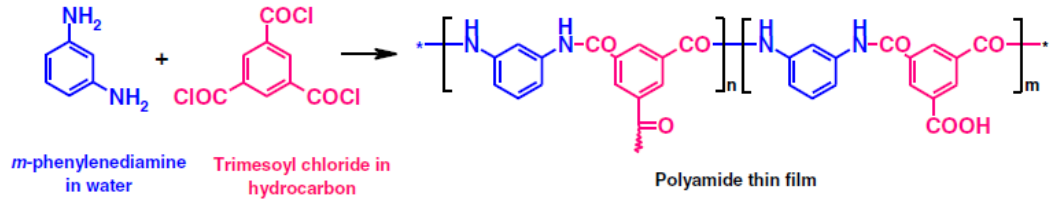

Figure 2.7: The reaction between MPD and TMC to form thin film composite membrane via IP [20].

There are various elements affect the final structure and composition of the membrane, such as monomer concentration, the reaction time at the interface, post-treatment conditions, and more importantly the nature of the support. Despite the fact that selectivity or salt rejection is accomplished by cross-linked thin layer, the structure of the support membrane has a significant impact on water flux. TFC membranes are widely used in RO desalination processes where high pressures are applied for water separation. The morphology of the microporous support has to be in such a porosity that not only it can resist the high pressures, but also contains high surface porosity in order not to block flow of water [10].

2.8 Thin Film Composite Membranes

Once the first thin film composite (TFC) membranes were introduced by Cadotte [36], they became a major research and application point for RO processes and in fact, many manufacturers managed to develop TFC membranes with numerous varieties. TFC membranes are advantageous in terms of enabling the modifications on porous support and thin layer separately. However, since their discoveries, the researches were focused mostly on improving the features of the active thin layer. It is known fact that top thin layer contributes the solute rejection and water permeation, but the support also does affect the flux of water, hence the resulted permeation of TFC membrane. Besides, it gives mechanical strength to the TFC as well. The properties of support were underestimated during TFC membrane preparation for a long time, but several research groups did prove that the relation between the substrate and polyamide layer cannot be ignored [20].

As describes in previous section, thin film composite membranes are comprised of an ultra-thin selective layer on the microporous support. This polyamide layer is formed at the surface of the substrate membrane as a result of crosslinking reaction of a polyfunctional amine dissolved in water and a polyfunctional acid chloride dissolved in a polar organic solvents [37]. Two of the most used monomers are; MPD and TMC as amine and as acid chloride source, respectively. The schematic representation of these reactants is shown in Figure 2.7. In addition to these, other amine monomers are also used as alternatives to MPD, which are piperazine [38], p-phenylenediamine [39], and triethylenetetramine [40]. Moreover, Tang et al. [41] reported the results on separation performances of the membrane when an aliphatic amine source that is triethanolamine (TEOA) reacts with TMC. Resultant membrane can be a good choice for acidic solution treatments, because the water flux is increased with decreasing the pH of the feed.

Despite the fact that the TFC membranes have better salt rejections with higher permeabilities compared with the conventional asymmetric counterparts, the attempts on the further improvements on separation properties of thin selective layer have been taken over the years [20]. The studies have been focused mainly on the IP reaction kinetics, reaction time, curing time, the use of additives, solvent solubility, solution composition, and the effect of porous support [37, 42-45]. The use of

additives in casting solution has a significant effect on the solubility, diffusivity, and hydrolysis by modifying the monomers. Furthermore, the additives can also behave as reaction byproduct scavengers [37]. In another study, the researchers have reported that the addition of amine salts for instance the trimethylamine salt of camphorsulfonic acid into the aqueous amine solution allows post-reaction curing at temperature higher than 100°C [46, 47]. By this way, increased crosslinking produced higher salt rejection without compromising the permeability. On the other hand, instead of mixing additives into the aqueous amine solution, the inclusion of additives into the organic acyl chloride solution is also possible. In fact, several patents have been disclosed on the addition of complexing agent into TMC [48, 49]. Phosphate-containing compounds, such as triphenyl phosphate, are one of the most preferred ones for their modification and elimination of repulsive interaction of acyl chloride with other compounds [42]. A major drawback of TFC membranes is the low resistivity against chlorine attacks. Systematic studies have proved that chlorine changes the chemical nature of the polyamide, hence affecting performance and shortening lifetime of the membrane [20]. Recent studies are mainly focused on overcoming the chlorine degradation.

Over the years, researchers have been trying to improve the interfacial properties of TFC membranes via employing various techniques in IP procedure. Zou et al. [50] developed novel method for minimizing the unreacted acyl chloride groups by means of the introduction of secondary amine solution. First, the PSf substrate was immersed in aqueous solution of 3.0 wt% MPD; the excess amount of solution was removed by rolling a rubber roller. Then, 0.15 wt% TMC in hexane was introduced. Subsequent employment of secondary amine solution of 3.0 wt% MPD formed the polyfunctional amine layer on the porous support. Results indicated that the topmost surface of the skin layer contained large amount of amino group ($-NH_2$) unlike the carboxylic acid groups (-COOH) prepared by conventional IP process. The authors also reported that this novel IP technique produced better antifouling property than that prepared by conventional IP procedure.

In addition to employment of the various techniques described above, there are several studies comprehensively investigated the TFC reaction conditions on the formation of PA layer in terms of interfacial polymerization reaction time, monomer concentrations, curing time and temperature [37, 51, 52]. It is a known fact that the

two monomers get together at liquid-liquid interface to form PA layer, which is formed in the organic phase because of low solubility of most acid chlorides in water and relatively high solubility of amines in organic phases. A dense cross-linked barrier is formed in a short time, which is stated as self-limiting reaction. The term self-limiting can be explained as the diffusion of MPD toward TMC slows down and gets more difficult to diffuse through, mainly because of the formation of the denser and thicker PA layer as the reaction progresses [52]. Since the reaction conditions are the major factor governing the final structure of PA layer and thus effecting the performance of the resultant membrane, special efforts have been devoted to understand the every factor influencing the IP film. Jin et al. [51] studied on forming a PA layer without growing it on a support membrane with the purposes of studying on the effects of various reaction conditions purely on the PA film. The experimental set-up is shown schematically in Figure 2.8. The variables were both monomer concentrations, reaction time and temperature. From the data obtained, more pendant –COOH groups which are the main responsible of the increased hydrophilicity of PA layer causing to obtain enhanced water flux, were found at higher TMC concentrations or lower MPD compositions.

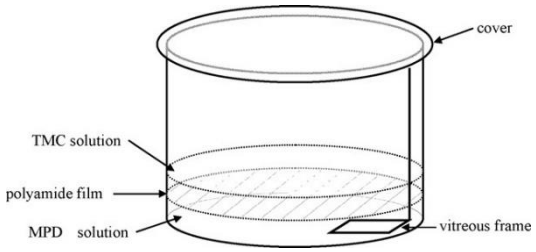

Figure 2.8: The experimental set-up of IP reaction of PA thin film without growing on a support membrane [51].

In addition to these, increased contact time and lower curing temperatures also facilitated the formation of the free acids by effecting the diffusion rate of MPD monomer for the passing through the interface.

On the other hand, Soroush et al. [52] were studied on the effects of reaction time, curing temperature, and curing time of PA layer formed on top of the PES substrate. Results have shown that the greatest effect on morphology and properties of PA layer was obtained from increasing the IP reaction time. As polycondensation time was increased, denser and more cross-linked PA thin layer was formed resulting increased thickness and altered surface morphology from nodular and leaf-like to

hill-and-valley structure. Eventually, the thicker PA layer and extended cross-linking resulted to obtain a decrease in water flux with the increased salt rejection. Similar results were also obtained from the increment in curing temperature. Up to a certain value, increasing curing temperature led to decreasing the water permeation and increasing salt rejection. Above this value, decreased water flux was obtained due to the chance of shrinkage of pores in the support membrane.

2.9 Thin Film Nanocomposite Membranes

Since the discovery of TFC membranes, many attempts have been dedicated to improve their water permeability, salt rejection, and antifouling properties. These efforts lead to form a new concept of TFC membrane called thin film nanocomposite (TFN) membrane which is basically the dispersion of nanomaterials into the ultra-thin PA layer formed by interfacial polymerization [53]. Schematic illustration of TFN membranes formation via IP is shown in Figure 2.9.

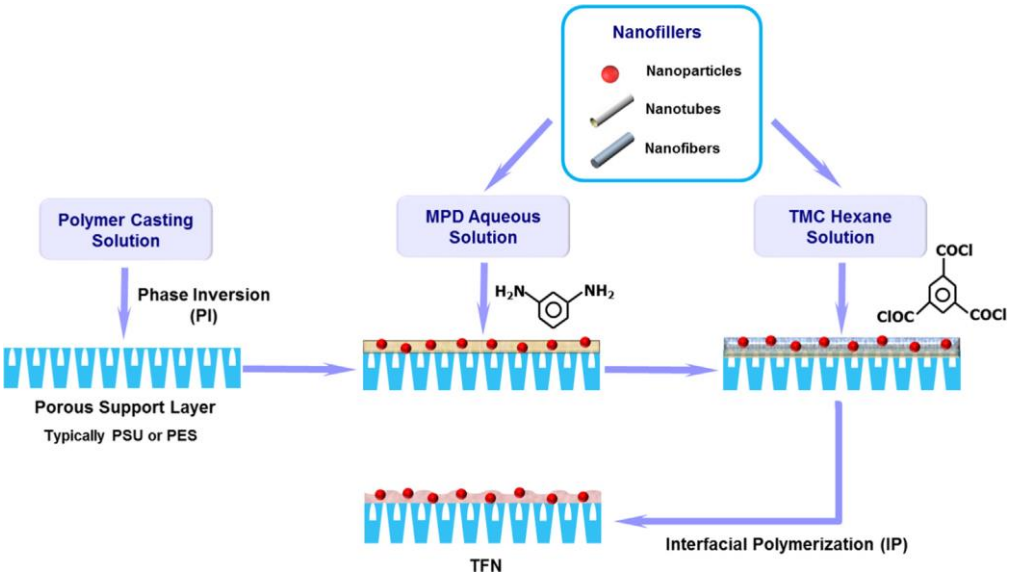

Figure 2.9: TFN membranes fabrication via IP process [53].

The term TFN membrane was first introduced by Hoek et al. in 2007 [54, 55]. Their groundbreaking study was based on the incorporation of zeolite NaA nanoparticles within the interfacially polymerized PA layer on top of the microporous PSf support. These embedded zeolite nanoparticles suggested a preferential pathway for the water molecules to pass through wherein happen to be super-hydrophilic and molecular sieve nanoparticle pores. As a result, a dramatical improvement in water permeability was obtained with comparable solute rejection to the conventional TFC membrane.

Despite the fact that the history of TFN membranes are not dated back earlier compared to TFC membranes, the idea of inclusion of nanofillers into the PA layer improves the membrane separation performances has been drawn much attention from the scientific community over the past 1-2 years [55]. Since their invention, various nanofillers have been employed with differing loading concentrations in TFN membranes such as zeolites, carbon nanotubes (CNTs), silica, Ag, and TiO_2 [53]. The permeability of water can be varied depending on not only the nanofiller type and its loading content, but also the IP process conditions. IP process conditions cover whether the nanoparticles disperse in organic or aqueous phase, in what concentrations the crosslinking monomers are mixed and what is the time duration required for the reaction of these reactants. All of the above-mentioned subjects can affect the resultant membrane flux and salt rejection. Lind et al. [56] reported that the smaller zeolite particles (~97 nm) have a tendency to yield higher water permeability whereas larger ones (~300 nm) give better surface properties when they are exposed to the PA layer [53, 55]. The exceptional structure of zeolite crystal with molecular sieve properties enabling not only a privileged pathway for water molecules but also providing an accommodation for them due to their hydrophilic and negatively charged natures; therefore having greater affinity to water molecules with increased repulsion of anions because of Coulombic effects is attained [54].

On the other hand, the effect of IP process conditions has been investigated by Fathizadeh and co-workers [57]. First, PA layer was produced from 2% (w/v) MPD reacted with 0.1% (w/v) TMC. Then, the second membrane was made from higher concentration of monomers that is 3 % MPD and 0.15 % TMC. The zeolite loading was same for both cases that of 0.2 wt% loading. As a result, the former case, which was the lower monomers concentration, produced better flux and solute rejection than latter one. However, despite lower concentration gives better rejection than higher concentration does, the rejection is still much lower than it is expected. There are other studies reporting that the crosslinking condition and the thickness of PA thin layer can affect the water flux and selectivity [37]. Generally, higher water flux is accomplished from thinner PA layer and lower degree of crosslinking. Inclusion of nanofillers into the PA matrix could disrupt the reaction between amine groups and acyl chloride groups or it can form nanovoids at the borders of nanofiller and PA matrix, and eventually causing the crosslinking reduction [53]. Although there are

numerous studies showing the inclusion of zeolite nanoparticles into the thin barrier membrane provides improved water flux, under certain conditions poor NaCl rejection is also reported by several studies [55]. The main reason of salt rejection decline is associated with the poor interaction between zeolite and PA layer eventually causing to form PA surface defects. Basically, inclusion of nanoparticles without any tailoring the IP process would not give enhanced performance. Therefore, additional adjustments are necessary for achieving good combination of water flux and salt rejection. For example, Lind et al. [56] and Fathizadeh et al. [57] have reported that improved separation performances obtained when the MPD and TMC concentrations were restricted around 2 and 0.1%, respectively.

Other than zeolite nanoparticles, nanotubes are also used as components of TFN RO membranes, such as CNTs and aluminosilicate single walled nanotubes (SWNTs). Baroña et al. [58] reported the effects on addition of aluminosilicate SWNTs into the PA layer. As a result, they found that incorporation of aluminosilicate SWNTs increases the surface hydrophilicity but conversely decreases the roughness. Furthermore, 0.59 wt% loading of nanotube produced 1.5 - fold increase in water flux in addition to small increment in NaCl rejection as well, when compared with the typical TFC membrane. The flux increase in TFN membranes is mainly attributed to the enhanced surface hydrophilicity of the membrane when a hydrophilic nanofiller is added [53]. In another study, oxidized multi walled CNTs (MWCNTs) were incorporated in PA membranes [59]. Characterization results showed that the water contact angle was declined from around 70° to 25°, while MWCNTs concentration was increased from 0 to 0.2 % (w/v). As result of increased surface hydrophilicity, the enhanced flux was obtained with increasing nanotube loading. Roy et al. [60] reported that improved permeability results are the indications the nanogaps around the MWCNTs surface and polymer matrix offering a very low resistance pathway for solvent. In TFN membranes, PA thin matrix is the major part performing the solute rejection.

On the other hand, the agglomeration of the nanofillers is the major challenge in the TFN membrane fabrication. Generally, they are introduced into the PA layer by mixing with either aqueous or organic solutions used in the IP process. These nanomaterials exhibit low dispersion rates in the IP solutions. Non-uniform dispersion of nanoparticles and nanotubes, especially in non-polar organic solvents,

causes to particles agglomerate, hence make them to be spread on the porous support surface unevenly. Because of these reasons, some part of the resultant PA membrane can remain untreated with nanomaterials at all. Another difficulty experienced in the TFN membrane fabrication is that the application of IP process itself. After introducing the aqueous amine solution, generally a rubber roller is rolled on top of the support to remove the excess amount of solution. Since the hydrophilic nanoparticles are introduced on the substrate by dispersing in aqueous phase due to having better dispersion than in organic phase, subsequent application of roller can remove not only the excess amine solution but also a large amount of nanoparticles from the substrate surface. Consequently, small amounts of nanoparticles are left behind in the support pores. One solution to that problem could be performing the surface modification of hydrophilic nanoparticles in order to make them more compatible with the organic phase [55]. For example, Shen et al. [61] first performed surface modification technique on MWCNTs with a mixture of acid solution (HNO_3 and H_2SO_4) which is nothing but oxidation of the nanotube walls. Then, micro-emulsion polymerization of methyl methacrylate (PMMA) was applied. As a result, well-dispersed nanotubes in organic phase were obtained. With the dispersion ability of nanomaterials, the precipitation of them in organic phase in the course of IP process is attenuated; as a result the extend of particle aggregation in the PA layer is decreased [55].

Various approaches have been introduced not only to modify the IP procedure of TFN membranes in terms of their interfacial properties, but also to increase the dispersion of the nanomaterial in the PA layer. Some of these adjustments are the preliminary employment of organic solution, then following the regular IP procedure. Wu et al. [14, 62] introduced above-mentioned technique on the PSf substrate and compared with the results of conventional IP procedure. Schematic representation of improved IP process is shown in Figure 2.10. As a first step, support was immersed in organic solution containing TMC for 30 min. Then, TMC-enriched substrate placed into the aqueous amine solution of triethanolamine (TEOA) containing 0.05 % (w/v) MWCNTs for a certain time. Subsequent immersion of the membrane into the TMC-organic phase finalized the IP process. Results pointed out that the improved IP process produced a TFN membrane with significant enhancement in both permeability and selectivity compared with the TFC

membrane without MWCNTs and TFN membranes fabricated by conventional IP. By this way, the improved process of IP can facilitate to surpass the permeability and selectivity trade-off.

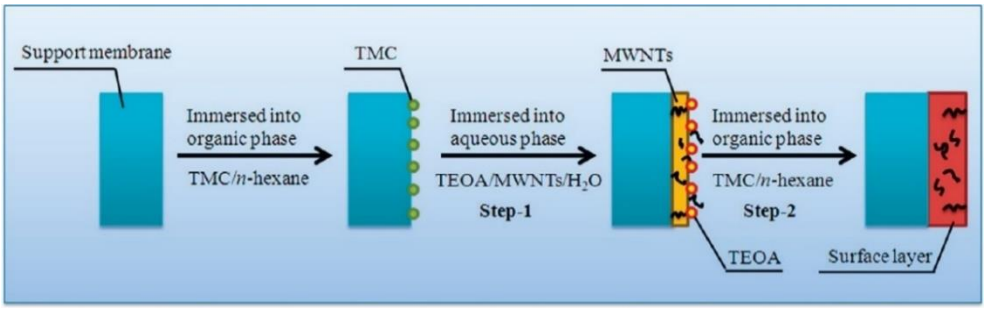

Figure 2.10: Schematic representation of improved IP process by Wu et al [14].

2.10 The Use of CNTs in Membranes for Desalination

Owing to having unique smoothness and orderliness of the CNT pores, in contrast to the other nanoporous materials significant enhancement of the transport property of fluids through these pores are achieved with the confirmation of both experimental and computational studies. The transport of water molecules by means of subnanometer nanotubes is realized by taking advantage of compliant and pulse-like movement of hydrogen-bonded molecules existing within the channel [63]. Studies conducted so far have shown that CNTs are promising material for using in desalination technology since they possess exceptionally high separation properties as well as have the ability of exhibiting superior durability [64]. Previous research studies have also shown that the potential of applying CNTs can increase due to the fact that combination of enhanced water transport with the pore diameter of nanotubes. Gerhard et al. [65] reported that water passed through in CNTs in a way that analogous to that of passing through in a polymeric membrane pore. They also stated that the water passage was similar to diffusion of a gas molecule through a membrane [66].

In order to obtain enhanced properties such as high selectivity and water flux, the incorporation of CNTs into the membrane requires employing chemical modification and functionalization on the CNTs [64]. Furthermore, computational and experimental work were conducted so far reveal that these advanced materials possess outstanding flux of water transport with the ability of excellent salt rejection

values mainly because of the potential combination of functionalization of nanotubes with their intrinsic ion channel transport.

Significant efforts have been devoted to develop new methods for the improvement and modification of the surface characteristics of CNTs to obtain products with enhanced properties. The common way is the functionalization of CNTs, which can be divided into two groups being chemical and physical functionalization. The latter one represents the non-covalent interaction and is a result of the van der Waals interactions or π-π stacking between CNT and mostly a polymer, while the former involves the covalent bonding of functional groups onto CNT skeleton.

The chemical functionalization can be accomplished by two different ways performed either at the open ends of the tubes or at their sidewalls. Sidewall functionalization is a consequence of change in hybridization from sp^2 to sp^3 with synchronized loss of π conjugation system on graphene layer [67]. Polymer wrapping, surfactant adsorption and endohedral methods are the examples for the physical functionalization [68]. On one hand, molecules having high chemical reactivity such as fluorine react with purified CNTs to form fluorinate nanotubes, which are an intermediate step for the subsequent replacement of fluorine by amino, alkyl, and hydroxyl groups [69]. The other derivatives of sidewall functionalization methods are cycloaddition, chlorination, bromination, and hydrogenation [67]. On the other hand, functionalization of open ends of the nanotubes also known as defect functionalization enabling chemical conversion of defect sites on CNTs. These defect sites are intentionally produced as a result of oxidation treatment by strong acids such as H_2SO_4, HNO_3 or a mixture of them with the purpose of purification, cutting or just functionalization [70]. These oxidant-induced sites are further stabilized with functional groups such as carboxylic acid (-COOH), hydroxyl (-OH), ketone and ester groups. COOH group-attached CNTs are the most prevalent type of amongst others owing to having higher reactivity and inherent multi-functionality towards chemical reactions in which acted as precursors for further treatment such as esterification, thiolation, alkylation, and polymer grafting. Chen et al. reported the first acylation-amidation process [71]. In this study, COOH-terminated shortened SWCNTs first reacted with acyl chloride, then subsequent treatment of octadecylamine (ODA) took place and as a result zwitterion-functionalized SWCNTs were obtained. The purpose of using long chain ODA is to facilitate the dissolution

of SWCNT in the common organic solvents. The proposed reaction is depicted in Figure 2.11 and ODA group is shown in red circle.

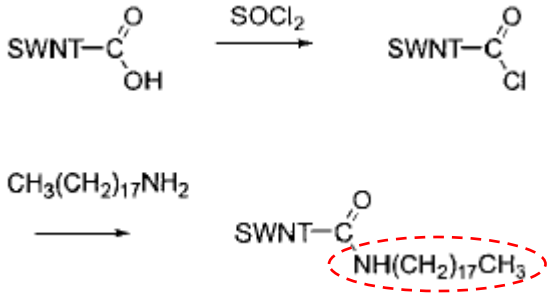

Figure 2.11: The proposed reaction between COOH-bound SWCNT with ODA [71].

In another study, same procedure was employed for the functionalization of nanotubes but in that case with the purpose of separating the metallic and semiconducting SWCNTs with gel-permeation chromatography (GPC) [72].

On the other hand, sidewall functionalization is another approach recently grown attention for studying the effect of CNTs inclusion on membrane performance. Qui et al. [66] reported the results on blending of PSf membranes with varying fractions of functionalized MWCNTs incorporated into membrane and fabricated by phase-inversion method. Carboxylated MWCNTs were functionalized by 5-isocyanato-isophthaloyl chloride (ICIC) groups as shown in Figure 2.12.

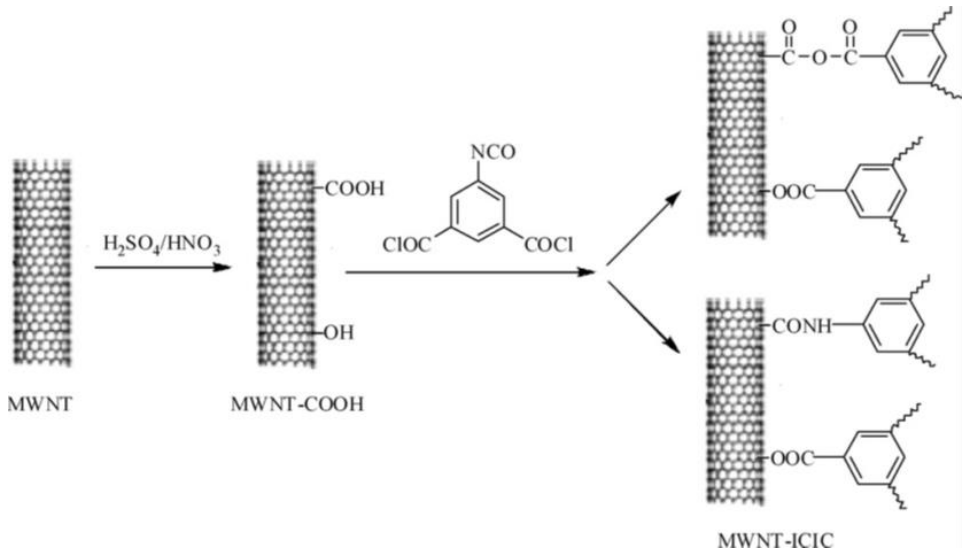

Figure 2.12: The synthesis of modified MWCNT-ICIC [66].

The amount of the functionalized CNTs was the major factor effecting the water flux and resultant morphology of the membrane. Regarding the permeation evaluation of

novel membranes, the pure water flux increased with the increment of the amount of CNTs up to 0.19% wt. The suggested explanation for water flux reduction after 0.19% wt. loading of CNTs was that the porosity of the membrane could be decreased because of high density of nanotubes in membrane and yielding decline in water permeation. Indeed, this explanation was in a good agreement with the average pore size measurements indicating the pore size reduction after 0.19% wt. MWCNT loading.

One of the promising approaches of employing CNTs in desalination technology is inclusion of this novel material into the selective PA layer of TFC membranes. A patent has been disclosed by Ratto et al. [73] defining the addition of CNTs with narrow diameter of approximately 0.8 nm into the PA layer by interfacial polymerization technique on a microporous support. The cross-sectional structure of TFC membrane with embedded CNTs into the selective layer is represented in Figure 2.13. Random orientation of CNTs throughout the polymer matrix offers channels for water passing through. The existence of these exceptional channels for the water transport yielded nearly two-fold increase in water permeation when compared with the membranes without containing CNTs in company with slight increment in the salt rejection from 96.2 to 97.7% [64].

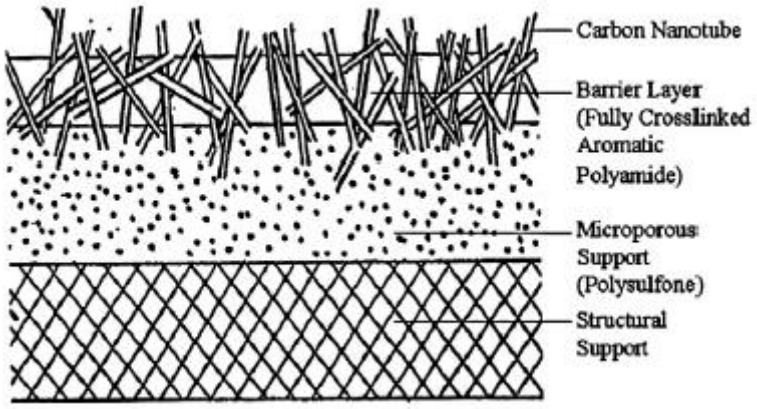

Figure 2.13: The cross-sectional structure of embedded CNTs into the selective layer of TFC membrane [64].

A more comprehensive research concerning the use of CNTs in the membrane field has been conducted by Chan et al focusing on incorporation of the zwitterion functionalized CNTs into the polyamide selective layer and evaluating their permeation tests [63]. It was assumed that the use of chain-like zwitterion groups -COO-$(CH_2)_3$-$N^+(CH_3)_2$-$(CH_2)_2COO^-$ at the open ends of CNTs caused to obtain

improved rejection of not only positive ions but also negative ones more effectively compared to CNTs functionalized with singly charged groups. These bulky groups acted as gate-keeper and narrowed the openings of the CNTs. They incorporated CNTs into PA selective layer by employing a high-vacuum filtration during membrane fabrication and as a result, partial alignment of CNTs was achieved. From the data obtained, the water flux increased by more than a factor of 4 as the CNT portion was varied from 0 to 20% wt. Furthermore, these improved permeability values were obtained without sacrificing from the selectivity of the membrane, which was also increased from 97.6% to 98.6%.

Table 2.4 lists a summary of thin film nanocomposite membranes; including the nanofiller properties, the IP reaction conditions, and the performance of the resultant membrane in a chronological order.

Table 2.4: Summary of thin film nanocomposite membranes prepared with CNT.

TFN		Particle Size	Aqueous Phase	Organic Phase	Loading wt%	Method	Application	Performance & Properties	Published year and Reference
Nanofiller	Polymer								
Carboxylic MWCNTs	Polyester	OD < 8 nm, L=10-30 μm	6% (w/v) TEOA in water	0.6% (w/v) TMC in hexane	0.05% w/v in aqueous phase	Modified IP O/A/O	NF	Improved water flux and salt rejection. Immersion of substrate into organic phase before IP improved TFN performance	2010 [14]
MWCNTs	PA	OD=9-12 nm L=10-15 μm	2% (w/v) MPD	0.1% (w/v) TMC	0.1, 0.5, 1.0, 5.0% w/v in aqueous phase	IP	RO	Enhanced chlorine resistance. Addition of surfactant facilitated the MWCNT dispersion.	2010 [74]
Functionalized MWCNTs	PA	OD=~30 nm L_1=10-30 μm L_2= 0.5-2.0 μm	0.5 wt % PEI in water	0.7 wt % IPD in xylene	0.01-0.06% wt in aqueous or organic phase	IP	NF	Improved water flux. Transport corridor between CNT and polymer chains provide a low-resistance solvent pathway	2011 [60]
Oxidized MWCNTs	PA	-	2% (w/v) MPD	0.2% (w/v) TMC	0.005-0.2% (w/v) in aqueous phase	IP	RO	Enhanced water flux due to increased surface hydrophilicity; decreased salt rejection.	2011 [59]
Zwitterion functionalized CNTs	PA	OD=1.5 nm L= 1 μm	2 wt% MPD	0.5 wt% TMC	9 and 20 wt% of PA	Deposition + IP	RO	Both water flux and salt rejection are increased.	2013 [63]

Table 2.4 (continued): Summary of thin film nanocomposite membranes prepared with CNT.

TFN		Particle Size	Aqueous Phase	Organic Phase	Loading wt%	Method	Application	Performance & Properties	Published year and Reference
Nanofiller	Polymer								
Carboxylic MWCNTs	PA	OD < 8 nm, L=10-30 μm	2 wt% MPD	0.15 wt% TMC	3 mg per membrane sample	Deposition + IP	RO	High water flux and fairly good salt rejection were obtained. Increased biofouling resistance under electrical potential	2013 [75]
PMMA modified MWCNTs	PA	OD=20-30 nm L< 50 μm	2 g/L PIP	4 g/L TMC	0-5.4 g/L in aqueous phase	IP	NF	Both increased water flux and salt rejection were achieved.	2013 [61]
Carboxylic MWCNTs	PA	OD < 8 nm L=10-30 μm	60 mg/mL TEOA	6 mg/mL TMC	0.2-2.0 mg/mL in aqueous phase	Modified IP O/A/O	NF	Optimum water flux with fairly good salt rejection > 70 % value.	2013 [62]
Amine functionalized MWCNTs	PA	OD= ~5 nm L_1= ~50 μm	1 wt% MPD	0.1 wt% TMC	0.01, 0.05, 0.1 % in aqueous phase	IP	FO	High water permeability with acceptable salt rejection. Hydrophilicity increases with CNT amount.	2013 [76]
Aluminosilicate SWNT	PA	OD= ~ 2.7 nm L=150 nm	2% (w/v) MPD	0.1% (w/v) TMC	0.05, 0.1, 0.2 % (w/v) in organic phase	IP	Low Pressure RO	Enhanced water permeation and high salt rejection were achieved.	2013 [77]
Carboxylic MWCNTs	PA	OD=20-40 nm L= 1-5 μm	2% (w/v) MPD	0.1% (w/v) TMC	0.001, 0.01, 0.1 wt% in aqueous phase	IP	RO	Increased water flux with increasing CNT loading, without sacrificing salt rejection. Better antifouling properties.	2014 [78]

Table 2.4 (continued): Summary of thin film nanocomposite membranes prepared with CNT.

TFN		Particle Size	Aqueous Phase	Organic Phase	Loading wt%	Method	Application	Performance & Properties	Published year and Reference
Nanofiller	Polymer								
Oxidized MWCNTs	PES	OD=10-15 nm	2 wt% MPD	0.15 wt% TMC	0.5 wt% in dope solution	Phase inversion	RO	Enhanced water permeability, due to the increased hydrophilicity. Better fouling resistance.	2015 [68]
Zwitterion functionalized CNTs	PA	OD= ~15 nm L= 10 µm	2 wt% PIP	0.06 wt% TMC	0.025, 0.1, 0.2 wt% in aqueous phase	IP	RO	1-fold higher permeability and more than 5-10 times larger fluxes in modules than pristine membrane.	2015 [79]
Oxidized MWCNTs	PES	OD=10-15 nm	2 wt% MPD	2 wt% MPD	2 wt% MPD	Phase inversion	PRO	Increased water flux due to CNT-induced porosity and hydrophilicity of the support layer.	2016 [80]

3. EXPERIMENTAL

3.1 Materials

All the chemicals were analytical grade. Suppliers and product codes of chemicals are listed in Table 3.1. Chemicals were used without extra purification.

Table 3.1: List of suppliers and product codes of chemicals used.

Chemical Name	Specifications	Supplier (Brand)	Code
Polysulfone (PSf)	Mw= 50,000	Sigma-Aldrich	374296
1-Methyl-2-pyrrolidone (NMP)	≥ 99.5 %	Merck	806072
Polyvinylpyrrolidone (PVP)	Mw= 10,000	Sigma-Aldrich	856452
2-Propanol (IPA)	98 %	Riedel-de Haen	121286
Methanol (MeOH)	≥ 99.9 %	Merck	106009
m-Phenylenediamine (MPD)	Flakes, 99 %	Sigma-Aldrich	P23954
Triethylamine (TEA)	Puriss. ≥99.5 %	Sigma-Aldrich	90340
Trimesoyl chloride (TMC)	98%	Sigma-Aldrich	147532
n-Hexane	≥ 95.0 %	Merck	104368
-COOH Functionalized SWCNT	Inner d= 0.8-1.6 nm Length= 1-3 μm	Nanografi	-
Sodium chloride (NaCl)	≥ 99.5 %	Merck	M106404
Sodium dodecylbenzenesulfonate (SDBS)	Technical grade	Sigma-Aldrich	289957

3.2 Fabrication of Polysulfone Support Membrane

3.2.1 Preparation of PSf membranes without additives

PSf microporous support membranes were fabricated via phase inversion method described in Section 2.7.3 in which a polymer dope solution is cast and immersed in a non-solvent bath for forming the desired porous structure. As a first attempt, the dope solution was prepared simply mixing the polymer and the solvent with varying concentrations. Two different non-solvents were employed as a coagulation bath to

achieve porous structure. PSf concentrations, solvent ratio, and coagulation baths are listed in Table 3.2.

Table 3.2: Dope formulation and coagulation baths used to prepare different types of support membranes.

Substrate	Dope formulation (wt.%)		Coagulation Bath (Non-solvent)		Temperature (°C)
	PSf	NMP	24 hours	8 hours	
*PSf-1	15	85	-	-	16
PSf-2	15	85	H_2O	MeOH	26
PSf-3	15	85	20%NMP+80% H_2O	MeOH	24
PSf-4	15	85	IPA	MeOH	24
PSf-5	15	85	IPA	MeOH	16

*PSf-1 was immersed in water bath just for about 10 min, then drying procedure was applied.

The PSf beads were dried at 60°C for 24 h before use to remove the adsorbed water. The certain amount of PSf was dissolved in the solvent, as described in Table 3.2. Then, the dope solutions were stirred with magnetic stirrer at 60°C for 24 h in order to obtain homogeneous solutions. Before casting the membranes, the solutions were sonicated in an ultrasonic bath for approximately 10 min to ensure there is no air bubble left in the solutions.

Flat sheet membranes were prepared via casting the prepared dope solutions on a glass substrate. The laboratory scaled automatic film applicator machine with a casting knife (Sheen branded) was utilized to cast the membranes at a constant velocity of 100mm/s. The air knife was set to a fixed thickness, which was 150 μm. The relative humidity and temperature values were 65% and 16°C, respectively. Then, the cast membranes were immediately immersed in coagulation bath at room temperature. Typically, water is used as a non-solvent in precipitation medium, but in this experiment, IPA was also employed. Polymer film coated glass was kept in coagulation bath for formation of the characteristics membrane structure until the film was pulled away from the glass substrate. Afterwards, the membranes were transformed into a clean medium filled with the corresponding coagulation bath composition and kept in for 24 h. Next, membranes were placed in methanol bath for 8 hours. This procedure was followed for all of the substrates, except the first one (PSf-1) which was immersed in water and precipitated until the cast film was come

off from the glass substrate. It took approximately 10 min to completely come off from the glass surface and without applying 24-hour coagulation bath treatment, the membrane was directly kept at atmospheric conditions. Following drying procedure was employed prior to SEM analysis: the formed membranes were left at ambient conditions for 24 h, then placed in an oven at 40°C for 24 h for drying and removing all the solvent residues. Finally, PSf membranes were kept in deionized (DI) water and stored at 4°C laboratory refrigerator for preventing from the biological growth.

3.2.2 Effect of pore forming agent on substrate characteristics

In order to obtain porous structure and to increase hydrophilicity of the PSf membranes, pore-former agents are added to the dope solution [37, 22, 81]. In literature, PVP is the most widely used one, thus we have decided to use PVP as the pore-former agent in varying concentrations. Dope solution compositions are listed in Table 3.3.

Table 3.3: Dope formulation with varying PVP compositions used to prepare different types of substrates.

Substrate	Dope formulation (wt. %)			Coagulation Bath	
	PSf	NMP	PVP	Non-solvent	Temperature (°C)
PSf-6	15	83	2	IPA	16
PSf-7	15	80	5	IPA	16
PSf-8	15	75	10	IPA	16

Specific amount of PVP was dissolved in NMP first, then PSf was added slowly, and dope solution was kept stirring for 24 h at 60°C. Then, solution was placed on a roller mixer for 48 h. Following 10 min ultrasonication produced well-dissolved and air bubble-freed dope solutions.

PVP-added dope solutions were cast exactly as described in previous section. Specific volume of polymer solution was poured on a glass surface and casting knife was drawn. The cast film was immediately immersed in coagulation bath containing IPA. Upon separation of film from glass surface was obtained, the membrane was placed in a clean IPA bath for 24 h. Then, the 8-hour MeOH bath was employed, before storing in DI water at 4°C in refrigerator. These UF membranes were dried only prior to characterization analyses as described in previous section.

3.2.3 Effect of coagulation bath temperature on substrate characteristics

Cold and hot precipitation media were used in order to investigate the effect of non-solvent temperature on membrane characteristics and porosity. Table 3.4 represents the dope compositions dipped into cold quench baths. The fabrication procedure was same as described previous section, the only difference was the temperature of the coagulation baths.

Table 3.4: Dope formulations of membranes by means of immersion in precipitation medium with varying temperatures.

Substrate	Dope formulation (wt. %)			Coagulation Bath	
	PSf	NMP	PVP	Non-solvent	Temperature (°C)
PSf-9	15	83	2	H_2O	7
PSf-10	15	83	2	40%IPA +60%H_2O	25
PSf-11	15	83	2	IPA	7
PSf-12	15	80	5	IPA	24
PSf-13	15	75	10	IPA	24

3.2.4 Effect of evaporation time on substrate characteristics

So far, different approaches have been employed to achieve porous structure and uniform pore distribution in PSf support membranes such as using IPA instead of water as precipitation medium, addition of pore-former to dope solution, and decreasing the coagulation bath temperature. In all above-mentioned approaches, the cast film was immediately immersed into the quench bath without applying specific evaporation time. However, the exposure time of cast film to the atmospheric conditions does affect the membrane structure, especially has significant impact on formation of skin layer on the membrane surface, which is a major drawback in fabrication of TFC membranes. In order to investigate the effect of exposure time to the atmospheric conditions, three different evaporation times were applied on the cast film before immersion to the coagulation bath. Dope formulations and evaporation times are listed in Table 3.5.

Same membrane fabrication procedure was employed with additional aspect, which was the cast film was exposed to ambient conditions for a definite amount of time before immersion into the coagulation bath.

Table 3.5: Dope formulations used to prepare different types of membranes with varying evaporation times.

Substrate	Dope formulation (wt. %)			Evaporation time (sec)	Coagulation Bath	
	PSf	NMP	PVP		Non-solvent	T (°C)
PSf-14	15	83	2	20	IPA	11
PSf-15	15	83	2	40	IPA	8
PSf-16	15	83	2	60	IPA	11
PSf-17	15	80	5	40	IPA	13

3.3 Fabrication of Thin Film Composite RO Membrane

Owing to the sensitivity of the interfacial polymerization (IP) of polyamide (PA) layer to the operating condition and reaction time, various recipes have been developed. The procedures vary in terms of monomers concentration, reaction time, air-drying time, curing temperature, etc. [63]. TFC membranes were prepared via in-situ IP method as result of the reaction between MPD and TMC as described in Figure 2.7, in Section 2.7.4 Two different solutions were prepared being aqueous and organic solution corresponding to MPD and TMC, respectively. 0.50 g of MPD and 690 µl of trimethylamine (TEA) were added to 25 ml of DI water to obtain 2 wt.% diamine solution. The solution was stirred for 10 min. Meanwhile, 0.015 g of TMC was mixed with 20 ml of n-hexane under continuous stirring for 10 min. Resultant solution was 0.07 wt. % in terms of TMC composition.

Initially, the PSf support was washed with DI water thoroughly and rolled with a rubber roller to remove the water from the surface. Then, the substrate was clamped on a glass plate with a frame. 2 wt.% of MPD was poured on the top of the PSf support for 15 s. Next, the solution was discarded and excess amount of MPD was removed by rolling a rubber roller over the membrane surface once. The membrane was clamped back for the next step, which was the introduction of TMC in hexane solution for 15 s. After removing the frame, heat-curing was applied at 68°C in an air-circulating oven for 10 min. Finally, the interfacially polymerized TFC membrane was stored in DI water at 4°C in the laboratory refrigerator before carrying out evaluation studies. A thin selective PA layer was formed at the interface of the two reactive monomers. The properties of PSf substrate, MPD concentration, and the reaction time between MPD and TMC are listed in Table 3.6. Representative picture of TFC membrane process is shown in Figure 3.1.

Table 3.6: The properties of PSf substrate and IP process conditions.

TFC Substrate	PSf Support Properties		MPD (wt.%)	TMC (wt %)	Reaction time (s)
	PVP (wt.%)	Evaporation time (s)			
TFC-1	2	40	2	0.07	15
TFC-2	5	40	2	0.07	15
TFC-3	5	40	2	0.07	30
TFC-4	2	40	4	0.07	15
TFC-5	10	0	2	0.07	15
TFC-6	Commercial PES membrane		2	0.07	15

Figure 3.1: TFC membrane preparation process.

3.4 Fabrication of Thin Film Nanocomposite RO Membrane

As a first sample, 0.05 mg of commercial carboxylated SWCNT were weighed and mixed with 10 mg of sodium dodecylbenzenesulfonate (SDBS) in 40 ml of water and sonicated for 30 mins by a sonication horn. Figure 3.2 shows the ultrasonic horn and the CNT mixtrure.

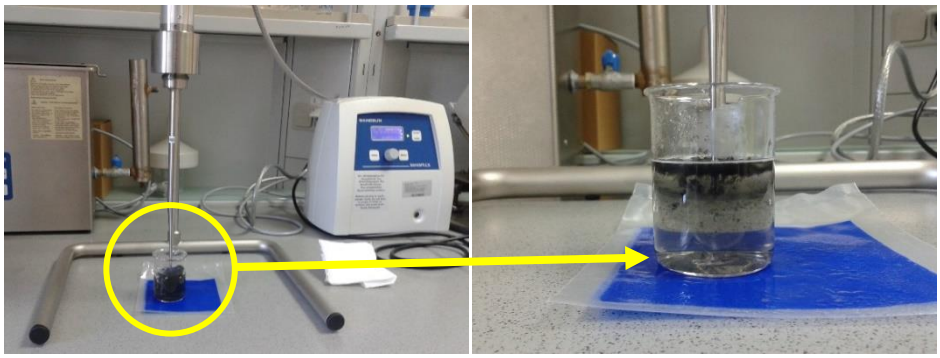

Figure 3.2: The ultrasonic horn and the CNT mixtrure.

After sonication, the support membrane was cut approximately 50 mm diameter and was placed on top of the filtration system (Merck Millipore). The selected support membrane was PSf-8 which contains 10 wt.% PVP and immersed in cold IPA. Then,

the CNT mixture was poured on top of the membrane. During the filtration a pump was used for the filtration and deposition of CNT; as the CNT being pulled by the vacuum the alignment of them was taken place. The experimental set-up is depicted in Figure 3.3.

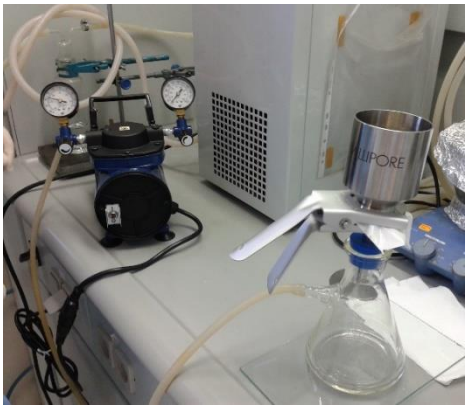

Figure 3.3: The experimental set-up for CNT alignment.

The CNT-deposited substrate dried in an oven under 100mbar vacuum at room temperature for 1 hour. Then, IP process was carried out on top of the CNT-deposited PSf substrate. First, MPD solution was introduced for 15 s, then excess solution were removed by rolling the rubber roller. After that, TMC was poured on top and allowed to react for 15 s. The resultant TFN membrane was dried in oven at 68°C for 10 min and placed in DI water in the refrigerator. Figure 3.4 shows the picture of CNT/PSf TFN membrane.

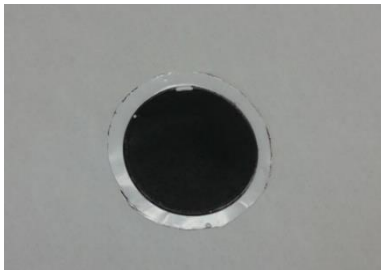

Figure 3.4: The picture of CNT/PSf TFN membrane.

3.5 Characterization of Fabricated Membranes

3.5.1 Scanning electron microscopy

The surface properties of the fabricated membranes were analyzed in Quanta Feg250 model FESEM device manufactured by FEI Company. Since the membranes were stored in water at 4°C in refrigerator, they dried for a one day at atmospheric

conditions before SEM analysis. Samples were cut in small pieces and coated with gold and palladium to obtain the conductivity requiring for SEM measurements. For cross-section images, the samples were fractured in liquid nitrogen.

3.5.2 Contact angle measurements

Hydrophilicity or hydrophobicity of the PSf substrate has a significant impact on TFC characteristics in terms of effecting PA layer, and consequently affects the performance of the resultant membrane. The contact angle measurements were carried out by using theta contact angle device manufacture by KSV CAM200 via employing the sessile drop technique. All membrane samples were kept under same conditions and analyzed in same way so that to eliminate all the systematic errors sourced from storage conditions that can disrupt the results rather than membrane own characteristics. For every membrane sample, at least three trials at different locations were done in order to results for reflecting good representatives of the samples and to indicate the standard deviation values as well.

3.5.3 Membrane performance tests

The performance evaluations of the fabricated membranes were studied using the setup built in the lab. Figure 3.5 represents the schematic of the water permeation setup.

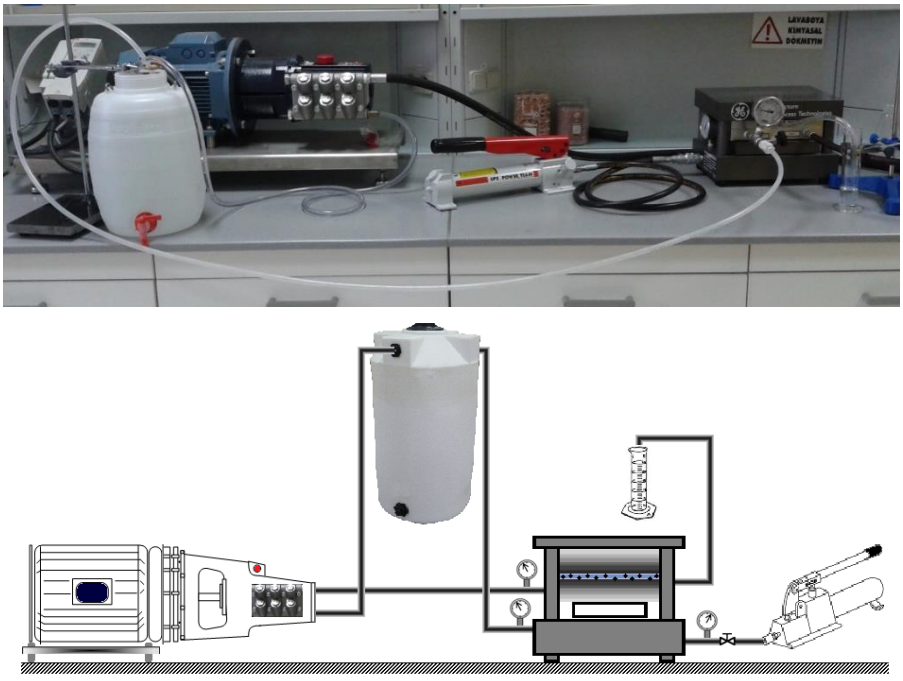

Figure 3.5: Schematic diagram of lab-scale cross-flow water permeation cell.

The permeation tests of the membranes were carried out in GE Osmonics Sepa^{TM} CF Cell cross-flow membrane test system shown schematically in Figure 3.5. The system consists of a stainless steel membrane cell, a high-pressure pump (Hydra-Cell 70 bar pump), a hand pump (Sepa System) and a feed tank. A known amount of permeant was collected in a beaker placed on a mass balance (Radwag branded) within a given period of time. The concentrate was recycled back to the feed tank. Figure 3.6 shows the cell body of the system.

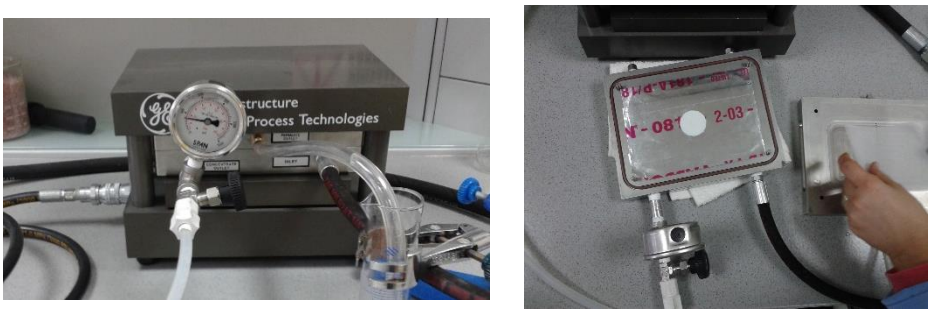

Figure 3.6: Pictures showing the GE Sepa^{TM} CF Cell-Body and placing a masked membrane sample into cell-body for performance evaluation.

Figure 3.7 represents membrane samples were masked with using aluminum foil duct tape in order to fit the large area of the test cell, which are shown in Figure 3.6. The masked membrane was placed inside the testing cell. The synthesize membranes had varying area values such as ranging from 3.0 cm^2 to 20 cm^2.

Figure 3.7: Pictures of a TFC and a CNT/TFN membrane masked with Al tape.

The pure water flux and salt rejection values of synthesized TFC membranes were tested under the standard testing conditions at which the transmembrane pressure for water flux and concentration of the feed solution were approximately 15.5 bar (225 psi) and 2000 ppm NaCl (34.18 mM NaCl) solution, respectively. The circulation flow rate was set to 0.37 m/s. At first, pure water flux values of the membranes were measured and data collected for at least 3 hours. The flow rate and flux calculations were done after the system had reached steady state conditions, which was around 30 min. Because of the permeate was collected on a balance in terms of grams, the

density of the water was taken to be 0.997 g/cm^2 for the calculation of the volumetric flow rate from the equation (3.1);

$$Q = \frac{\Delta V}{t \cdot A} \tag{3.1}$$

where ΔV is the permeant volume in liter, t is the permeation time in hours and A is the area of the membrane in m^2, hence the flow rate, Q, was reported in the units of liter per square meter per hour (LMH). On the other hand, a conductometer (WTW, Cond 7110) was used for determination of the salt concentration, in which was calibrated with 0.1 KCl standard solution having a known conductance.

Salt rejection value (R) was calculated from the reduction in the conductance of permeate according to the equation (3.2); where C_p represents the conductance of the cation in the permeate, and C_f in the feed.

$$R(\%) = \left(1 - \frac{C_p}{C_f}\right) \times 100 \tag{3.2}$$

4. RESULTS & DISCUSSIONS

4.1 Morphology of PSf Support Membranes

FESEM analysis was used for the structural and cross-sectional morphology, while contact angle analysis was employed for the determination of hydrophilicity of the surface properties of the prepared PSf substrates.

4.1.1 FESEM analysis

4.1.1.1 Effect of non-solvent type

Figure 4.1 presents the FESEM images of top surfaces of each PSf support membrane made of dope solution containing just polymer and solvent without addition of any modifiers. Due to the atmospheric conditions have significant impact on the film formation such as temperature and relative humidity of the medium; all substrates were cast at the same conditions, which were recorded as 16°C and 65%, respectively. As described in Section 3.2.1 the cast films were immersed in various coagulation baths for 24 hours to complete the precipitation process and followed by 8-hour MeOH bath, except the first sample, PSf-1 which was prepared by immersing in water only for 5 minutes and stored in DI water at 4°C in refrigerator. The recipe of PSf-1 was taken from the literature [10].

As can be seen from the first two FESEM images in Figure 4.1 corresponding to PSf-1 substrate, the pores on the surface of the membrane were so small that they can be even negligible note that the magnification was set at 400,000x. When water was used as the coagulation bath, the membrane surface was smooth with no clear pores. After reviewing the literature for the pore formation thoroughly, following findings were obtained:

1. Keeping the cast film in the coagulation bath for 24 hours can help the completion of the precipitation process.

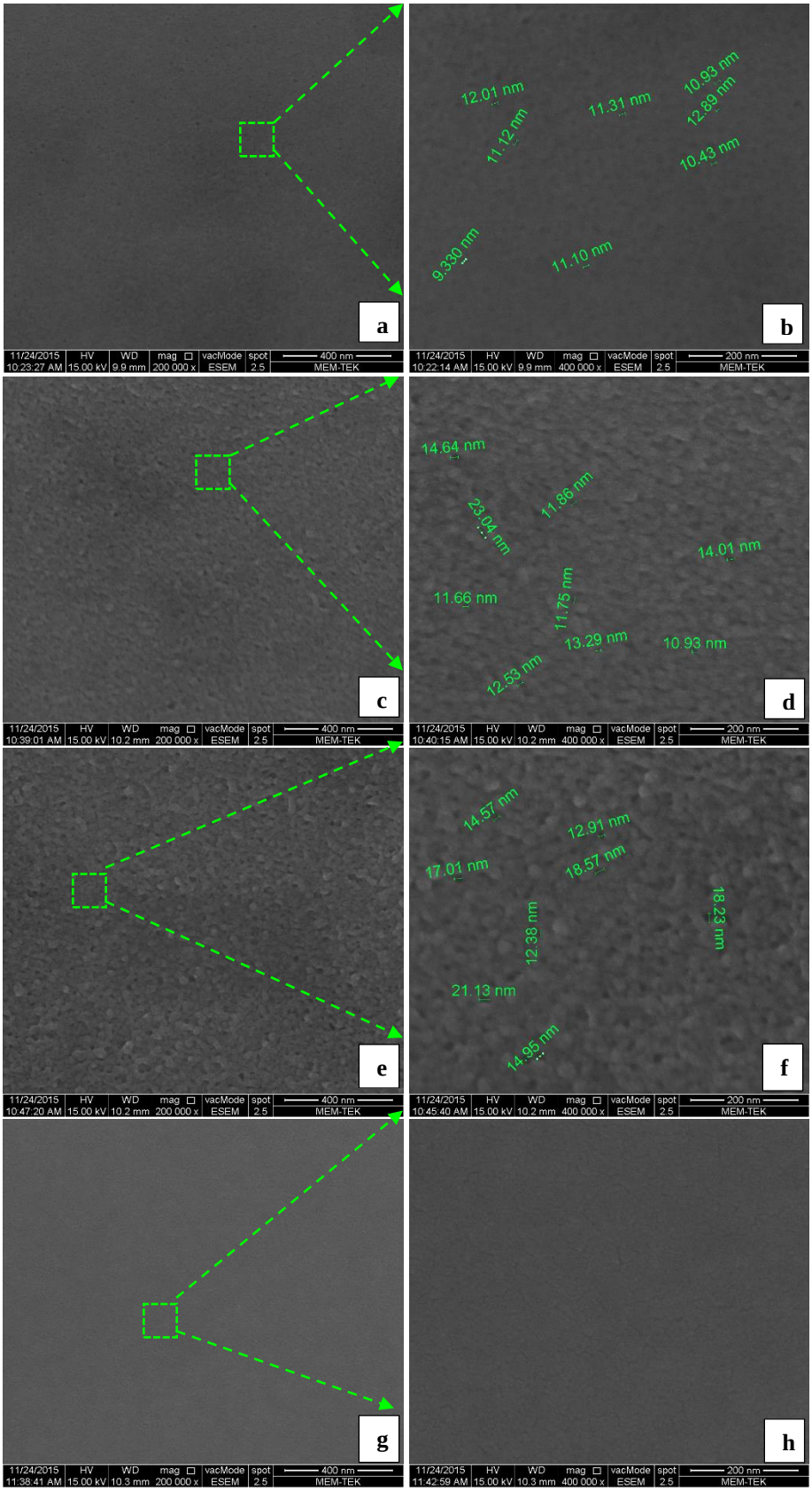

Figure 4.1: FESEM images of (a) and (b) PSf-1; (c) and (d) PSf-2; (e) and (f) PSf-3; (g) and (h) PSf-4; (i) and (k) PSf-5.

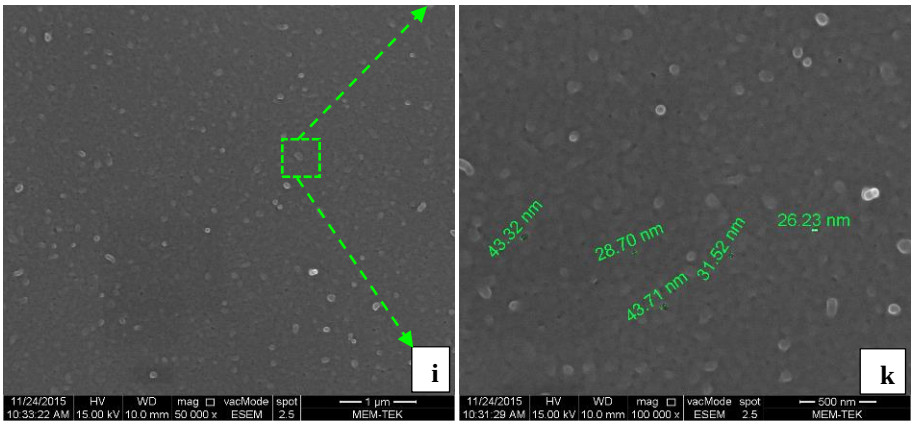

Figure 4.1 (continued): FESEM images of (a) and (b) PSf-1; (c) and (d) PSf-2; (e) and (f) PSf-3; (g) and (h) PSf-4; (i) and (k) PSf-5.

2. Decreasing the non-solvent quality by addition of the solvent to the coagulation bath can facilitate to alter the morphology from finger-like to the sponge-like structure [85]. The tendency for macrovoid formation can be reduced.

3. Using non-solvents rather than water in coagulation bath can lead to the formation of sponge-like structure. Bai et al. [86] reported that the use of a non-solvent containing hydroxyl group in the coagulation bath can accelerate the diffusion rate between solvent and non-solvent thus leading to the production of short finger-like pores with many macrovoids. According to the results they presented, the maximum acceleration in the diffusion rate was obtained in the case of using isopropanol (IPA) in the coagulation bath.

4. In another study, the choice of the solvent system and the non-solvent has significant effects on the structure formation of the resultant membrane [87]. They stated that Hansen solubility parameters of the selected polymer, solvent, and non-solvent should be close to each other as much as possible, which means that they are compatible with each other and good demixing can be obtained. They also reported that the use of inappropriate non-solvent for their polymer-solvent system caused swelling of the polymer. Table 4.1 lists Hansen solubility parameters for the used system in this study.

5. Employment of subsequent non-solvent mainly methanol can increase the formation of bigger sponge-like pores [86]. Figure 4.2 shows cross-sectional pictures of membranes indicating the difference between membrane immersed in water and a membrane placed in MeOH bath after immersion in water bath.

Table 4.1: Hansen solubility parameters for polymer, solvent, and non-solvents used in this study.

	Compound	δ [(MPa)$^{0.5}$]
Dope composition	PSf	23.7
	NMP	22.9
Non-solvent	Water	47.1
	IPA	23.6
	MeOH	29.7

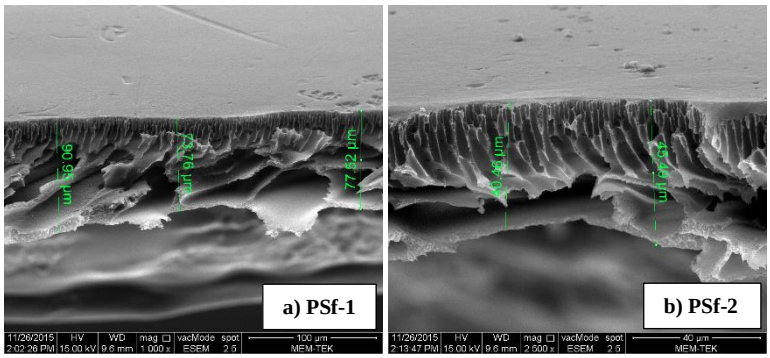

Figure 4.2: The cross-sectional images of membranes PSf-1 and PSf-2 indicating the use of subsequent 8-hour MeOH bath after coagulation bath.

PSf-1 sample was immersed in water for 5 min, while PSf-2 was kept in 8-hour MeOH bath after immersing a coagulation bath for 24 h. The major difference between two images is the thickness of the membrane. The thickness of PSf-1 is approximately 80 μm, while PSf-2 is around 45 μm. Furthermore, there is a clear distinction in cross-section of the membranes in terms of the structural formation of the sublayers just underneath the surface. The 5-min-water-precipitated membrane (PSf-1) has shapeless and bigger macrovoids close to the bottom, which will not withstand the high pressures of the RO process, compared to membrane kept in MeOH bath (PSf-2). On the other hand, both membrane type have a skin layer on top of the cast film indicating that either no pore or very small pore formation on the surface, which is a unfavorable situation for a UF membrane.

As can be seen from the Table 4.1, water is not a proper non-solvent for the PSf-NMP system in terms of comparing the solubility parameters, while IPA and MeOH can be appropriate choices due to having solubility values close to both polymer and solvent. FESEM images of PSf-2 (Figure 4.1, c and d) show slightly better surface property in terms of porosity. This insignificant change in the structure can be attributed to the use of MeOH bath, which was employed after coagulation in 24-

hour water bath. In addition to these, from the pictures of PSf-3 sample it is clearly observed that increasing the solvent content in the coagulation bath did not produce the desired porous structure. In the light of above-mentioned findings from the literature, we decided to use IPA as a non-solvent to obtain porous structure on the surface of the support membranes.

All the images showed no clear pore formation on the surface, except the last pictures representing PSf-5 that was immersed and kept at cold IPA bath. Interesting findings observed in PSf-4 and PSf-5 results, which were immersed in same non-solvent being in room temperature and cold IPA bath, respectively. FESEM pictures of PSf-5 substrate produced in cold IPA shows porous structure on the surface, while PSf-4 support precipitated in room temperature IPA did not yield any pore formation at all. On the other hand, it was obvious that the experimental procedure needed to be modified for further structural improvement.

4.1.1.2 Effect of pore forming agent

The effect of pore former agents was studied by adding three different PVP concentrations into the dope solutions. Figure 4.3 depicts the FESEM images of 2, 5, and 10 wt.% corresponding to PSf-6, PSf-7, and PSf-8, respectively.

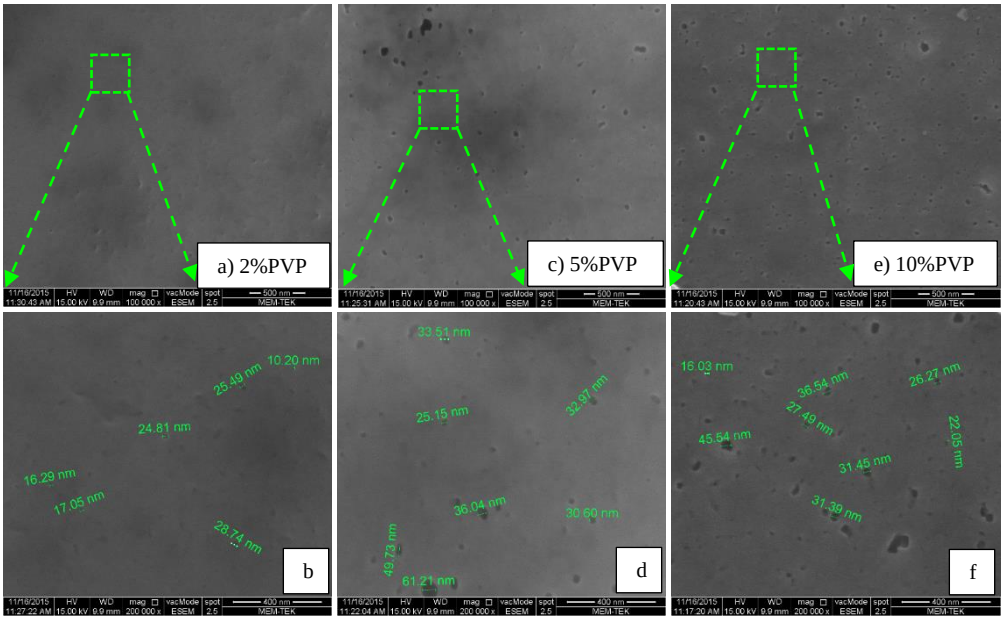

Figure 4.3: FESEM images of (a) and (b) PSf-6; (c) and (d) PSf-7; (e) and (f) PSf-8 containing 2, 5, 10 wt% PVP, respectively.

As can be seen from the images, addition of PVP did induce the pore formation. The average pore diameter obtained from addition of the three compositions

approximately same varying in the interval 25-40 nm, but the pore distribution shows dissimilarities. The pore size distribution follows an increasing trend which has reached its maximum value when PVP concentration was 10 wt.%. Results indicate that the addition of pore former agent induced the pore formation on the surface of the support. Due to relatively weaker affinity of the solvent, NMP, for IPA, homogeneous pore distribution and uniform-sized pores were obtained as result of slow coagulation [88].

Figure 4.4 shows the cross-section images of the PVP-added samples with a general overview and at a higher magnification for closer look to the structures.

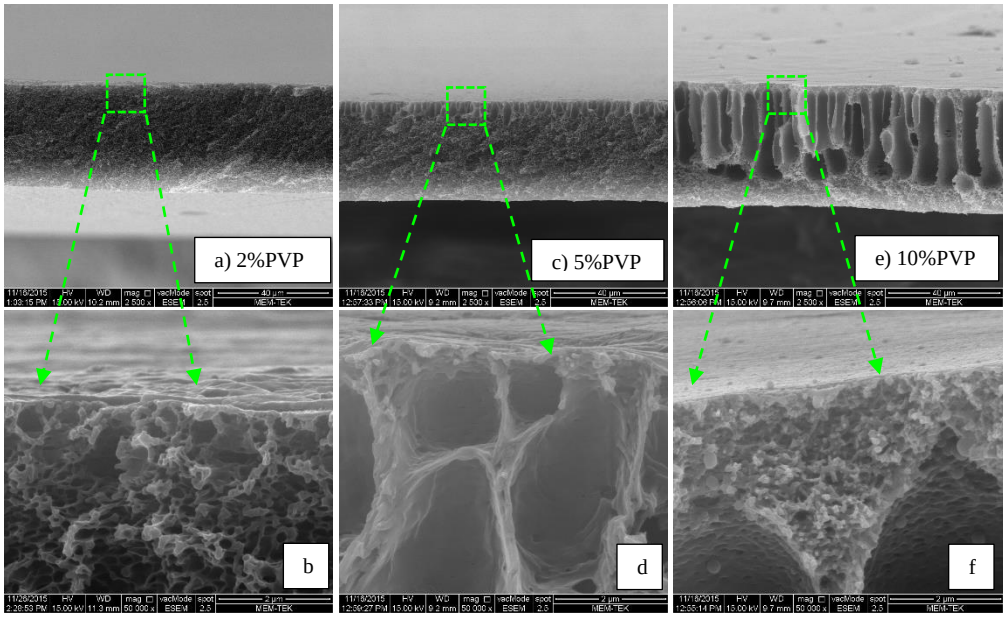

Figure 4.4: Cross-sectional images of (a) and (b) PSf-6; (c) and (d) PSf-7; (e) and (f) PSf-8 containing 2, 5, 10 wt% PVP, respectively.

Results showed that even though the pore sizes of the membranes showed similar behaviour the cross-sections of them were completely different. The use of 2 wt.% PVP resulted sponge-like structure in the entire cross-section of the substrate, whereas 5wt.% PVP produced macrovoids under the surface. On the other hand, a finger-like structure at the middle of the substrate cross-section was obtained with the use of 10 wt.% PVP. An increasing trend in the macrovoid formation was observed with increasing the PVP amount in the casting solution. This is mainly because of the effect of PVP on the pore formation [89]. Nevertheless, there are contradictory studies on the results of PVP addition to the membrane solution. On one hand, Wienk et al. [90] stated that the addition of pore forming additives suppress the macropore formation in the phase inversion membrane. On the other

hand, in another study Han et al. [89] reported that the macrovoid enlargements were induced by the addition of PVP in company with the substantial permeability increase of the membranes. In the present case, the latter study supported our results, thus the addition of PVP caused to form more finger-like structure with well-organized arrangements rather than shapeless channel-like configuration obtained from inverted in water.

4.1.1.3 Effect of coagulation bath temperature

Figure 4.5 represents the FESEM images of PSf-9, PSf-10, and PSf-11 supports (with higher magnification at bottom part) fabricated with the purpose of studying the effect of coagulation bath temperature on the morphology of the membranes.

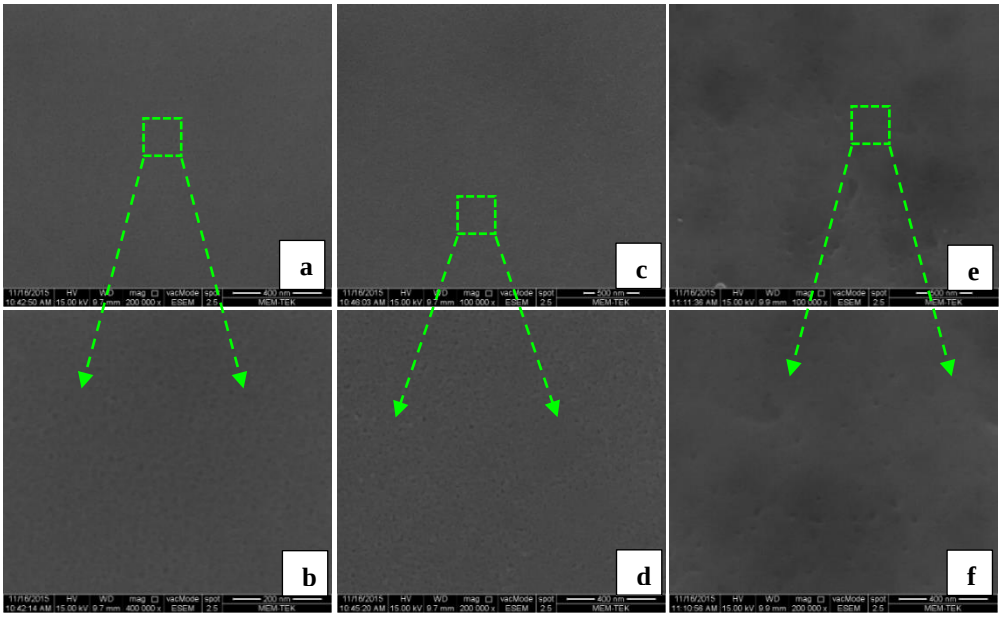

Figure 4.5: FESEM images of (a) and (b) PSf-9; (c) and (d) PSf-10; (e) and (f) PSf-11.

All the pictures in Figure 4.5 showed no clear pore formation on the surface. This may resulted from casting in different ambient conditions. Even though the use of 2wt.% PVP could not produce the pore formation on the surface.

To investigate the effect of different non-solvents with varying temperatures thoroughly, cross sectional micrographs were also taken. Figure 4.6 represents cross sectional image of PSf-9. Both surface and cross-section images proved that the use of water as coagulant caused to form a skin layer on top of the surface preventing the pore formation. These membranes were cast under same conditions: temperature was 16°C and at 65% relative humidity.

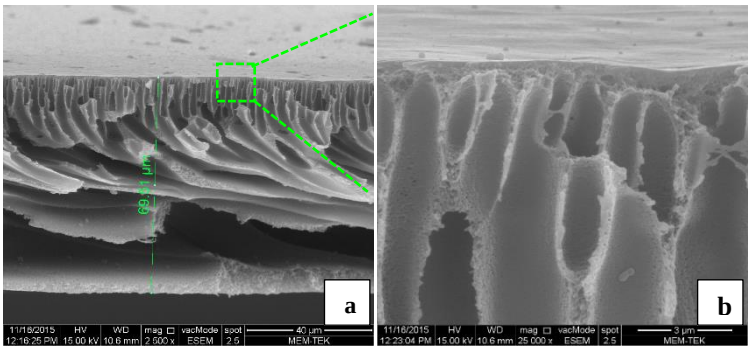

Figure 4.6: The cross-sectional image of PSf-9 prescipitated in cold water and formation of skin layer on top of the surface.

Figure 4.7 shows cross-sectional micrographs of PSf-10 and PSf-11 inverted in the system of 40%IPA+60% water and IPA, respectively. The structure of PSf-10 shows similarities with PSf-9 (Figure 4.6) in terms of general overview except the finger-like structures at the middle of the cross-section which has more well-ordered than water inverted counterpart. In addition, there was skin layer on the surface as well. These are mainly resulted from the rapid demixing phenomenon in the case of presence of water in the non-solvent indicating larger pore formation [88]. The higher affinity of NMP for water than IPA leads the formation of very thin top layer with many macrovoids underneath, which are mainly used in UF or hyperfiltration processes [91]. The mechanism behind is simple that owing to rapid precipitation takes place, there is not enough time for both movement of polymer chains and formation of a dense skin layer and a sublayer by aggregation. On the other hand, the image of PSf-11 shows a sponge-like structure with relatively thinner cross-section compared to water-inverted membranes. Sponge-like structure is indication of a slow coagulation process [88].

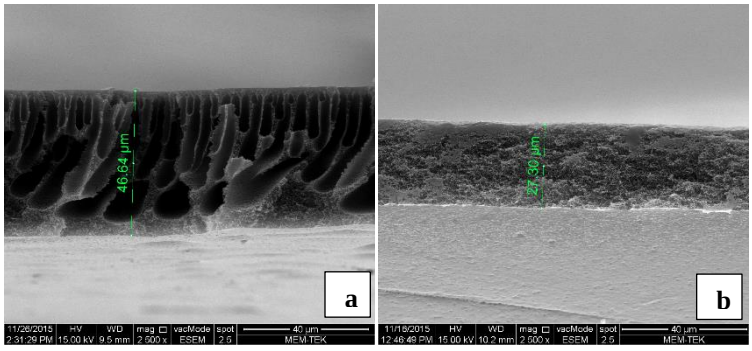

Figure 4.7: The cross-sectional micrographs of PSf-10 and PSf-11 inverted in the system of 40%IPA+60% water and IPA, respectively.

In order to visualize a more clear distinction, 5 wt.% PVP and 10 wt.% PVP containing substrates but inverted in either cold or room temperature IPA were compared. Figure 4.8 depicts the cross-sectional micrographs of PSf-7 and PSf-8 immersed in 16°C IPA, while PSf-12 and PSf-13 precipitated in 24°C IPA, either case both samples contain 5 wt.% PVP and 10 wt.% PVP.

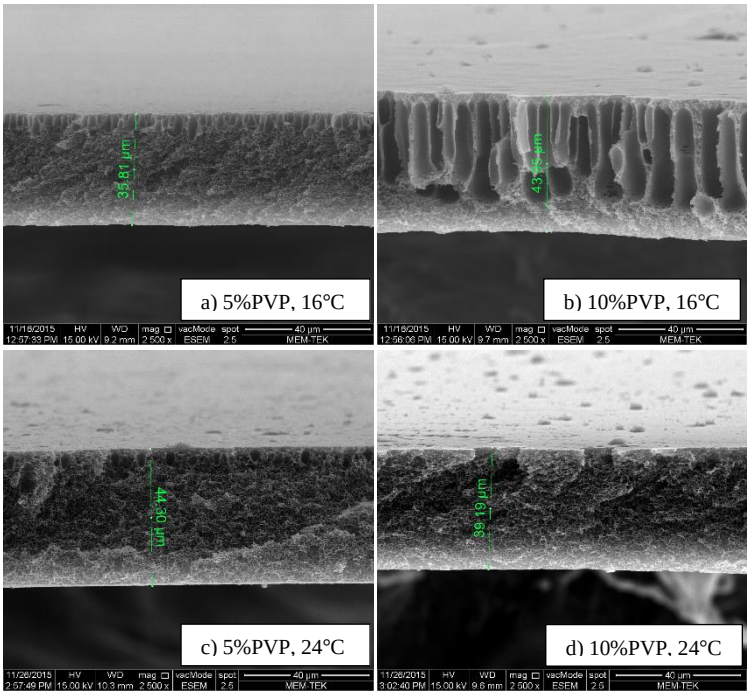

Figure 4.8: The cross-sectional micrographs of (a) PSf-7 and (b) PSf-8 immersed in 16°C; (c) PSf-12 and (d) PSf-13 precipitated in 24°C IPA.

Although, the membranes containing 5 wt.% PVP show similarities with precipitated in cold and room temperature IPA, the cross-section of 10 wt.% PVP membrane inverted in cold non-solvent shows a clear distinction from corresponding membrane precipitated in 24°C IPA. The substrate precipitated in room temperature IPA, which is indicated by PSf-13, is purely sponge-like with no clear macrovoids formation; while PSf-8 contains large macrovoids at the middle of the cross-sections sandwiched with sponge-like structure. It is noteworthy to mention that there is a formation of large pores at sublayer of the surface of PSf-7 comprised of 5 wt.% PVP, whereas corresponding sample PSf-12 contains relatively lower macrovoid density at the cross-section. The cross-sectional pictures indicate that cold non-solvent induced the formation of macrovoids that is the finger-like structure just under the top layer, whereas non-solvent used at room temperature led sponge-like sublayer independent of the PVP content. In the light of these results; as a non-

solvent, cold IPA can be selected over room temperature IPA for the fabrication of ultrafiltration PSf support membranes.

The corresponding surface micrographs of samples precipitated in room temperature IPA are shown in Figure 4.9. It can be seen clearly that there are pores on the surface. Despite the fact that the varying cross-sectional images between inversion in cold non-solvent and room temperature conditions, the surface morphology of these membranes show similarities in terms of pore formations and distributions (Figure 4.3 (c) and (e)).

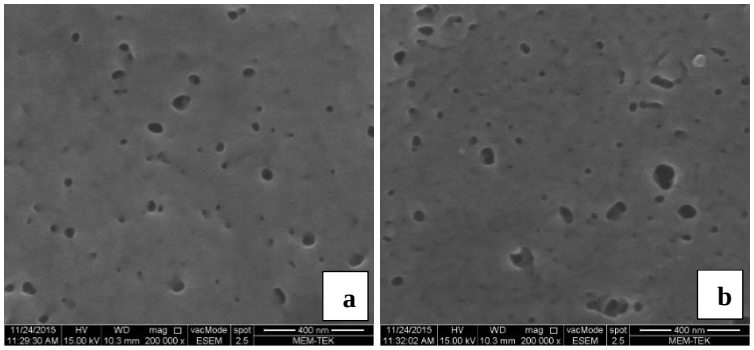

Figure 4.9: FESEM images of (a) PSf-12 and (b) PSf-13 containing 5 wt% and 10 wt.% PVP, respectively.

4.1.1.4 Effect of evaporation time

Besides the effect of coagulation bath temperature, the atmospheric conditions, such as temperature and the relative humidity, have significant effects on the membrane in terms of solvent evaporation. Figure 4.10 shows FESEM images corresponding to two sets of trials; prepared under summer and autumn conditions. Table 4.2 lists the details of the atmospheric conditions of the two sets of experiments.

Table 4.2: The atmospheric conditions of Group A and B.

	Group A	Group B
Temperature (°C)	16	~ 26
Relative Humidity (%)	65	~ 85

The properties of the membrane solutions and casting condition details were listed in Table 3.5, in Section 3.2.4 .

The most significant difference was observed in PSf-17 and PSf-17-1 substrates in terms of the pore sizes. Even though these samples were prepared in same compositions, the former membrane has pore size around 20-70 nm, while the latter

one has 250-400 nm. The main reason for this dissimilarity is the effect of atmospheric conditions on the film casting procedure.

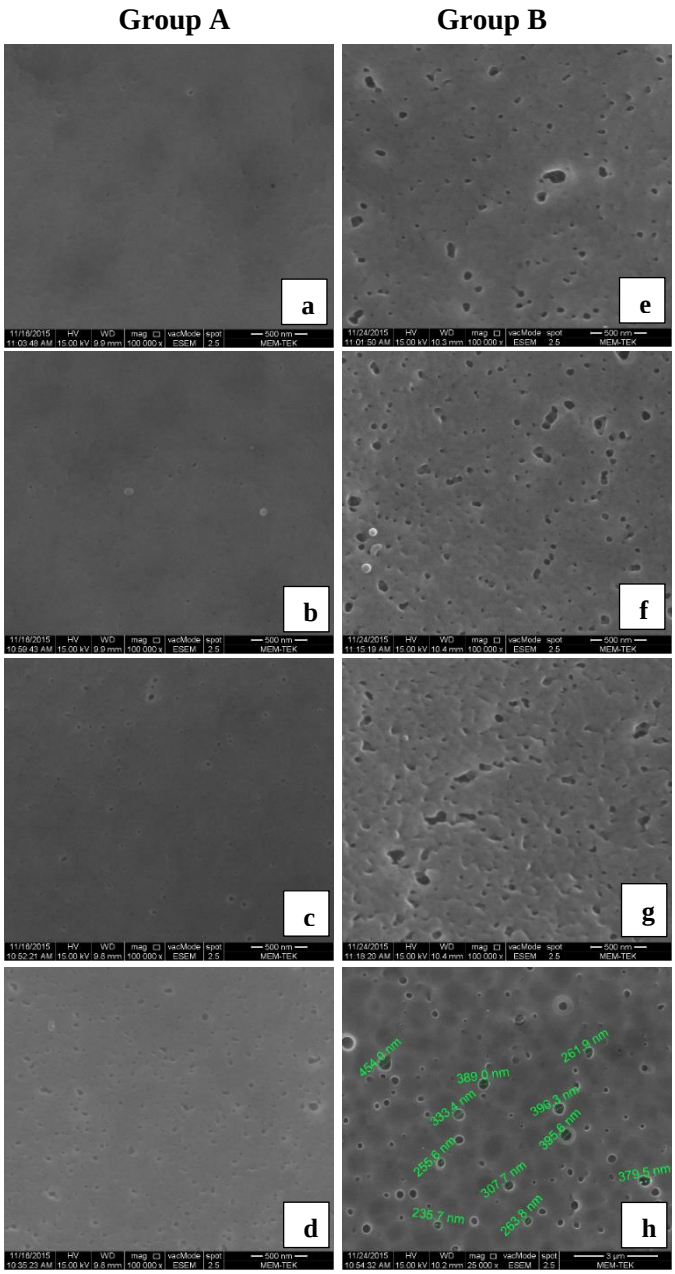

Figure 4.10: FESEM images corresponding to two sets of trials: a) PSf-14; b) PSf-15; c) PSf-16; d) PSf-17; e) PSf-14-1; f) PSf-15-1; g) PSf-16-1; h) PSf-17-1.

Figure 4.10 also represents varying evaporation times being 20s, 40s, and 60s as well as variation in PVP content. FESEM results show that more open pores and porous structures were obtained from group B experiments corresponding to relative warmer and higher humidity. On the other hand, Figure 4.10 (d) gave the best structure with good pore distribution and optimum pore sizes.

Table 4.3 lists the average pore sizes of all types of membranes and pore distribution relative to each other. It is noteworthy to emphasize that these results were drawn from FESEM images by visual inspection, thus indicate relative results to one another.

Table 4.3: Average pore size and pore distribution of the support membranes based on FESEM images.

Membrane Code	Average pore size	Pore distribution
PSf-1	No pore formation	-
PSf-2	~ 15 nm	Poor
PSf-3	~ 20 nm	Poor
PSf-4	No pore formation	-
PSf-5	~ 35 nm	Poor
PSf-6	~ 25 nm	Poor
PSf-7	~ 30 nm	Medium
PSf-8	~ 40 nm	High
PSf-9	No pore formation	-
PSf-10	No pore formation	-
PSf-11	~ 20 nm	Poor
PSf-12	~ 60 nm	High
PSf-13	~ 40 nm	High
PSf-14	~ 15 nm	Poor
PSf-15	~ 20 nm	Poor
PSf-16	~ 30 nm	Poor
PSf-17	~ 60 nm	High
PSf-14-1	~ 50 nm	High
PSf-15-1	~ 60 nm	High
PSf-16-1	~ 100 nm	High
PSf-17-1	~ 300 nm	High
PES	~ 20 nm	Poor

4.1.2 Contact angle results

Contact angle measurement is the most practical and the easiest way of determination the hydrophilicity and hydrophobicity of a species in terms of evaluating the wettability characteristics. The idea behind the concept of contact

angle is simple; on one hand, a contact angle greater than 90° representing the hydrophobic surface in which the interaction between surface and water droplet is so unfavorable that the fluid reduces its contact with the surface and produces a compact liquid droplet. On the other hand, contact angle smaller than 90° indicating a favorable interaction between surface and water droplet and as a result, the fluid spreads over a large area on the surface. The measured results of PSf substrates cast in different conditions and compositions are depicted in Figure 4.11.

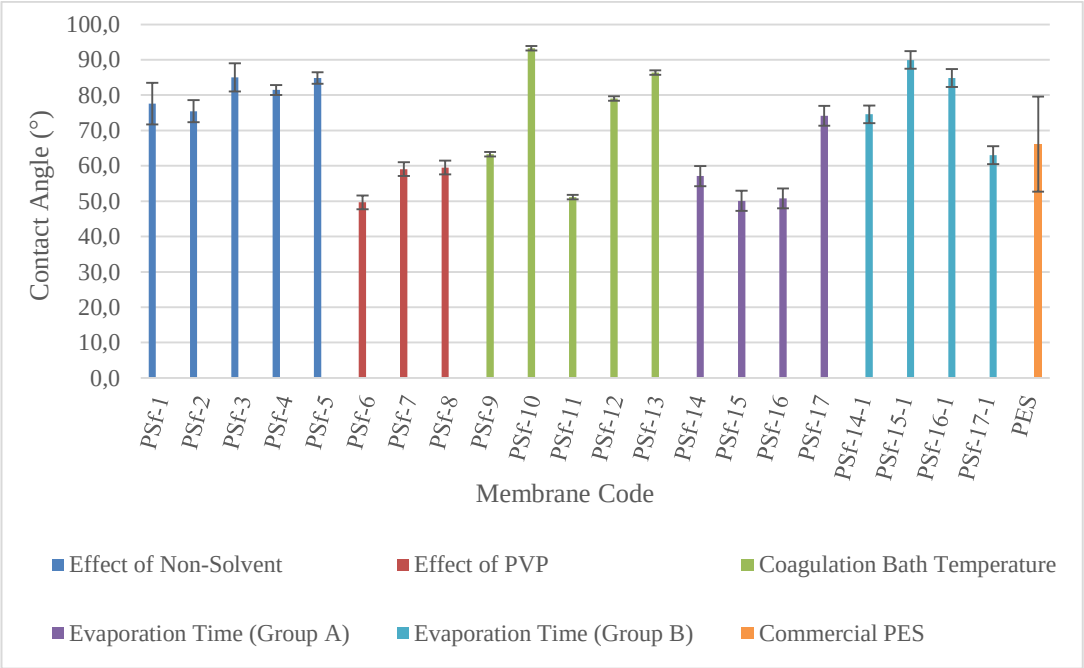

Figure 4.11: The measured contact angle results of PSf substrates cast in different conditions and compositions.

According to the results: PSf-3 membrane, which was inverted in the mixture of 20%NMP + 80% water; PSf-10 precipitated in 40% IPA+60% water mixture; and PSf-15-1 coagulated in IPA but cast relatively hotter and more humid conditions have the highest contact angle value. In other words, these membranes are the most hydrophobic samples among others. The effect of PVP addition can be observed from the results of PSf-6 to PSf-17. Basically, the pure PVP effect can be investigated from the outcomes of PSf-6, PSf-7, and PSf-8 containing 2 wt.%, 5 wt.%, and 10 wt.%, respectively. The use of hydrophilic additive-PVP yielded hydrophilic membranes with contact angle between 50° and 60°. This result support the idea of use of a hydrophilic pore forming agent did enhance the wettability of a membrane, since not all PVP could leach out of the cast film during the precipitation process.

The effect of coagulation bath temperature can be observed from the results of between PSf-9 to PSf-13 in Figure 4.11. PSf-9, PSf-10, and PSf-11 samples indicate the membranes containing 2 wt.% PVP and immersed in 7°C water, 25°C 40% IPA + 60% water, and 7°C IPA, respectively. Results have shown that use of cold IPA as a non-solvent produced more hydrophilic membrane compared with other counterparts, such as PSf-11. PSf-10, which was immersed in the mixture of IPA and water, had more hydrophobic surface than precipitated in either IPA or water. This difference might be mainly sourced because of the temperature of the coagulation bath. The more significant difference for the effect of coagulation bath temperature can be observed from the results of data set between PSf-7 and PSf-8 precipitated in cold IPA; and PSf-12 and PSf-13 immersed in 24°C IPA. Both data sets were comprised of 5 and 10 wt.% PVP, respectively. The results were consistent with overall outcomes confirming that decreasing the temperature of precipitation medium enabled to form more hydrophilic membranes.

The effect of evaporation time on the surface characteristics can be evaluated from the results of PSf-14, PSf-15, PSf-16, and PSf-17. According to the results, applying different evaporation time did not cause too many changes in the wettability of the membranes having same amount of additive inside, such as membranes comprised of 2 wt.% PVP but cast at increasing evaporation times. The only difference with respect to evaporation time can be sourced from containing varying amount of PVP in the dope solution, like PSf-17. However, the contact angle results of membranes cast under different atmospheric conditions indicated significant differences. The membranes within the interval of PSf-14 to PSf-17 formed under both lower relative humidity and temperature, while the interval of PSf-14-1 to PSf-17-1 signifies the corresponding membranes but under both higher temperature and relative humidity. It can be clearly seen that the latter conditions produced more hydrophobic substrates. On the other hand, commercial PES substrate was also analyzed in order to make comparison between our cast PSf membranes. PES support has a moderate water contact angle value which is close to 65° and is comparable to our membranes.

4.2 Morphology of TFC Membranes

The prepared TFC membranes were analyzed in terms of cross-sectional and surface properties by FESEM and contact angle measurements, respectively.

4.2.1 FESEM analysis

The fabrication procedures were described in Section 3.3 in details. Figure 4.12 represents the cross-sectional FESEM images of prepared TFC membranes.

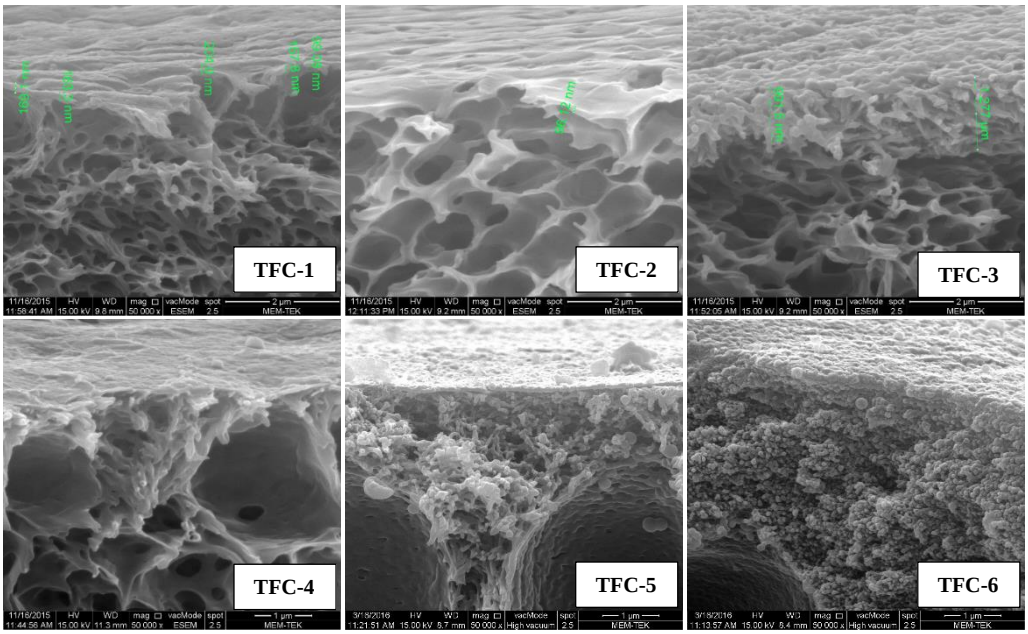

Figure 4.12: The cross-sectional FESEM images of prepared TFC samples.

According to the above results, the PA layer thickness depends greatly on the reaction conditions thus the reaction time, the monomer concentrations and even the support membrane porosity. In other words, the thickness of the PA layer is a result of a cross-linking reaction between MPD and TMC, and subsequent heat curing. TFC-1 yields around 200 nm PA in thickness, while others are ~ 100 nm, ~ 1 μm, and 300 nm, for TFC-2, TFC-3, and TFC-4, respectively. Moreover, the PA layer thickness of TFC-5 is approximately 350 nm, whereas the PA layer formed on top of the commercial PES membrane coded as TFC-6 is ~ 400 nm. Results were compared in terms of support characteristics, IP reaction time, and MPD concentration in following sections. Additionally, kinetics of IP reaction and mechanism behind the formation of cross-linked PA layer are also provided.

4.2.1.1 Kinetics of interfacial polymerization

In order to gain further insights on formation of PA layer, the interfacial polymerization kinetics should be thoroughly investigated. Due to the fact that TMC is trifunctional, branching and linear chain propagation take place at the same time. Figure 4.13 illustrates the IP reaction between MPD and TMC and schematic

drawing of simultaneous branching, cross-linking, and linear chain formation of polyamide chains. Thus, resultant PA structure is obtained accordingly. When the acid chloride group of an available branch reacts with an amine group of another linear chain, a film with totally cross-linked character is formed. On the other hand, linear structure is a result of hydrolysis of unreacted acid chloride groups causing to form pendant carboxylic acid groups, which are in fact, main responsible of both the acidic nature and increased hydrophilicity of the PA layer and eventually effecting the water flux as well as salt rejection [52, 92]. Furthermore, according to Khare et al. the extend of acid chloride groups is a function of both degree of branching and cross-linking.

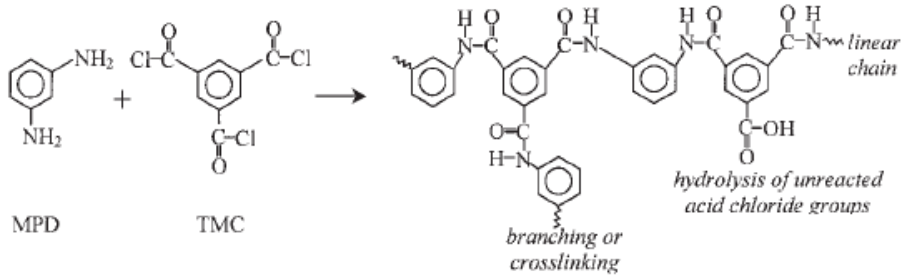

Figure 4.13: The IP reaction between MPD and TMC; and simultaneous illustration of branching, cross-linking, and linear chain formation [92].

4.2.1.2 Effect of support pore size

The main contributor affecting the resultant PA layer characteristics is might be the properties of PSf substrate, more specifically pore sizes on which IP reaction will be carried out. With the aim of that, TFC-1 and TFC-2 were prepared and compared in order to designate the impact of PSf support. TFC-1 was fabricated on support membrane coded as PSf-15-1 having pore size around ~ 60 nm in average, while TFC-2 was prepared on PSf-17-1 having pore size approximately ~ 350 nm in average. According to FESEM micrographs represented in Figure 4.10, the thickness of TFC-1 was around 200 nm, whereas in TFC-2 thinner PA layer was formed having approximately 100 nm thickness. In addition to these, TFC-5 was prepared using PSf-8 as substrate, which had average pore size about 40 nm and produced ~ 350 nm PA layer, while the PA layer fabricated on commercial PES membrane, which had 20 nm pore size in average, was around 400 nm. These results have shown that PSf substrate with smaller pore sizes give thicker PA layer, while bigger pores produce relatively thinner selective barrier. Moreover, the judgment was also

supported by TFC-6 formed on the commercial PES substrate. These outcomes were consistent with the study of Singh et al. [93] suggesting a mechanistic explanation how pore size can affect the thickness of the resultant PA layer. They claimed that smaller pores of PSf substrate somehow complicate the penetration of components, which later form PA layer, into the pores. Consequently, restricted diffusion of MPD deep into the smaller pores develops thicker PA layer formation on the surface. On the other hand, MPD solution can diffuse deep into the pore channels of larger pores and thus causing to arise of a possibility to form cross-linking inside those pores. As a result, thinner PA layer is obtained. Years later, another extensive study was also conducted by Misdan et al. [81] reporting that when the surface pore size of substrate membrane decreases, the thickness of formed PA layer increases. Therefore, they remark the fact that how much PSf substrate characteristics, particularly pore size, can affect the final cross-linked PA layer as evidenced in the work of Singh et al. [93]. Figure 4.14 schematically represents possible structural difference between TFC-1 and TFC-2.

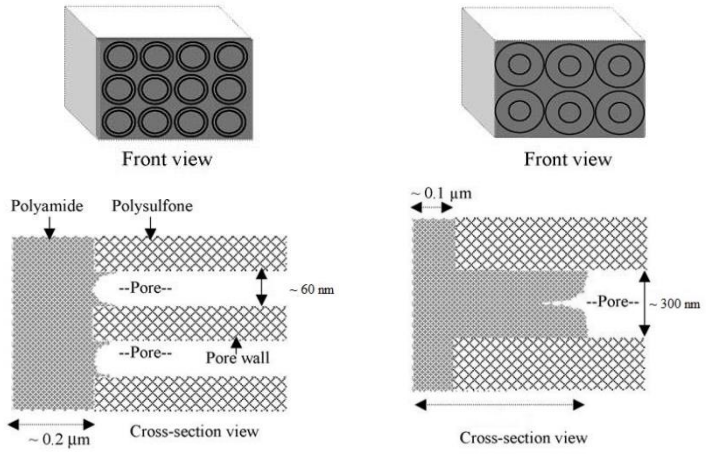

Figure 4.14: Schematic representation of possible structural difference between PSf substrated having small and larger pores corresponding to TFC-1 and TFC-2, respectively [93].

4.2.1.3 Effect of IP reaction time

For determining the impact of reaction time on the PA film formation; TFC-2 and TFC-3 were compared which were the products of 15 s and 30 s polymerization time, respectively. They both formed on PSf substrate having same characteristics and pore sizes on which substrate coded as PSf-17-1. Results have shown that the more obvious effect of the cross-linking can be observed in TFC-3 sample, which has the

maximum thickness. This is mainly because of doubling the reaction time and a clear evidence of the fact that the polymerization time is one of the governing factors in IP process. This outcome was consistent with the study of Jin and Su [51] stating that longer reaction times produce thicker films. They proposed an explanation for the effect of reaction time on PA film formation in terms of acid content sourced from TMC. According to them, increasing the reaction time leads first to drop the acid content in the film to a minimum value rapidly, and then to increase gradually. The main reason for this behaviour was explained with "self-limiting" phenomenon of the IP reaction itself. In order to form an initial PA layer with many pendant acid chlorides; once MPD molecules are introduced, at first they diffuse to organic side of the interface to react with TMC. As more MPD monomers keep coming, these acid chlorides can react with them and form a denser and more cross-linked film with a lower acid content. In order to enable the further film growth, MPD molecules have to diffuse through this initially formed layer to the organic/film interface. In this manner, excess TMC presents in polymerization process and more linear amide units with pendant acid group are formed. It is noteworthy to state that the diffusion of MPD through the initially formed PA film is slower when compared to the diffusion of TMC from the bulk solution to the interface. As a result, thicker films are formed at longer reaction times because of MPD diffusion is more difficult and excess TMC leads to form more residual acid groups.

4.2.1.4 Effect of MPD concentration

The effect of MPD concentration was determined by comparing FESEM images of TFC-1 and TFC-4 in Figure 4.10, which were prepared from 2 wt.% and 4 wt.% MPD, respectively. Other IP parameters were kept constant. As stated before, TFC prepared from lower MPD concentration has slightly thinner PA layer (~ 200nm) than membrane fabricated from 4 wt.% MPD which has a thickness of around 300 nm. In the literature, there are several studies reporting the effect of different reaction conditions including the monomer concentrations, reaction time, and heat-curing temperature. There are several systematic studies reporting the effect of monomer concentration on cross-linking process. Khare et al. [92] claimed that cross-linking density is strongly dependent on TMC concentration in such a way that it reaches maximum with TMC concentration at 0.1 wt.%, and after that point increasing TMC amount decreases the cross-linking density. They stated the results on MPD

concentration as well, thus lower degree of cross-linking took place with more branching at lower MPD concentrations; whereas at higher MPD concentrations of 1-4 wt.% produced relatively constant degree of cross-linking and branching. In another study, Jin et al. also studied on the effect of monomer concentrations to the PA layer [51]. They also found that decreasing MPD concentration yields reduced degree of cross-linking; while higher MPD contents produce more cross-linked PA network, which are in a good agreement with the outcomes of Khare et al. Our results are also in a good agreement with the literature stating that slightly thicker PA layer was attained with increased MPD concentration.

4.2.2 Contact angle results

Figure 4.15 shows the results of contact angle measurements of six different prepared TFC membranes. The membranes coded as TFC-1 and TFC-4 were interfacially polymerized on PSf-15-1 support membrane, while the PA layer of TFC-2 and TFC-3 were formed on PSf-17-1 substrate. On the other hand, PSf-8 was used as support for TFC-5, whereas TFC-6 signified the PA layer formed on commercially available PES substrate. The results were grouped into two groups and six groups overall signifying the contact angle value of TFC and its corresponding UF support membrane. The first bar implies contact angle of TFC membrane and second bar refers to its substrate hydrophilicity.

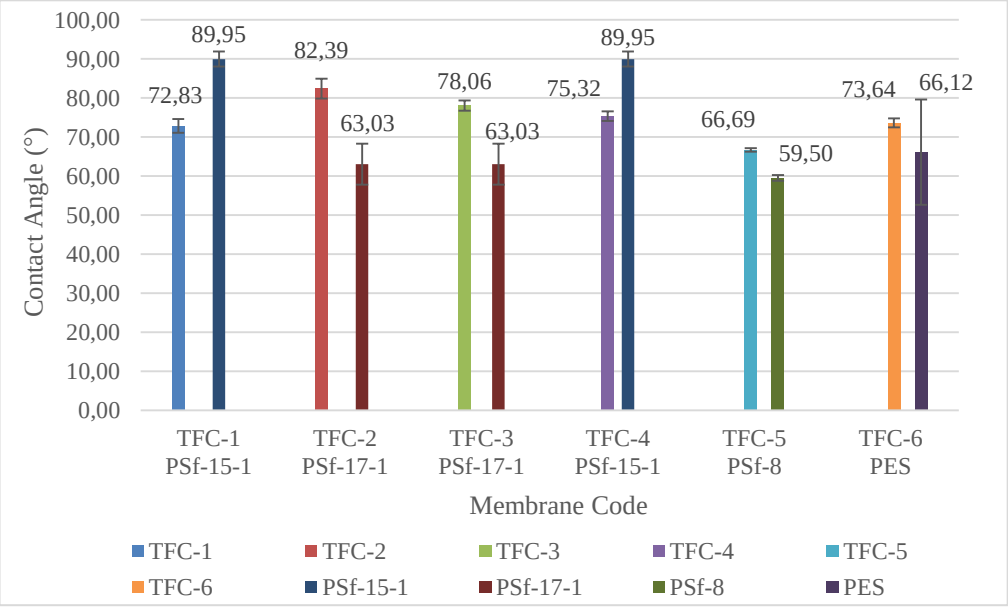

Figure 4.15: The measured contact angle results of six different TFC membranes and their corresponding UF support membranes.

For all produced TFC membranes except the ones formed on PSf-15-1 support, regardless of the IP reaction conditions, the contact angle results of TFC membranes were increased indicating the formation of more hydrophobic layer on the surface than PSf supports. Only TFC-1 and TFC-4 had the contact angle value less than its corresponding substrate, which was PSf-15-1. According to the results, PA layer formed on hydrophobic surface produced hydrophilic layers such as TFC-1 and TFC-4. On the other hand, PA layer polymerized on hydrophilic substrates yielded more hydrophobic layers than its equivalent supports at the end. This conclusion can be drawn clearly from the results of TFC-2, TFC-3, TFC-5, and TFC-6.

Among other counterparts, TFC-2 has the highest hydrophobicity mainly because of the effect of pore size characteristics of PSf support. The pore size distribution of substrate PSf-17-1 was around 250-400 nm, whereas PSf-15-1 had a pore size distribution of around 50-60 nm. The most hydrophilic sample was TFC-4, mainly because of MPD concentration was doubled as 4 wt.% which was introduced in aqueous solution. On the other hand, the effect of doubling MPD concentration can be observed best at the difference in contact angle results between TFC-1 and TFC-4. Even though same PSf support was used as substrate, there is a significant distinction in hydrophilicity and the thickness of the resultant membranes. This can be attributed to the use of higher monomer concentration.

TFC-1 and TFC-2 were compared to see the effect of PSf support on PA layer formation. PSf-15-1 (TFC-1) was the more hydrophilic support with larger pores than PSf-17-1 (TFC-2) and produced thicker layer.

Lastly, PA layer formed on commercially available PES substrate (TFC-6) had a contact angle value around 75°, which was consistent with the overall outcomes of data stating that more hydrophobic layer was formed on the surface as a result of interfacial polymerization than its corresponding support membrane.

4.3 Membrane Performance Test

Performance assessment is one of the factors having significant effect on the characterization of fabricated membranes.

Synthesized TFC membranes were tested in lab-scale cross flow RO system. However, owing to having small area they could not be tested without proper

masking. As a start, commercial polyvinylidene fluoride (PVDF) and polyethersulfone (PES) UF membranes were tested both in the size of testing cell without masking and in a small area cut from the same membrane with masking. The reason for this application was twofold; on one hand to check the whole RO testing unit if we will get the same results reported by the supplier. On the other hand, to designate whether the masked membranes will meet the results of membrane without masking, eventually to determine that the masking works properly without any leakage. After testing, results showed that the masked membrane did not overlap with the reported data such that even though the area was small the flux was almost three times higher than it was as in the without masking case.

After thorough literature review, it was found that there was a severe lack of information on masking procedure of membranes having small areas. From this point forward, countless trials were carried out in order to eliminate the leaking problem and to develop a proper masking procedure, such as either changing the masking material or the way of masking technique. The entire masking procedure was described extensively in APPENDIX A with the addition of problems encountered in each masking method supported by the supplementary pictures.

After developing a successfully working masking technique, one of the fabricated membrane was tested as a representative result. The tested membrane was TFC-5, which was formed on PSf-8 support. Since the membrane area was 12.66 cm^2, masking was necessary which was masked with Al tape 425 (3M^{TM}, Product number 425) as described in APPENDIX A section. Test conditions were 2000 ppm (34 mM NaCl) salt concentration at 18 bar. Membrane was compacted under 20 bar for around one hour before starting the actual measurement, then the pressure was decreased to 18 bar. The salt rejection, which signifies the selectivity of a membrane, was calculated as 85 % and was accompanied by the salt water flux of 1.03 L/m^2h.

4.4 Morphology of TFN Membrane

In order to settle the alignment of CNTs on substrate and optimize preparation procedure of TFN membranes, different conditions were tried such as deposition of CNTs on support membranes having varying pore size and structures. With the purpose of that, fabricated PSf support membranes, which have the most proper structure and pore size were tried such as PSf-8 and PSf-17. According to FESEM

images, PSf-17 has sponge-like structure with pore size around 60 nm, while PSf-8 has surface pore size approximately 40 nm and shows finger-like structure sandwiched between two sponge-like structures. In order to achieve alignment of CNTs, a filtration system was utilized. When PSf-17 was used as support membrane, owing to having stringent structure in its cross-section, CNTs could not be filtered out; thus the deposition and alignment were failed. Then, it was decided to use a substrate, such as PSf-8, in which has a finger-like structure in its cross-section so that it could not show any internal resistance to flow of the solution during the CNT deposition and filtration.

Other than the choice of substrate structure, the loading amount of CNTs was also the other parameter that has to be optimized. As a starting point, 0.05 mg and 0.01 mg of –COOH functionalized SWCNTs (as they purchased) were tried. These were the preliminary studies for the fabrication of the state-of-the-art membranes containing CNTs, which will be zwitterionically functionalized in the future and will be used for fabrication of membranes having high boron rejection values.

Figure 4.16 shows representative FESEM images of TFN-1 membrane containing 0.05 mg –COOH functionalized SWCNTs and deposited on PSf-8 support prior to TFC formation on top layer.

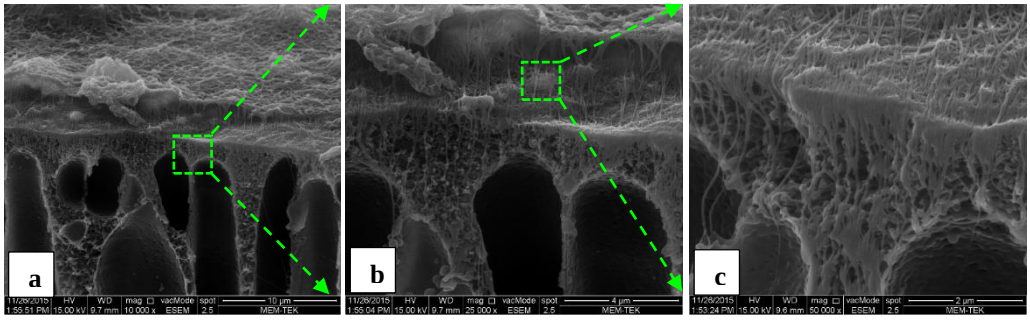

Figure 4.16: The cross-sectional FESEM images of TFN-1 membrane.

The results show that the alignment of CNTs were accomplished by applying vacuum filtration, as there are CNTs fibers in the substrate pores representing the integration of into the porous support. However, the amount of CNT was so much that they formed bundles and accumulations in some locations. The 0.05 mg of COOH-SWCNT corresponds to approximately 12% of the thin selective layer. On top of the CNTs, the characteristic ridge-and-valley structure of the PA layer is observed indicating the IP process was followed successfully.

5. CONCLUSION & RECOMMENDATIONS

Thin film nanocomposite membranes with zwitterion-functionalized carbon nanotubes on microporous PSf substrate were fabricated for desalination applications. PSf supports with varying conditions were fabricated to obtain the porous structure on the surface of the membrane. Results have shown that:

- The use of water as non-solvent caused to form a skin layer on top of the membranes, besides long finger-like structures were obtained which cannot withstand the high operation pressures in RO process. In addition to these, water caused to swell the polymer.

- According to the Hansen solubility parameters isopropanol was used as a non-solvent instead of water, and subsequent 8-hour methanol bath was employed for inducing the formation of sponge-like structure.

- Addition of pore forming compound did induce the formation of pore on the surface and sponge-like structure were achieved in the cross-section as well.

- Other than changing the type of non-solvent and addition of PVP in the dope solution, the temperature of the coagulation bath has a significant effect, too. Decreasing the non-solvent temperature produced more pores on surface, due to the slow precipitation of the polymer.

- Another factor governing the final membrane structure is the evaporation time of the cast film to the atmospheric conditions that is the time of exposure of the film to environment before immersing into the precipitation medium. According to the results, 40 s evaporation time produced more uniform and relatively bigger pores.

- With the purpose of studying effect of environmental conditions to the film morphology and evaluating the reproducibility of the results, two sets of experiments were conducted; one was in summer condition in which both temperature and relative humidity were high, the other set was cast in autumn. The group of samples

prepared during summer condition showed better porosity and pore formations on the surface.

- After fabrication of the microporous PSf membrane, the next was to prepare the PA layer in-situ by interfacial polymerization technique. According to the available literature data, the most common amine and acyl chloride monomers were used that is MPD and TMC, respectively. PA layer is formed as result of cross-linking reaction of these monomers. Therefore, the concentration of the monomers, the reaction time, and curing conditions play a significant role in the final PA layer. If the TMC amount is not enough branching takes place instead of cross-linking and produces thicker PA layer which will yield low water flux. The thinner the PA layer, the more cross-linked it is.

- The maximum PA layer was observed when changing the reaction time from 15 s to 30 s.

- As a first attempt, TFN membrane containing commercially COOH- functionalized SWCNTs were deposited on top of the prepared PSf substrate by means of applying vacuum filtration. Consequently, the CNTs were semi-aligned by shear forces and some of them went into the pores of the PSf support.

- Taking everything into the consideration, the pore size of the fabricated PSf membranes should be optimized in order to determine the best structure for the CNT deposition and following TFN fabrication.

- Last but not least, not only the optimum CNTs loading in the PA layer should be specified, but also a method for the vertical-alignment of CNTs should be developed such as applying electrical field.

REFERENCES

[1] **Tu, K. L.** (2014). *Boron Removal by Nanofiltration and Reverse Osmosis Membranes* (PhD thesis) University of Wollongong.

[2] **UNESCO**. (2003). Water for People, Water for Life, The United Nations World Water Development Report, (WWDR1). UNESCO Publishing. Retrieved from http://www.unesco.org/new/en/natural-sciences

[3] **Greenlee, L., Lawler, D., Freeman, B., Marrot, B., & Moulin, P.** (2009). Reverse osmosis desalination: Water sources, technology, and today's challenges. Water Research, 43(9), 2317-2348.

[4] **Hilal, N., Kim, G., & Somerfield, C.** (2011). Boron removal from saline water: A comprehensive review. Desalination, 273(1), 23-35. http://dx.doi.org/10.1016/j.desal.2010.05.012

[5] **Oo, M.** (2012). *Boron removal by reverse osmosis membranes* (PhD thesis). National University Of Singapore.

[6] **WHO.** (2011). Guidelines for drinking-water quality, 4th Edition. Geneva: WHO.

[7] **Güler, E., Kaya, C., Kabay, N., & Arda, M.** (2015). Boron removal from seawater: State-of-the-art review. *Desalination*, *356*, 85-93.

[8] **Güler, E., Kabay, N., Yüksel, M., Yavuz, E., & Yüksel, Ü.** (2011). A comparative study for boron removal from seawater by two types of polyamide thin film composite SWRO membranes. *Desalination*, *273* (1), 81-84. http://dx.doi.org/10.1016/j.desal.2010.10.045

[9] **Koseoglu, H., Kabay, N., Yüksel, M., Sarp, S., Arar, Ö., & Kitis, M.** (2008). Boron removal from seawater using high rejection SWRO membranes — impact of pH, feed concentration, pressure, and cross-flow velocity. *Desalination*, *227*(1-3), 253-263.

[10] **Baker, R.** (2004). *Membrane technology and applications* (2nd ed.). Chichester: J. Wiley.

[11] **Url-11**< *http://web.ornl.gov.jpg*> date retrieved 17.10.2015.

[12] **Mulder, M.** (1996). *Basic principles of membrane technology*. Boston: Kluwer Academic Publishers, Netherlands, pp.6.

[13] **Loeb, S., & Sourirajan, S.** (1963). Sea Water Demineralization by Means of an Osmotic Membrane. *Advances in Chemistry*, 117-132.

[14] **Wu, H., Tang, B., & Wu, P.** (2010). MWNTs/Polyester Thin Film Nanocomposite Membrane: An Approach to Overcome the Trade-Off Effect between Permeability and Selectivity. *J. Phys. Chem. C*, *114*(39), 16395-16400. http://dx.doi.org/10.1021/jp107280m

[15] **Lalia, B., Kochkodan, V., Hashaikeh, R., & Hilal, N.** (2013). A review on membrane fabrication: Structure, properties and performance relationship. *Desalination*, *326*, 77-95.

[16] **U.S. Bureau of Reclamation Sandia National Laboratories.** (2003). *Desalination and Water Purification Roadmap – A Report of the Executive Committee*. DWPR Program Report #95. Denver. U.S.

Department of the Interior, Bureau of Reclamation and Sandia National Laboratories.

[17] **Fritzmann, C., Löwenberg, J., Wintgens, T., & Melin, T.** (2007). State-of-the-art of reverse osmosis desalination. *Desalination*, *216*(1-3), 1-76. http://dx.doi.org/10.1016/j.desal.2006.12.009

[18] **Nath, K.** (2008). *Membrane separation processes*. New Delhi: Prentice-Hall of India.

[19] **Wei, J., Jian, X., Wu, C., Zhang, S., & Yan, C.** (2005). Influence of polymer structure on thermal stability of composite membranes. *Journal of Membrane Science*. http://dx.doi.org/10.1016/j.memsci.2005.02.012

[20] **Lau, W., Ismail, A., Misdan, N., & Kassim, M.** (2012). A recent progress in thin film composite membrane: A review. *Desalination*, *287*, 190-199. http://dx.doi.org/10.1016/j.desal.2011.04.004

[21] **Ghosh, A., & Hoek, E.** (2009). Impacts of support membrane structure and chemistry on polyamide–polysulfone interfacial composite membranes. *Journal of Membrane Science*, *336*(1-2), 140-148. http://dx.doi.org/10.1016/j.memsci.2009.03.024

[22] **Ly, A., Chu, C., & Nguyen, T.** (1990). US4970034 Process for preparing isotropic microporous polysulfone membranes. *U.S. Patent No. 4970034 A.*

[23] **Kools, W.** (1998). *Membrane Formation by Phase Inversion in Multicomponent Polymer Systems Mechanisms and Morphologies* (PhD thesis). University of Twente.

[24] **Strathmann, H.** (1985). Production of Microporous Media by Phase Inversion Processes. In D. Lloyd, *Materials Science of Synthetic Membranes* (1st ed., pp. 165–195). Washington, DC: *American Chemical Society*. http://dx.doi.org/10.1021/bk-1985-0269.ch008

[25] **Kim, J., Lee, H., & Kim, S.** (2000). Liquid-liquid phase separation during polysulfone membrane preparation. *Korean Journal of Chemical Engineering*, *17*(5), 564-569. http://dx.doi.org/10.1007/bf02707167

[26] **Liu, Y., Koops, G., & Strathmann, H.** (2003). Characterization of morphology controlled polyethersulfone hollow fiber membranes by the addition of polyethylene glycol to the dope and bore liquid solution. *Journal of Membrane Science*, *223* (1-2), 187-199.

[27] **Chuang, W., Young, T., Chiu, W., & Lin, C.** (2000). The effect of polymeric additives on the structure and permeability of poly(vinyl alcohol) asymmetric membranes. *Polymer*, *41*(15), 5633-5641.

[28] **Lafreniere, L., Talbot, F., Matsuura, T., & Sourirajan, S.** (1987). Effect of poly(vinylpyrrolidone) additive on the performance of poly(ether sulfone) ultrafiltration membranes. *Industrial & Engineering Chemistry Research*, *26*(11), 2385-2389.

[29] **Saljoughi, E., Amirilargani, M., & Mohammadi, T.** (2009). Effect of poly(vinyl pyrrolidone) concentration and coagulation bath temperature on the morphology, permeability, and thermal stability of asymmetric cellulose acetate membranes. *Journal of Applied Polymer Science*, *111*(5), 2537-2544. http://dx.doi.org/10.1002/app.29354

[30] **Marchese, J., Ponce, M., Ochoa, N., Prádanos, P., Palacio, L., & Hernández, A.** (2003). Fouling behaviour of polyethersulfone UF membranes made with different PVP. *Journal of Membrane Science*, *211*(1), 1-11. http://dx.doi.org/10.1016/s0376-7388(02)00260-0

[31] **Wang, H., Yu, T., Zhao, C., & Du, Q.** (2009). Improvement of hydrophilicity and blood compatibility on polyethersulfone membrane by adding polyvinylpyrrolidone. *Fibers Polymer*, *10*(1), 1-5.

[32] **Ochoa, N., Prádanos, P., Palacio, L., Pagliero, C., Marchese, J., & Hernández, A.** (2001). Pore size distributions based on AFM imaging and retention of multidisperse polymer solutes. *Journal of Membrane Science*, *187*(1-2), 227-237.

[33] **Saljoughi, E., Amirilargani, M., & Mohammadi, T.** (2010). Effect of PEG additive and coagulation bath temperature on the morphology, permeability and thermal/chemical stability of asymmetric CA membranes. *Desalination*, *262*(1-3), 72-78.

[34] **Lee, H.** (2002). Solution properties of poly(amic acid)–NMP containing LiCl and their effects on membrane morphologies. *Journal of Membrane Science*, *196*(2), 267-277.

[35] **Ng, L., Mohammad, A., Leo, C., & Hilal, N.** (2013). Polymeric membranes incorporated with metal/metal oxide nanoparticles: A comprehensive review. *Desalination*, *308*, 15-33.

[36] **Cadotte, J., Petersen, R., Larson, R., & Erickson, E.** (1980). A new thin-film composite seawater reverse osmosis membrane. *Desalination*, *32*, 25-31.

[37] **Ghosh, A., Jeong, B., Huang, X., & Hoek, E.** (2008). Impacts of reaction and curing conditions on polyamide composite reverse osmosis membrane properties. *Journal of Membrane Science*, *311*(1-2), 34-45.

[38] **Veríssimo, S., Peinemann, K., & Bordado, J.** (2006). Influence of the diamine structure on the nanofiltration performance, surface morphology and surface charge of the composite polyamide membranes. *Journal of Membrane Science*, *279* (1-2), 266-275.

[39] **Tarboush, B., Rana, D., Matsuura, T., Arafat, H., & Narbaitz, R.** (2008). Preparation of thin-film-composite polyamide membranes for desalination using novel hydrophilic surface modifying macromolecules. *Journal of Membrane Science*, *325*(1), 166-175.

[40] **Huang, S., Li, C., Hu, C., Tsai, H., Lee, K., & Lai, J.** (2006). Polyamide thin-film composite membranes prepared by interfacial polymerization for pervaporation separation. *Desalination*, *200*(1-3), 387-389.

[41] **Tang, B., Huo, Z., & Wu, P.** (2008). Study on a novel polyester composite nanofiltration membrane by interfacial polymerization of triethanolamine (TEOA) and trimesoyl chloride (TMC). *Journal of Membrane Science*, *320* (1-2), 198-205.

[42] **Lee, K., Arnot, T., & Mattia, D.** (2011). A review of reverse osmosis membrane materials for desalination—Development to date and future potential. *Journal of Membrane Science*, *370*(1-2), 1-22.

[43] **Song, Y., Sun, P., Henry, L., & Sun, B.** (2005). Mechanisms of structure and performance controlled thin film composite membrane formation via interfacial polymerization process. *Journal of Membrane Science*, *251*(1-2), 67-79.

[44] **Karode, S., Kulkarni, S., Suresh, A., & Mashelkar, R.** (1998). New insights into kinetics and thermodynamics of interfacial polymerization. *Chemical Engineering Science*, *53*(15), 2649-2663.

[45] **Dhumal, S., Wagh, S., & Suresh, A.** (2008). Interfacial polycondensation—Modeling of kinetics and film properties. *Journal of Membrane Science*, *325*(2), 758-771.

[46] **Tomaschke, J.E.** (1990). Interfacially synthesized reverse osmosis membrane containing an amine salt and processes for preparing the same. *U.S. Patent No. 4948507 A.*

[47] **Chau, M.M., Light, W.G., & Chu, H.C.** (1991). Dry High Flux Semipermeable Membranes. *U.S. Patent No. 4983291 A.*

[48] **Mickols, W.E.** (2005). Composite Membrane and Method for Making the Same. U*.S. Patent No. 6878278 B2.*

[49] **Mickols, W.E.** (2002). Composite Membrane and Method for Making the Same. *U.S. Patent Application No. 6337018.*

[50] **Zou, H., Jin, Y., Yang, J., Dai, H., Yu, X., & Xu, J.** (2010). Synthesis and characterization of thin film composite reverse osmosis membranes via novel interfacial polymerization approach. *Separation and Purification Technology*, *72* (3), 256-262.

[51] **Jin, Y., & Su, Z.** (2009). Effects of polymerization conditions on hydrophilic groups in aromatic polyamide thin films. *Journal of Membrane Science*, *330* (1-2), 175-179.

[52] **Soroush, A., Barzin, J., Barikani, M., & Fathizadeh, M.** (2012). Interfacially polymerized polyamide thin film composite membranes: Preparation, characterization and performance evaluation. *Desalination*, *287*, 310-316.

[53] **Yin, J., & Deng, B.** (2015). Polymer-matrix nanocomposite membranes for water treatment. *Journal of Membrane Science*, *479*, 256-275. http://dx.doi.org/10.1016/j.memsci.2014.11.019

[54] **Jeong, B., Hoek, E., Yan, Y., Subramani, A., Huang, X., Hurwitz, G., & Jawor, A.** (2007). Interfacial polymerization of thin film nanocomposites: A new concept for reverse osmosis membranes. *Journal of Membrane Science*, *294* (1-2), 1-7. http://dx.doi.org/10.1016/j.memsci.2007.02.025

[55] **Lau, W., Gray, S., Matsuura, T., Emadzadeh, D., Paul Chen, J., & Ismail, A.** (2015). A review on polyamide thin film nanocomposite (TFN) membranes: History, applications, challenges and approaches. *Water Research*, *80*, 306-324. http://dx.doi.org/10.1016/j.watres.2015.04.037

[56] **Lind, M., Ghosh, A., Jawor, A., Huang, X., Hou, W., Yang, Y., & Hoek, E.** (2009). Influence of Zeolite Crystal Size on Zeolite-Polyamide Thin Film Nanocomposite Membranes. *Langmuir*, *25*(17), 10139-10145. http://dx.doi.org/10.1021/la900938x

[57] **Fathizadeh, M., Aroujalian, A., & Raisi, A.** (2011). Effect of added NaX nano-zeolite into polyamide as a top thin layer of membrane on water flux and salt rejection in a reverse osmosis process. *Journal of Membrane Science*, *375*(1-2), 88-95.

[58] **Baroña, G., Choi, M., & Jung, B.** (2012). High permeate flux of PVA/PSf thin film composite nanofiltration membrane with aluminosilicate single-walled nanotubes. *Journal of Colloid And Interface Science*, *386*(1), 189-197. http://dx.doi.org/10.1016/j.jcis.2012.07.049

[59] **Zhang, L., Shi, G., Qiu, S., Cheng, L., & Chen, H.** (2011). Preparation of high-flux thin film nanocomposite reverse osmosis membranes by

incorporating functionalized multi-walled carbon nanotubes. *Desalination and Water Treatment*, *34*(1-3), 19-24.

[60] **Roy, S., Ntim, S., Mitra, S., & Sirkar, K.** (2011). Facile fabrication of superior nanofiltration membranes from interfacially polymerized CNT-polymer composites. *Journal of Membrane Science*, *375*(1-2), 81-87. http://dx.doi.org/10.1016/j.memsci.2011.03.012

[61] **Shen, J.N., Yu, C.C., Ruan, H.M., Gao, C.J., & Van der Bruggen, B.** (2013). Preparation and characterization of thin-film nanocomposite membranes embedded with poly(methyl methacrylate) hydrophobic modified multiwalled carbon nanotubes by interfacial polymerization. *Journal of Membrane Science*, *442*, 18-26.

[62] **Wu, H., Tang, B., & Wu, P.** (2013). Optimization, characterization and nanofiltration properties test of MWNTs/polyester thin film nanocomposite membrane. *Journal of Membrane Science*, *428*, 425-433.

[63] **Chan, W., Chen, H., Surapathi, A., Taylor, M., Shao, X., Marand, E., & Johnson, J.** (2013). Zwitterion Functionalized Carbon Nanotube/Polyamide Nanocomposite Membranes for Water Desalination. *ACS Nano*, *7* (6), 5308-5319.

[64] **Goh, P., Ismail, A., & Ng, B.** (2013). Carbon nanotubes for desalination: Performance evaluation and current hurdles. *Desalination*, *308*, 2-14. http://dx.doi.org/10.1016/j.desal.2012.07.040

[65] **Kalra, A., Garde, S., & Hummer, G.** (2003). Osmotic water transport through carbon nanotube membranes. *Proceedings of The National Academy Of Sciences*, *100* (18), 10175-10180.

[66] **Qiu, S., Wu, L., Pan, X., Zhang, L., Chen, H., & Gao, C.** (2009). Preparation and properties of functionalized carbon nanotube/PSF blend ultrafiltration membranes. *Journal of Membrane Science*, *342*(1-2), 165-172.

[67] **Ma, P., Siddiqui, N., Marom, G., & Kim, J.** (2010). Dispersion and functionalization of carbon nanotubes for polymer-based nanocomposites: A review. *Composites Part A: Applied Science and Manufacturing*, *41*(10), 1345-1367.

[68] **Son, M., Choi, H., Liu, L., Celik, E., Park, H., & Choi, H.** (2015). Efficacy of carbon nanotube positioning in the polyethersulfone support layer on the performance of thin-film composite membrane for desalination. *Chemical Engineering Journal*, *266*, 376-384.

[69] **Stevens, J., Huang, A., Peng, H., Chiang, I., Khabashesku, V., & Margrave, J.** (2003). Sidewall Amino-Functionalization of Single-Walled Carbon Nanotubes through Fluorination and Subsequent Reactions with Terminal Diamines. *Nano Letters*, *3*(3), 331-336.

[70] **Yang, Y., Xie, X., & Mai, Y.** (2011). Functionalization of carbon nanotubes for polymer nanocomposites. In T. McNally & P. Pötschke, *Polymer-Carbon Nanotube Composites* (1st ed., pp. 55-91). *Woodhead Publishing Series in Composites Science and Engineering*.

[71] **Chen, J., Hamon, M. A., Hu, H., Chen, Y., Rao, A. M., Eklund, P. C., & Haddon, R.C.** (1998). Solution Properties of Single-Walled Carbon Nanotubes. *Science*, *282*(5386), 95-98.

[72] **Chattopadhyay, D., Lastella, S., Kim, S., & Papadimitrakopoulos, F.** (2002). Length Separation of Zwitterion-Functionalized Single Wall Carbon Nanotubes by GPC. *J. Am. Chem. Soc.*, *124*(5), 728-729.

[73] **Ratto, T. V., Holt, J. K., & Szmodis, A. W.** (2010). Membranes with embedded nanotubes for selective permeability. *U.S. Patent No. 20100025330 A1*.

[74] **Park, J., Choi, W., Kim, S., Chun, B., Bang, J., & Lee, K.** (2010). Enhancement of Chlorine Resistance in Carbon Nanotube Based Nanocomposite Reverse Osmosis Membranes. *Desalination and Water Treatment*, *15*(1-3), 198-204.

[75] **de Lannoy, C. F., Jassby, D., Gloe, K., Gordon, A. D., & Wiesner, M. R.** (2013). Aquatic Biofouling Prevention by Electrically Charged Nanocomposite Polymer Thin Film Membranes. *Environmental Science & Technology*, *47* (6), 2760-2768.

[76] **Amini, M., Jahanshahi, M., & Rahimpour, A.** (2013). Synthesis of novel thin film nanocomposite (TFN) forward osmosis membranes using functionalized multi-walled carbon nanotubes. *Journal of Membrane Science*, *435*, 233-241.

[77] **Baroña, G., Lim, J., Choi, M., & Jung, B.** (2013). Interfacial polymerization of polyamide-aluminosilicate SWNT nanocomposite membranes for reverse osmosis. *Desalination*, *325*, 138-147.

[78] **Zhao, H., Qiu, S., Wu, L., Zhang, L., Chen, H., & Gao, C.** (2014). Improving the performance of polyamide reverse osmosis membrane by incorporation of modified multi-walled carbon nanotubes. *Journal of Membrane Science*, *450*, 249-256.

[79] **Liu, T., Yuan, H., Li, Q., Tang, Y., Zhang, Q., & Qian, W. et al.** (2015). Ion-Responsive Channels of Zwitterion-Carbon Nanotube Membrane for Rapid Water Permeation and Ultrahigh Mono-/Multivalent Ion Selectivity. *ACS Nano*, *9*(7), 7488-7496.

[80] **Son, M., Park, H., Liu, L., Choi, H., Kim, J., & Choi, H.** (2016). Thin-film nanocomposite membrane with CNT positioning in support layer for energy harvesting from saline water. *Chemical Engineering Journal*, *284*, 68-77. http://dx.doi.org/10.1016/j.cej.2015.08.134

[81] **Misdan, N., Lau, W., Ismail, A., & Matsuura, T.** (2013). Formation of thin film composite nanofiltration membrane: Effect of polysulfone substrate characteristics. *Desalination*, *329*, 9-18.

[82] **Surapathi, A. K.** (2012). *Functionalized Single Walled Carbon Nanotube/Polymer Nanocomposite Membranes for Gas Separation and Desalination* (PhD thesis). Virginia Polytechnic Institute and State University.

[83] **Jain, A., Dubey, V., Mehra, N., Lodhi, N., Nahar, M., Mishra, D., & Jain, N.** (2009). Carbohydrate-conjugated multiwalled carbon nanotubes: development and characterization. *Nanomedicine: Nanotechnology, Biology and Medicine*, *5*(4), 432-442.

[84] **Zhang, Z., Chen, S., & Jiang, S.** (2006). Dual-Functional Biomimetic Materials: Nonfouling Poly(carboxybetaine) with Active Functional Groups for Protein Immobilization. *Biomacromolecules*, *7*(12), 3311-3315.

[85] **Pakizeh, M., Mansoori, S., Pourafshari Chenar, M., & Namvar-Mahboub, M.** (2013). Modification of PSf membrane nanostructure using

different fabrication parameters and investigation of the CO_2 separation properties of PDMS-coated PSf composite membranes. *Brazilian Journal of Chemical Engineering*, *30*(2), 345-354.

[86] **Bai, H., Zhou, Y., & Zhang, L.** (2014). Morphology and Mechanical Properties of a New Nanocrystalline Cellulose/Polysulfone Composite Membrane. *Advances In Polymer Technology*, *34*(1), 21471-21479.

[87] **Hahn, J., Filiz, V., Rangou, S., Clodt, J., Jung, A., Buhr, K., Abetz, C., & Abetz, V.** (2012). Structure formation of integral-asymmetric membranes of polystyrene -block -Pol y (ethylene oxide). *J. Polym. Sci. B Polym. Phys.*, *51*(4), 281-290.

[88] **Subrahmanyan, S.** (2003). *An investigation of pore collapse in asymmetric polysulfone membranes* (PhD thesis). Virginia Polytechnic Institute and State University.

[89] **Han, M.** (2002). Thermodynamic and rheological variation in polysulfone solution by PVP and its effect in the preparation of phase inversion membrane. *Journal of Membrane Science*, *202*(1-2), 55-61.

[90] **Wienk, I., Boom, R., Beerlage, M., Bulte, A., Smolders, C., & Strathmann, H.** (1996). Recent advances in the formation of phase inversion membranes made from amorphous or semi-crystalline polymers. *Journal of Membrane Science*, *113*(2), 361-371.

[91] **van de Witte, P., Dijkstra, P., van den Berg, J., & Feijen, J.** (1996). Phase separation processes in polymer solutions in relation to membrane formation. *Journal of Membrane Science*, *117*(1-2), 1-31.

[92] **Khare, V., Greenberg, A., & Krantz, W.** (2004). Investigation of the viscoelastic and transport properties of interfacially polymerized barrier layers using pendant drop mechanical analysis. *Journal Of Applied Polymer Science*, *94*(2), 558-568.

[93] **Singh, P., Joshi, S., Trivedi, J., Devmurari, C., Rao, A., & Ghosh, P.** (2006). Probing the structural variations of thin film composite RO membranes obtained by coating polyamide over polysulfone membranes of different pore dimensions. *Journal Of Membrane Science*, *278*(1-2), 19-25.

APPENDICES

APPENDIX A: Membrane Masking Procedure Using Aluminum Tape & Foil

APPENDIX A

The permeation cell in which synthesized membranes tested has a 140-cm^2 area for testing operation. On the other hand, synthesized membranes had varying area values ranging from 3.0-20 cm^2. Due to the limited area of the fabricated membranes, masking procedure was inevitable in order to characterize the resultant membranes in terms of their performance. Certainly, membranes having larger effective area could be synthesized however, this study was preliminary study and will be the base for the fabrication of TFN membranes comprised of functionalized SWCNTs with high boron selectivity. The main restriction is the deposition procedure of the CNTs on the UF support in which a filtration system is used for the alignment of nanotubes by shear forces.

The masking material has to be impermeable to water so that it cannot allow any sort of leaking that can interfere the performance of the fabricated membranes. Any kind of material made of aluminum (Al) is the best choice for masking of to-be-tested samples. Therefore, Al foil duct tape and Al foil were our primary choices owing to having not only heavy-duty performance against high hydraulic pressure but also inert behavior to the salty water.

In order to eliminate leaking problem, numerous types of masking were tried and overall three different kinds of Al duct tapes were used having varying width and thicknesses. The applied masking procedures were described hereafter, supported by supplementary images and reasons of why they were failed.

At first, an Al duct tape (Avery Dennison; Fasson 0810) was used as a masking material. This tape is in overall 0.12 mm in thickness with having acrylic adhesive at the backside of the foil. First trials were carried out with Al tape 810, which was cut in the dimensions of testing cell; folded half from its length and superimposed on one to other because of the width of the tape was 7.5 cm. Next, the tape was fold in half from its length, and a circle in the diameter of the membrane was cut. Membrane was placed into that circle and sandwiched between two tapes. Initially, commercially available membranes with known flux and salt rejection values were tested to check if there is a leak. It is important to mask membranes as in round shape in order to prevent leaking or creating extra stress around the corners in the circle of Al tape. Then, two-component epoxy (Bison Epoxy) was applied to the edge of the hole to

seal the openings. The masked membrane was placed in a vacuum oven for 3-4 hours for the completion of the epoxy reaction. A representative masked TFC membrane placed into the cell are shown in Figure A.1.

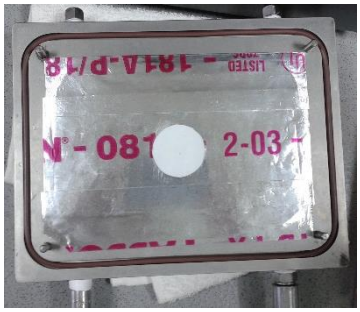

Figure A.1: A representative placement of masked TFC membrane into the cell.

After consecutive unsuccessful trials in terms of not overlapping with the unmasked case, the masked procedure was changed began with switching the masking material Al tape 810 to Al tape 802 (Avery Dennison; Fasson 802) which has rubber adhesive relatively thinner overall thickness being 0.18 mm. We believed that the leaking was sourced mainly because of the thickness of the Al 810. That is why; same masking procedures were applied but this time with thinner Al tape. When masked UF membranes were tested for pure water flux values, it was found out that the results could not meet with their commercial values. Once more, it was obvious that the leaking problem could not be solved. We believed that the masking material has to be much thinner than what we used so far. Therefore, we decided to use heavy-duty Al foil 18 μm in the thickness. By this way, not only the overall thickness of the masked was reduced but also the overlapping problem in duct tape was minimized. In this type of masking, one side was comprised of one piece Al foil stuck to Al duct tape. The one-piece side that was the Al foil part was placed to the feed side with the intention of eliminating or at least minimizing the leaking problems through the superimposed parts. Furthermore, epoxy or any kind of glue was not used for sealing, masking used without

All tried masking techniques were listed in the followings supported with pictures of samples:

i. 3-piece Al tape 810 / 3-piece Al tape 810: Three pieces of Al duct tape 810 were superimposed to each other containing membrane in the center of the middle

tape. Epoxy was used to seal the membrane. Figure A.2 shows the masked membrane coded M1.

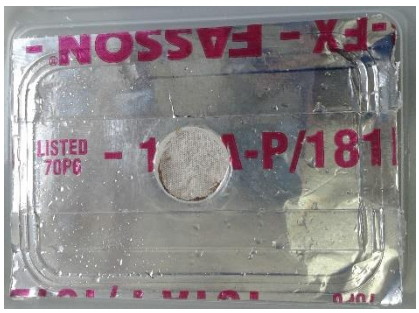

Figure A.2: The masked membrane coded M1.

ii. 3-piece Al tape 802/ 3-piece Al tape 802: As described above, due to the thickness of the Al tape 810, the masking material was switched to relative thinner one named Al tape 802. Epoxy was used for sealing. Figure A.3 represents the masked membrane coded M2.

Figure A.3: the masked membrane coded M2.

iii. 3-piece Al tape 802/ 3-piece Al tape 802: Membrane was placed without any sealing. Figure A.4 depicts the masked membrane coded M3.

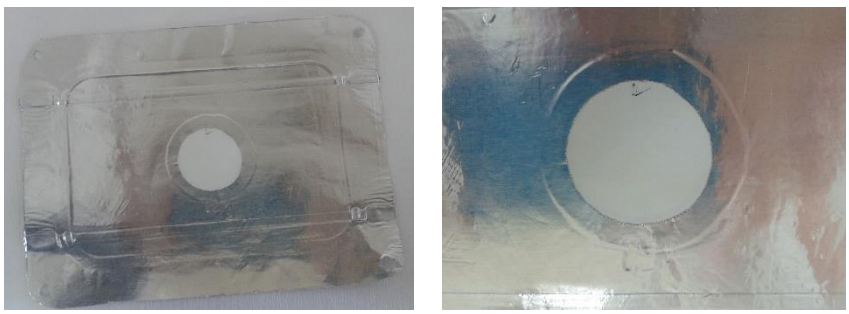

Figure A.4: The masked membrane coded M3.

iv. 3-piece Al tape 802/ 3-piece Al tape 802: It was assumed that the leaking possibly sourced from the epoxy seal and it was decided to use silicone adhesive for

the sealing. Figure A.5 represents the membrane coded M4, which was sealed with silicone adhesive.

Figure A.5: The membrane sample sealed with silicone adhesive and coded M4.

v. 2-piece Al tape 802/ 1-piece Al foil: After repetitive studies resulted with failure, we changed the duct tape to thinner one and decided to use two pieces of Al tape instead of three. Two pieces of Al tape were stuck to one-piece of Al foil with the purpose of minimizing the thickness of the intersection points. Because it was clear that, the superimposed parts came across right to the turn-offs of the inner O-ring creating stress over there and hence causing to increase the measured water flux by leaking. Membrane was placed to the intersection of the two Al tapes. Meanwhile, it was understood the sealing adhesive was not the problem; it was leaked because of the intersections of the tape came across the O-ring turnoffs. Therefore, from this point forward no adhesive or epoxy was used for sealing. Figure A.6 shows the membrane masked with Al tape and Al foil coded M5.

Figure A.6: The membrane sample masked with Al tape and Al foil coded M5.

vi. 3-piece Al tape 802/ 3-piece Al tape 802 (Positioned horizontally): In this type of masking, the masked sample was placed under the inner O-ring and the intersections positioned horizontally to the testing cell. The tape was pasted on the cavity of the inner O-ring. After the measurement, the cell was opened and there were holes at the superimposed points where two pieces of Al tapes came across. A representative picture of the membrane is shown in Figure A.7, which was pasted

under inner O-ring and was placed in horizontal position. The membrane code was M6. The picture was taken right after the membrane was tested and cell was opened. The water flux was so high even though for such a small area which was an indication of possible intervention from feed side to the permeate side. The water droplets can be noticed easily on top of the Al mask representing the leaking from overlapped points.

Figure A.7: The masked membrane sample pasted under inner O-ring as horizontal position and coded M6.

vii. 3-piece Al tape 802/ 3-piece Al tape 802 (Positioned vertically): Subsequently, every alternative variations of mask were tried such as positioning the intersection vertically to the cell; using foil on one side instead of tape; preparing masks that as big as the cell so that it pasted at the cavity of the inner O-ring. Fig. depicts the masked membrane M7, which was positioned in vertical arrangement to the cell and was pasted under the inner O-ring. However, this masking type did not worked either, since the droplets in the Figure A.8 indicate of the leakage from overlapped points. This outcome led us to a point that the leaking problem may be sourced from the shim and spacer combination of cell, thus it should be rearranged.

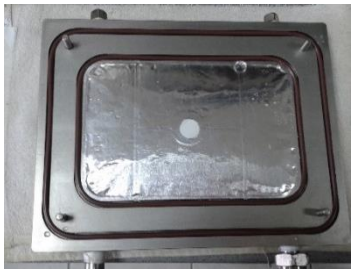

Figure A.8: The masked membrane sample pasted under inner O-ring as vertical position and coded M7.

viii. 3-piece Al tape 810/ 2-piece Al tape 810 (Shim and spacer combination of the cell): The membrane test cell has three different foulant spacers and five different shims. The spacer and shim are used for adjusting the cavity of the effective area of

the cell and thus the combination of them has a significant impact on the performance results. The spacers have knitted-type structures with varying thicknesses being 17 mil, 47 mil, and 65 mil. The thinnest spacer is represented as 17 mil being low foulant spacer, while 65 mil is the thickest one and named high foulant spacer. On the other hand, shims are made of Al plate having different thickness values coded with numbers being No.4, No.7, No.8, No.9, and No.10. The thinnest shim is No.4, whereas No.10 signifies the thickest one. Figure A.9 shows two representative pictures of spacers and shim.

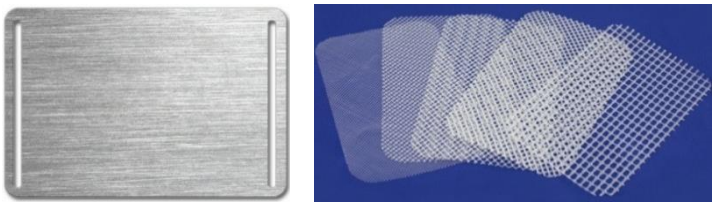

Figure A.9: Representative pictures of spacers and a shim.

Figure A.10 shows masked membrane samples, which were coded M8.

Figure A.10: The masked membrane sample coded M8.

ix. 3-piece Al tape 810/ 1 piece Al foil: One-piece tape, which had a hole with membrane at the center of it, was pasted to the one-piece of Al foil. The Al foil was placed under inner O-ring in order to avoid any possible disturbance on the O-ring that might affect the sealing of it and eventually can cause to leak. Figure A.11 depicts the membrane sample M9.

Figure A.11: The masked membrane sample coded M8.

x. 3-piece Al tape 810/ 1 piece Al foil: Al tape was in the dimensions of inner O-ring, while Al foil was of outer O-ring. The purpose was to eliminate the overlapped points, which were the main leaking source, at the same time using Al can reduce the overall thickness of the masked membrane. A representative picture of membrane sample which was coded M10 is shown in Figure A.12.

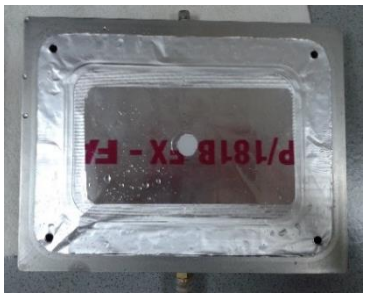

Figure A.12: The membrane sample coded M10.

xi. 1-piece Al tape 802/ 1 piece of Al foil sandwiched between 2-piece of Al foil: This type of masking was comprised of one piece Al tape pasted on a one piece of Al foil, which was cut as in the dimensions of cell. Additionally, it was sandwiched between two pieces of Al foils. Masked membrane was tested under both pure and salt water conditions to calculate the pure water flux and salt rejection values, respectively. Since the tested membrane has known specifications, it was also tested without masking and compared with the masked case. Results matched up with the specifications indicating that the masking technique did work properly. However, the technique is not robust enough because of the thin nature Al foil, after a few trials foil was torn where the O-ring came across. Masked membrane M11 is depicted in Figure A.13.

Figure A.13: The membrane sample M11 which was masked with Al foil and sandwiched between two piece of Al foil.

In fact, this method led us to proceed with one piece of masking material without any tape intersections that can cause possible leaks. New type of Al tape (3M^{TM}; Product

Number 425) was purchased which has a slightly wider width than the size of cell has. A hole for the membrane to be placed was cut at the center of the tape. Then, this one-piece tape was stuck on Al foil. This type of masking is the only type works properly without any leaks. Figure A.14 shows two different membrane samples masked by one-piece of Al tape and coded as M12.

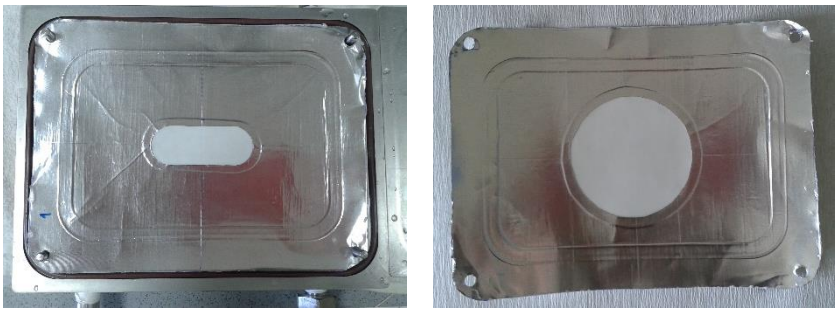

Figure A.14: Two different membrane samples masked by one-piece of Al tape and coded as M12.

The overall masking methods and materials are listed in Table A.1 with their specifications and corresponding codes.

Table A.1: The list of masking methods and materials with their specifications and codes.

Membrane Code	Masking Technique	Specification
M1	3 pieces Al tape 810 + 3 pieces Al tape 810	Sealed with epoxy
M2	3 pieces Al tape 802 + 3 pieces Al tape 802	Sealed with epoxy
M3	3 pieces Al tape 802 + 3 pieces Al tape 802	No sealing
M4	3 pieces Al tape 802 + 3 pieces Al tape 802	Sealed with silicone adhesive
M5	2 pieces Al tape 802 + 1 piece Al foil	No sealing
M6	3 pieces Al tape 802 + 3 pieces Al tape 802	Horizontal positioning to the cell
M7	3 pieces Al tape 802 + 3 pieces Al tape 802	Vertical positioning
M8	3 pieces Al tape 810 + 2 pieces Al tape 810	Shim and spacer combination
M9	3 pieces Al tape 810 + 1 piece Al foil	Al foil was placed under inner O-ring
M10	3 pieces Al tape 810 + 1 piece Al foil	Placed under outer O-ring
M11	1 piece Al tape 802 + 1 piece of Al foil	Sandwiched between 2 pieces of Al foil
M12	1 piece Al tape 425 (3M^{TM}; Product Number 425)	No leak! The best masking technique.

Masking technique was tested with membranes having known water flux and rejection. The membrane sample was tested with both a mask and unmasked case. The test results of SMTC-TFC membrane, which was fabricated in Singapore Membrane Research Center, were shown in Table A.2.

Table A.2: The performance results of SMTC-TFC membrane tested with Al tape 425.

Membrane	Pressure	Salt Concentration	Flux	Rejection	Commercial Data
SMTC-TFC (Unmasked, A=140 cm^2)	10 bar	2000 ppm (34 mM)	23.62 L/m^2h (Pure water flux)	~ 93 %	Pure water flux: 25 L/m^2h Rejection: ~96% (at 10 mM NaCl)
SMTC-TFC (Masked, A= 34.21 cm^2)	10 bar	585 ppm (10 mM)	5.83 L/m^2h (Salt water flux)	~ 95 %	

CURRICULUM VITAE

Name Surname **:** Kader ÖZGÜR

Place and Date of Birth **:** Dulovo - Bulgaria, 18/07/1989

E-Mail **:** kderozgur@gmail.com

EDUCATION:

M.Sc. **:** Istanbul Technical University, Graduate School of Science Engineering and Technology, Department of Nano Science and Nano Engineering, (2013-)

B.Sc. **:** Izmir Institute of Technology, Faculty of Science, Department of Chemistry, (2008- 2013)

PROFESSIONAL EXPERIENCE AND REWARDS:

- Researcher at TÜBİTAK MAM - Energy Institute (2016-)
- Project Specialist at Sampas Nanotechnology Ltd. (2014 - 2016)
- B.Sc. honour graduate (2008-2013)

PUBLICATIONS, AND PRESENTATIONS:

- B.Sc. Graduation Project: "Molecular Design of Organic Inhibitors for Silica-Based Geothermal Scaling", under the supervision of Prof. Dr. Mustafa M. Demir, 2013